

Design and control of a portable take-home laboratory rig for control systems teaching.



Prepared by:
Reginald Tamuka Nyakonda
Student Number: NYKREG001

Department of Electrical Engineering
University of Cape Town

Supervised by:
Dr M. S. Tšoeu
DEPARTMENT OF ELECTRICAL ENGINEERING
University of Cape Town

6 November 2021

Submitted to the Department of Electrical Engineering at the University of Cape Town in partial fulfilment of the academic requirements for a Bachelor of Science degree in Electrical Engineering

Declaration

1. I know that plagiarism is wrong. Plagiarism is to use another's work and pretend that it is one's own.
2. I have used the IEEE convention for citation and referencing. Each contribution to, and quotation in, this final year project report from the work(s) of other people, has been attributed and has been cited and referenced.
3. This final year project report is my own work.
4. I have not allowed, and will not allow, anyone to copy my work with the intention of passing it off as their own work or part thereof

Name: REGINALD TAMUKA NYAKONDA

Student No: NYKREG001

Signature: R.T.N

Date: 06 November 2021

Word count = 19 982 words

Terms of Reference

DESCRIPTION:	The COVID-19 pandemic has accelerated the move to blended forms of teaching and learning. For Engineering education, the single most critical constraint is laboratory work. Ways of carrying out laboratory work have been through virtualization, on-campus presence and miniaturization of laboratory rigs. This project is intended to design and build a multi-tank fluid flow and level control system that has deadtime (delay), second order integrating dynamics, multivariable coupling as well as carefully designed hard nonlinearities of deadzone and saturation. Tanks of this will be designed to have both linear and nonlinear operating regions such as cylindrical tanks with hemisphere or cone base. This system will be designed using sensors, actuators and Arduino components available at Communica, RS components and 3D printed parts. The cost of this system is to be kept below R5000.00. The system will be replicated and loaned out to students of Control Engineering and Measurements and Instrumentation for off-campus study and experimentation.
DELIVERABLES:	<ol style="list-style-type: none">1. A well designed and tested laboratory rig.2. Implementation of a software framework for interfacing different controllers and displaying results.3. All code source files in Git repository.4. Research report, oral presentation and project exhibition with poster.

Acknowledgements

This project was one of the most challenging things I have had to do as a student and its completion would have not been possible without the help of the following people.

First and foremost, I would like to thank my family for being a constant support pillar in my life. The long nights discussing my progress as an engineer and hearing me rant about school have not been in vain and I hope this project gives you guys' another reason to be proud of me as a son and as a brother.

Secondly, I would like to thank Dr Tšoeu for being a guiding hand throughout the duration of this project. Thank you for keeping my expectations in check and for always being available when I needed your help. Good luck in your future endeavours and I hope our paths will cross again in industry or academia.

Thirdly, I would like to thank the Klaus Jurgen Bathe Leadership programme for their generous scholarship which has allowed me to complete the last 2 years of my undergraduate degree.

Finally, I would like to thank all the friends I have made during this rigorous undergraduate degree. You guys have sharpened my mind and I am grateful for all our interactions. Good luck with the rest of your careers and let's stay in touch.

To all those who have supported me throughout this journey, this one is for you!

Abstract

COVID-19 has changed all aspects of our lives and the way in which control engineering students conduct their experiments has been dramatically changed due to social distancing rules. There is a need to rethink how practical experiments can be adapted for the online, physically distanced learning environment. This project sought to develop a low-cost, portable prototype that can be used for control systems teaching. The system was built to demonstrate concepts such as instrumentation aswell as process control after having designed an initial computer aided design prototype. A coupled 2 tank liquid level control rig was developed for a combined cost of R2883. The sensors and actuators of the motor were calibrated and a prototype was assembled before the combined rig was tested using a tuned PID controller. The PID controllers implemented all improved the settling time of the plant and thereby suggesting that the system was well designed aswell as well integrated. Investigations into non-linear control of the laboratory rig was not possible due to time constraints.

All the code aswell as CAD models used for the purposes of this project are available at the following link:

<https://github.com/rtnyakonda/EEE4022S>

Table of Contents

Declaration	i
Terms of Reference	ii
Acknowledgements.....	iii
Abstract.....	iv
Table of Contents.....	v
List of Figures and Tables	vii
1. Introduction.....	1
1.1 Background to the study	1
1.2 Problem statement, research aims, questions and objectives.....	3
1.2.1 Problem statement.....	3
1.2.2 Research aims.....	3
1.2.3 Research questions.....	3
1.2.4 Research objectives	3
1.3 Scope and Limitations.....	3
1.4 Research Contributions.....	3
1.5 Plan of development	4
1.6 Report Outline.....	6
2. Literature Review.....	7
2.1 System Dynamics	7
2.1.1 Dead time.....	7
2.1.2 Saturation.....	9
2.1.3 Dead zone	10
2.1.4 Non-linear and Linear regions of operation.....	11
2.1.5 Multivariable coupling	12
2.1.6 Second order dynamics	13
2.2 Component choices	15
2.2.1 Valves	15
2.2.2 Water pump.....	16
2.2.3 Water level sensors.....	17
2.2.4 Flow rate sensors.....	18
2.3 Laboratory rig control	19
2.3.1 Model Predictive Control (MPC) vs PID control	19
2.4 Controller implementation.....	20
2.4.1 Analogue controllers	20
2.4.2 Digital controllers	20
3. Research Design.....	22
3.1 Design Process.....	22
3.2 System Requirements Analysis	22
3.2.1 User Requirements.....	22
3.2.2 Technical Requirements.....	23
3.3 Testing	24
3.3.1 Module testing.....	24
3.3.2 System Integration testing	25
3.3.3 Acceptance test procedures	26
4. Design.....	27

4.1	System Design	27
4.1.1	Model 1.....	27
4.1.2	Model 2.....	28
4.2	Hardware Design	29
4.2.1	Microcontroller	29
4.2.2	Flow rate sensor.....	30
4.2.3	Level sensor	30
4.2.4	Actuators (Pumps/Valves).....	30
4.2.5	Water tank	31
4.3	Software Design.....	34
4.3.1	Flow rate sensor.....	34
4.3.2	Level sensor	35
4.3.3	Software Packages	36
4.4	Implementation.....	37
4.4.1	Laboratory rig.....	37
4.4.2	Hardware integration.....	40
4.4.3	Bill of materials	42
5.	Results and Data Analysis.....	43
5.1	Level sensor calibration.....	43
5.1.1	Tank 1 level sensor.....	43
5.1.2	Tank 2 level sensor	44
5.2	Flow sensor calibration.....	45
5.2.1	Input flow rate sensor.....	45
5.2.2	Output flow rate sensor	46
5.3	Motor testing	47
5.4	Noise filter testing	48
5.5	System testing	50
5.5.1	Tank testing.....	50
5.5.2	Multivariable coupling	52
5.5.3	System identification.....	54
5.5.4	Controller testing.....	59
6.	Discussion.....	63
6.1	Water Level Readings	63
6.2	Tank 1 outflow.....	63
7.	Conclusions	64
8.	Recommendations	65
9.	List of References	66
10.	Appendices	68
10.1	Quote for the Quanser double tank	68
10.2	GitHub repository link.....	68
10.3	Controller simulations in Simulink.....	69
10.4	PID controller validation in software	69
11.	ECE Faculty: Assessment of Ethics in Research Projects	72

List of Figures and Tables

List of Figures

Figure 1.1 Gantt chart illustrating the project timeline.....	5
Figure 2.1 A system with input delay.....	8
Figure 2.2 Saturation on the output of an arbitrary component.....	9
Figure 2.3 Deadzone nonlinearity as it typically appears in DC motors and other actuators.....	10
Figure 2.4 Inverse nonlinearity of the deadzone show in figure 2.3	11
Figure 2.5 Schematic of a typical DC motor.....	13
Figure 2.6 Water level can be determined by knowing the values shown in the figure	17
Figure 3.1 V model approach that will be used as the project management methodology [25].....	22
Figure 4.1 Piping and instrumentation diagram of the system	27
Figure 4.2 First iteration of the CAD design.	28
Figure 4.3 Second iteration of the system with improvements made	28
Figure 4.4 Hemisphere bottom shaped tank for the first tank design	32
Figure 4.5 Cone bottom tank for the second design	33
Figure 4.6 Reservoir tank design with multiple inlet and outlet pipes	34
Figure 4.7 Flow chart for reading and processings flow sensor readings.....	35
Figure 4.8 Flow chart for successfully using two I2C VL53L0X level sensors.....	36
Figure 4.9 CAD design of the final laboratory rig to be prototyped aswell as the dimensions in mm.....	37
Figure 4.10 Practical implementation of the designed system (front view)	38
Figure 4.11 Practical implementation of the designed system (back view)	39
Figure 4.12 Fritzing diagram of the hardware illustrating how it is integrated.....	40
Figure 4.13 Schematic of the hardware showing connection points.	41
Figure 5.1 Calibration of the level sensor in tank 1 using analogue readings from a meter rule.	43
Figure 5.2 Calibration of the level sensor in tank 2 using analogue readings from a meter rule.	44
Figure 5.3 Calibration curve for the flow rate sensor on the inflow of tank 1	45
Figure 5.4 Calibration of the flow sensor on the outflow of tank 1 which is the inflow of tank 2.....	46
Figure 5.5 Plot of measured fluid flow rate for different armature voltage values on motor 1.....	47
Figure 5.6 Plot of measured fluid flow rate for different armature voltage values on motor 2.....	47
Figure 5.7 Frequency spectrum of motors obtained by performing an FFT on an audio recording of the motors both operating at maximum flow rate.....	48
Figure 5.8 Bode plot of the low pass filter with a 1Hz cut-off.....	49
Figure 5.9 Filter performance verification using MATLAB Simulink	49
Figure 5.10 Filter performance zoomed in at the peak of the sinusoid	50
Figure 5.11 Testing of tank 1 using a constant flow rate into the tank with the outflow closed	50
Figure 5.12 Testing of tank 2 using a constant flow rate whilst the outflow was closed	51
Figure 5.13 Multivariable coupling test done by providing 4V to the motor connecting outflow of tank 1 to the inflow of tank 2 .Both tanks were in the linear region of operation. Outflow of tank 2 was closed during this test aswell as the inflow of tank 1.....	52
Figure 5.14 Experimental results of measuring pipe resistance. No actuation was provided to the motor joining the outflow of tank 1 with the inflow of tank 2.	53
Figure 5.15 Step response of motor. Voltage of the motor was stepped from 4.2V to 4.42V.....	54
Figure 5.16 Step response of tank with motor voltage stepped from 7.5V to 8V	55
Figure 5.17 Step response of tank with motor voltage stepped from 7.52V to 8.47V	56
Figure 5.18 Step response of tank after voltage was stepped from 8V to 7.5V	56
Figure 5.19 Stepping voltage from 0V to 5.65V and noting the time delay it takes for water level to increase	57

Figure 5.20 Stepping pump voltage from 0V to 8.5V and noting the input delay	58
Figure 5.21 Stepping pump voltage from 0V to 12V and noting the input delay	58
Figure 5.22 The plant to be controlled in negative feedback	59
Figure 5.23 Bode plot of the system.....	60
Figure 5.24 Response of the system at the ultimate gain	60
Figure 5. 25System response with the control action shown.....	61
Figure 5.26 Step response of system with Ziegler-Nichols tuned PID controller. $K_p = 1.481$, $K_i = 0.07148$, $K_d=2.108$	61
Figure 5.27 Step response of tuned PID controller along with the control action.....	62
Figure 5.28 Step response of the PID controller with $K_p = 0.9138$, $K_i = 0.1$, $K_d = -1.917$	62
Figure 6.1 'Tornado' bubble caused by turbulent flow in the tank when water was pumped in with the outflow open	63

List of Tables

Table 2-1Pro's and cons of different software frameworks available to use in this project	21
Table 3-1 User requirements tracking table	23
Table 3-2 Technical requirements tracking table	23
Table 4-1 Summary of key motor specifications.....	31
Table 4-2 Tank dimensions in the different CAD designs	32
Table 4-3 Bill of materials for the laboratory rig prototype	42
Table 5-1 Calibration gains for the level sensor over different regions	44
Table 5-2 Calibration gains for the level sensor in tank 2 over different regions	44
Table 5-3 Calibration gains for the flow sensor over different flow rates.....	46

1. Introduction

This report documents research, design and prototyping work done to build a laboratory rig for control systems teaching. This chapter gives a brief background, summary literature and related works on laboratory rigs that have been designed to teach control systems concepts followed by a statement of the research aims, objectives and questions. The scope and limitations of the research are given followed by research contributions, plan of action and report outline.

1.1 Background to the study

Practical experience in engineering education plays a significant role in the development of one's skills as an engineer. One cannot simply "learn on the job" when it comes to practicing engineering as such, laboratories have been an essential part of many engineering curriculums[1]. The Engineering Council of South Africa (ECSA) is the regulating body for the engineering profession in South Africa and one of its responsibilities is to ensure that engineering degrees are awarded to only those students that show competencies in a range of areas they identified are essential to the profession. To be awarded an engineering degree, the student must demonstrate their competency in all these areas, at exit-level. These key areas that one needs to demonstrate their competency in are known as graduate attributes. Practical experience is so important to the engineering curriculum that the ability to conduct investigations and experiments is one of the 11 graduate attributes identified by ECSA [2].

Control systems engineering is one area of specialisation in Electrical Engineering, and it is often taught in the penultimate and final years of study. The first control device on record dates to ancient Egypt where Ktesibios – a mathematician and inventor, wanted to optimise the operation of a water clock. These ancient devices used water in a small tank to fill up a much larger reservoir which would in turn raise a float that would then move the time pointer. Slaves had to be used to replace the water in the smaller tank as it was used up when filling up the tank with the float. Ktesibios, in his bid to automate the process, made a regulator device which would use the water level indicated by the float to operate a valve which let in more water into the small tank whenever it was needed [3]. This simple device summarises the key points about what control systems engineering is all about. The field is concerned with the implementation of a controller that can control dynamic systems using information from sensors and in most cases, some form of feedback behaviour.

The current syllabus for undergraduate level control systems engineering at the University of Cape Town deals with topics including dead time (delay), second order integrating dynamics, hard nonlinearities such as dead zone and saturation, linear as well as nonlinear systems and multivariable coupling. In the advanced control systems courses, an introduction to instrumentation is also presented. The position control of a DC motor has been used extensively to practically demonstrate the topics that are taught in control systems engineering. Students must typically implement proportional-integral-derivative (PID) control as done by Khalifa et al. [4] and state feedback control as done by Iswanto et al. [5] among other controller configurations used in classical control theory to control the DC motor plant . A typical setup of the DC motor position control system consists of an operational amplifier, power amplifier, D.C motor, h-bridge, tachometer, digital to analogue converter (DAC), analogue to digital converter (ADC) and an output potentiometer. This experimental setup, which is currently being used for control systems teaching at the University of Cape Town (UCT), falls short by not being portable due to the bulky footprint of the DC motor that is used. In addition, to investigate multivariable coupling and control, two DC motors would need to be mechanically coupled using a belt where the control objective would be to simultaneously control belt speed and tension. Teaching of multivariable control in this manner has been investigated by Kocijan et al. [6] and the control of such a system was found to be well within

reach of final year students. The downside of this solution is that it would not only dramatically increase the size of the setup, but it would also increase the cost of the system overall.

A much more affordable and portable alternative to the bulky DC motor experiment described earlier was proposed by Reck [7]. The setup that was proposed used a Raspberry Pi, DC motor, sensors, and custom 3D printed parts to implement the DC motor position control experiment on a miniature scale. The cost of the proposed alternative set up was approximately \$125.93 in 2015 which is approximately \$144 after adjusting for inflation. In local currency, this translates to a cost of approximately R2120 as of the 15th of August 2021. Although the setup is much cheaper than the DC motor setup in the Control Lab at UCT, this solution does not allow for multivariable coupling experiments which would make it non ideal for purposes of teaching control systems. The setup could be adapted by mechanically coupling the DC motors on 2 of these miniature laboratory rigs as discussed earlier and as investigated by Kocjan et al. [6]. However, as mentioned before, a major downside of coupling 2 of these systems together is that the overall cost of the system would increase by a factor of at least two since each component would now be needed twice and additional sensors are required to measure the torque and belt speed.

Kadhim et al. [8] proposed a liquid tank level control system that uses an Arduino microcontroller, LabVIEW software, ultrasonic sensors and a single tank that is filled from a reservoir with the help of a motor. This solution has most of the functionality required to teach control systems concepts but it falls short by not including multivariable coupling since only a single tank is being filled up with fluid. Furthermore, the shape of the tank used in this experiment was cylindrical which means that only linear system characteristics and control can be demonstrated with this system. This experimental setup was expanded on by Johansson et al. [9] who used four cylindrical tanks and 2 pumps to control the water level to illustrate multivariable control of what is called the Quadruple-Tank Process (QTP) [10]. Though control of the QTP allows for investigations into multivariable control, it introduces added complexity because its control characteristics depend on the position of the valve joining the tanks which subsequently dictates whether the multivariable zeros are minimum phase or nonminimum phase [10]. This added complexity is not necessarily a bad thing as it allows more concepts to be demonstrated by the setup but the configuration of the tanks does not allow for the system to have both a linear and nonlinear operating range. Replacing the linear cylindrical tanks used by Kadhim et al.[8] and Johansson et al.[9] with a nonlinear tank with a cone shape such as the one used by Urrea et al. [11] would not solve the issue of not having both nonlinear and linear operating ranges. However, combining a nonlinear tank with a linear one to form a composite tank with a nonlinear region at the base and a linear region throughout the rest of the length of the tank (or vice versa) would allow for inclusion of all the necessary system dynamics needed to adequately teach these concepts in a laboratory. PID controllers[9],[12] and model predictive control (MPC) [12],[13] among other control methods have been used to control systems with either linear tanks or nonlinear tanks with great success. Such controllers should therefore be sufficient to control a composite system with both linear and nonlinear operation regions.

In addition to the laboratory rigs discussed earlier, a few international companies such as Quanser and Feedback Instruments also have a variety of experimental setups that investigate most of the control theory taught in the control systems courses at the University of Cape Town. Quanser has a local South African distributor called Test Dynamics and a quotation for the coupled tank system offered by them had a grand total of R165 237.11 (see Appendix A). Using these off the shelf laboratory rigs is not financially viable for a large institution like the University of Cape Town where there can be over 100 students in the introductory control systems course.

1.2 Problem statement, research aims, questions and objectives

1.2.1 Problem statement

Engineering problem:

Due to the new mode of teaching that has been brought about due to the COVID-19 pandemic, laboratory experiments are sometimes not feasible due to physical constraints such as geographical location, COVID-19 restrictions, necessitating the use of miniaturized and portable take-home laboratory rigs that can be used for experimentation as part of teaching.

1.2.2 Research aims

The aim of this research is to design and control a portable laboratory rig that can demonstrate key concepts taught in undergraduate level control systems engineering courses. The topics of interest that the rig should allow students to investigate by designing controllers to control the system are:

1. Dead time (delay)
2. Second order integrating dynamics
3. Linear and nonlinear regions of operation
4. Time-varying dynamics
5. Hard nonlinearities such as dead zone and saturation
6. Multivariable coupling.

1.2.3 Research questions

- How can the Quadruple-tank process be adapted into a portable laboratory rig for use as a practical tool that allows students at the University of Cape Town to get adequate exposure to concepts taught in introductory and advanced level undergraduate courses in control systems?

1.2.4 Research objectives

- Design a computer aided design prototype model of the portable laboratory rig.
- Design the electronic components that will be used on the laboratory rig.
- Design software to interact with the hardware.
- Assemble the prototype as per the computer aided design model.
- Evaluate the functionality of the laboratory rig and make refinements.
- Design and implement basic controllers for the laboratory rig using classical control to test the design.

1.3 Scope and Limitations

The scope of the research includes designing and testing of a multi-tank fluid flow and level control laboratory rig. Although other systems exist that can demonstrate all the aforementioned concepts, this research focuses primarily on using a fluid flow and level control system. In addition, a classical controller (PID control) will be used to control the plant with the objective being purely to demonstrate the control capabilities of the system and not for obtaining the best possible plant dynamics. Lastly, the cost of the system must be kept below R5 000.

1.4 Research Contributions

COVID-19 has affected the way undergraduate students interact with the practical aspect of their courses. Control systems engineering is a practically intensive course and students have had to resort to virtual laboratories to gain practical exposure to concepts taught in class. However, virtual laboratories are exactly as the name implies – they are virtual, and they do not allow the learner to engage with tangible hardware which

in most cases behaves differently compared to the idealised simulations that software packages offer. The laboratory rig that will be developed through this research will allow for students to have a portable hardware-based laboratory rig to use in their control systems experiments and this rig will be more affordable than the off the shelf setups that exist on the market.

1.5 Plan of development

The first task of the project is to determine a set of technical specifications that can meet the user requirements. These technical specifications will be used to develop and evaluate software models of the system. This task is estimated to take approximately 2 weeks to complete.

Having completed the first task, components that will be used in developing the prototype will need to be carefully chosen so that they exhibit some of the desired system characteristics. Decisions of which devices can be used in this system will be informed by what is in the literature. Therefore, the literature review will last for 4 weeks. Decisions of which components to choose will occur in the 2nd week of the 4-week literature review and components that are not available at the University of Cape Town will be ordered from external vendors.

Whilst waiting for components to arrive from the external vendors, computer aided design (CAD) models of the system will be made in SOLIDWORKS and simulations of the proposed design and its electronic components will be carried out in Simulink in parallel with the CAD modelling. This phase is estimated to take approximately 2 weeks. Once components have been delivered, the components will be tested as well as different subsystems before assembling the prototype. This will approximately take one week. The performance of the overall system needs to be investigated and any short comings need to be investigated and resolved as appropriate. The result of completing this subtask will be a fully functional system that can be controlled. In parallel with evaluating and improving the performance of the system, different controller configurations will be investigated in software and those that exhibit satisfactory performance will be implemented digitally on the final laboratory rig. This can be considered the testing stage of the project, and it is estimated to take approximately 4 weeks to complete. Finally, experiments will be conducted and data collected for analysis. This stage will take approximately 1 week to complete. In parallel with all the aforementioned tasks, the documentation for this project will be compiled throughout the duration of the project (13 weeks). The Gantt chart on the following page summarises the projects plan of development.

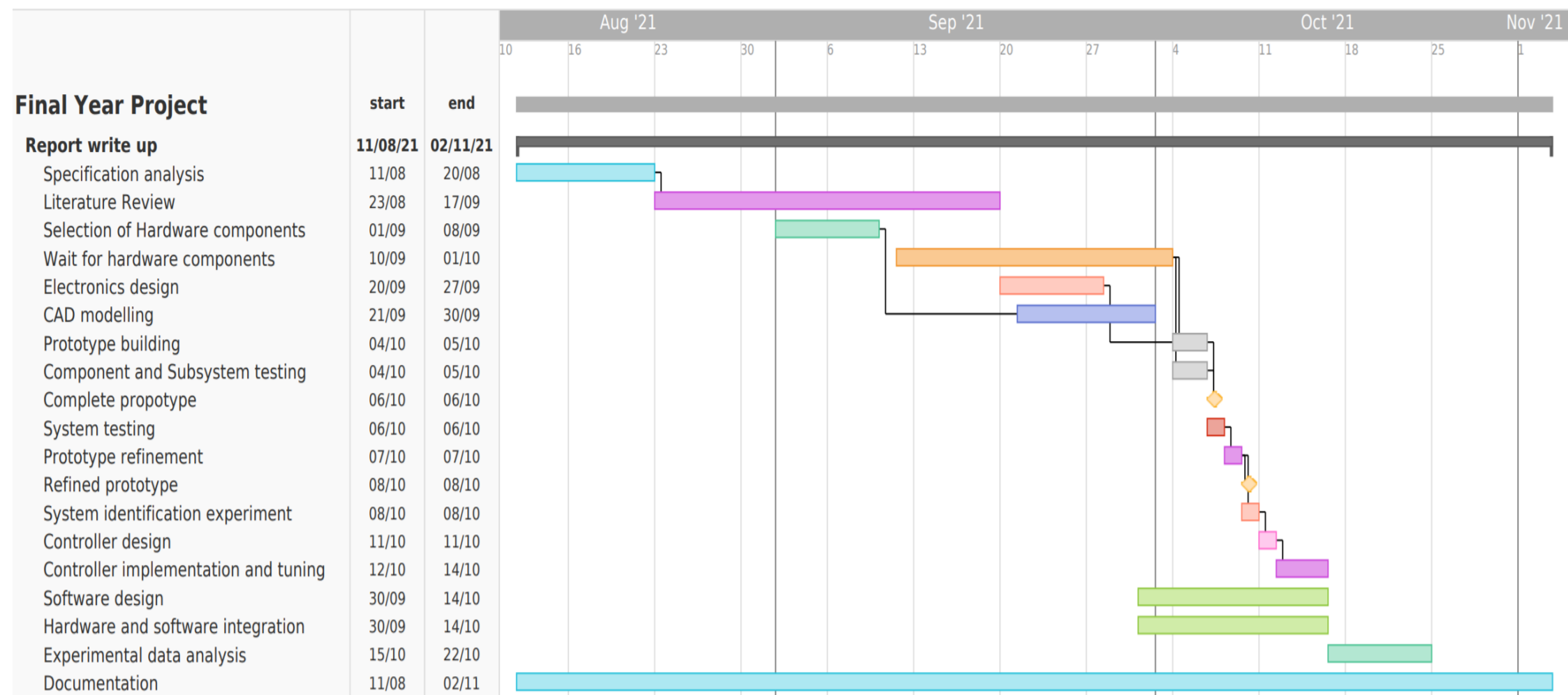


Figure 1.1 Gantt chart illustrating the project timeline

1.6 Report Outline

Following on from the discussion about the relevant literature, a detailed description of the research design procedure will be given. This section describes, at a high level, the methodologies used to perform various testing of the system and how each of these tests relate to the larger project objectives. Following from that, the design of the system will be discussed where justifications will be given for why certain components and software tools were chosen for the system design. The results of testing the system will then be presented along with a critical engagement of these results culminating in a conclusion and recommendations to improve on the work done in this project.

2. Literature Review

This chapter seeks to provide an overview of the system dynamics that need to be displayed by the laboratory set up. The dynamics of this system will be dictated by the choice of actuator and sensor types used in the construction of the laboratory rig and because of that, different sensor and actuator types will be compared. Finally, the literature for different controller configurations that can be used to control a system with the dynamics that this laboratory rig will have will be reviewed.

2.1 System Dynamics

Undergraduate courses typically cover content relating to dead time, second order integrating dynamics, linear and nonlinear regions of operation, hard nonlinearities such as dead zone and saturation and finally, multivariable coupling. Each of these concepts will be discussed in detail below.

2.1.1 Dead time

In physical systems, the output rarely reacts instantaneously to inputs provided to the system – there is usually a time delay between the control action being applied and the system reacting to that control action – this is a form of input delay. Signals often need to travel in space and potentially be processed before reaching their intended destination which typically causes these delays.

Given an n^{th} order differential equation that describes a system with an output $y(t)$ and input $x(t)$ up to its m^{th} derivative, it is easy to represent that system in the Laplace domain. Using a 3^{rd} order ($n=3$) differential equation with $x(t)$ differentiated up to its 2^{nd} derivative ($m=2$) as an example, the differential equation for such a system is shown below:

$$b_3y'''(t) + b_2y''(t) + b_1y'(t) + b_0y(t) = a_2x''(t) + a_1x'(t) + a_0x(t)$$

The Laplace transform of the above differential equation (assuming zero initial conditions) allows this differential equation to be transformed into a transfer function. The differentiation operation in time is equivalent to multiplication by the Laplace variable – s . Since the $a_0, a_1, a_2, b_0, b_1, b_2, b_3$ terms are constants, they are not affected by taking the Laplace transform. The result of taking the Laplace transform of the above differential equation is shown below:

$$b_3s^3Y(s) + b_2s^2Y(s) + b_1sY(s) + b_0Y(s) = a_2s^2X(s) + a_1sX(s) + a_0X(s)$$

By grouping like terms and noting that the transfer function is the ratio of the output to the input, the transfer function of this system is:

$$G(s) = \frac{Y(s)}{X(s)} = \frac{a_0 + a_1s + a_2s^2}{b_0 + b_1s + b_2s^2 + b_3s^3 + b_n s^n}$$

For the general case of an n^{th} order differential equation with m derivatives of the input, the transfer function is:

$$G(s) = \frac{Y(s)}{X(s)} = \frac{a_0 + a_1s + \dots + a_ms^m}{b_0 + b_1s + \dots + b_ns^n}$$

The above equation only holds for systems in which the output reacts instantaneously to the input. However, the real translation law for Laplace transforms allows for the dead time to be included in the transfer function

by the introduction of an exponential term. If we now define the transfer function of the system with a delay in cooperated as $g_d(s)$, as well as defining τ_d as the time difference between the input being applied and the system reacting, we can use the real translation law to define $g_d(s)$ as shown below.

$$g_d(s) = \frac{y(s)}{u(s)} = g(s)e^{s\tau_d}$$

Figure 2.1 graphically shows a system with dead time.

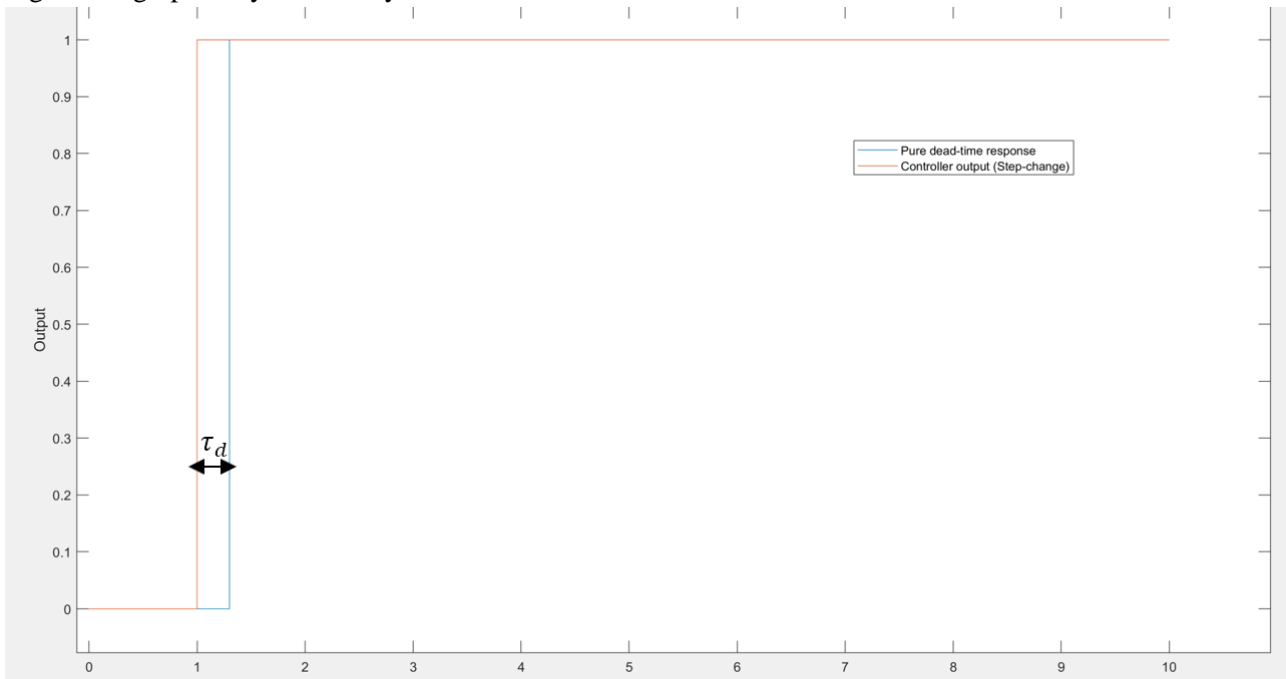


Figure 2.1 A system with input delay.

Many industrial systems have time delay properties such as what is shown in the above figure, including oil processing factories, piping systems, and even air-conditioning systems. Systems that can be described by ordinary differential equations (ODEs) result in transfer function models that imply the output reacts instantaneously to the input. Controller design is much easier for such systems and they are preferred when modelling systems as the future behaviour of the system can be computed by summing up only the present state. Time delays result in a different scenario - suppose that a system has an output delay of τ_d seconds and is connected in a negative feedback loop, at any instance in time, the error term is defined as the difference between the reference signal and the output. If the output is always τ_d seconds behind, the calculated error signal will be an overestimate of the actual error in the system. This causes the controller to output large control actions as it overcompensates and this results in the output being perturbed further away from the reference signal. This can cause instability and as such, systems with little to no delay are preferred for their simplicity [14]. Furthermore, systems with very large delays will require buffers and in very large systems, this extra storage often comes at a monetary cost. Time delay systems on the other hand, belong to a different class of differential equations known as functional differential equations (FDE's) and as explained before, these pose a significant challenge for control engineers. FDE systems can be modelled as approximate ODE systems using Pade's approximation [15] which seeks to represent the exponential term introduced in the overall transfer function using a ratio of infinite polynomial series. The infinite series is usually truncated because the higher order terms have less influence on the system but the Pade approximations can cause performance deterioration in the form of instability as well as oscillations[15]. Robust controller design approaches aim to create stability margins such that factors not accounted for in the design such as delays do not destabilise the system. Predictive control techniques are also popular for dealing with delays as they seek to estimate future values using the value available to the system at the present time [14].

The cause of dead time can be attributed to the time needed to transport information or materials from one point to another. In addition, information processing delays can also cause dead time. In the liquid level control laboratory rig that is to be designed, dead time could be incorporated into the design by using a sufficiently long pipe between the motor and the tanks. This will ensure that when the control signal is sent to pump water from the reservoir into the tank, there will be some time that will elapse before the water travels through the pipe and into the tank. Furthermore, non-ideal valves and pumps can be used as these typically contain gaps between the actuator gear teeth which leads to delays when used in this application.

2.1.2 Saturation

All practical actuators and electrical components such as operational amplifiers are subject to saturation due to the physical limitations of such devices which dictate their minimum and maximum limits. For example, a valve can either be in its fully closed or fully open position – it cannot allow more water to flow through it than what it was designed to allow. Figure 2.2 demonstrates saturation graphically.

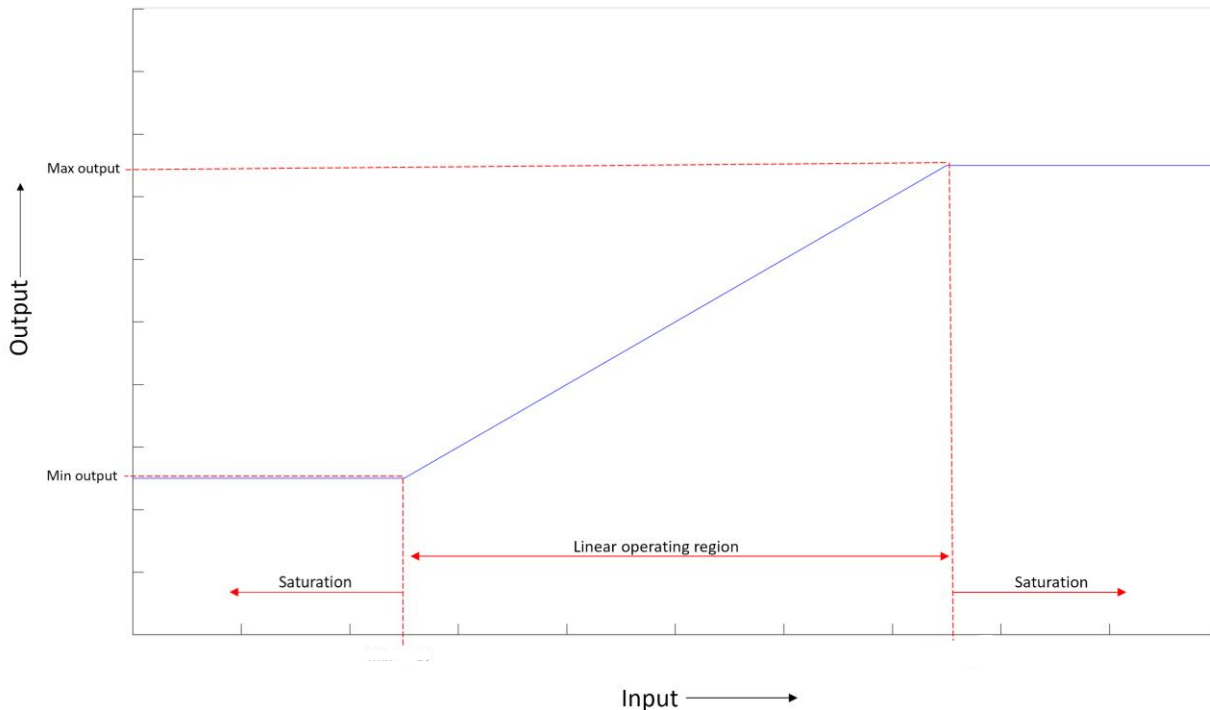


Figure 2.2 Saturation on the output of an arbitrary component.

The saturation non-linearity, which is shown in figure 2.2, belongs to the class of hard nonlinearities and it can occur both at the input or at the output. Saturation is notorious for causing performance degradation such as overshoot as well as cause slow system responses in uncompensated systems and it can sometimes lead to instability. In systems that involve an integrator such as a PID compensator, saturation can lead to what is called integrator windup[16]. As the systems' components saturate, the integrator cumulatively sums up the errors in the output values and this causes large control actions that are outside the linear operating range of the saturating components to be passed on to the actuators. This results in large overshoots and slow settling times [16]. Model predictive control has been used in the literature to compensate for input and output saturation due to its ability to include this nonlinearity in the control law in the form of input and output constraints[17]. In addition, anti-windup schemes can also be introduced in the form of additional feedback loops that regulate the control action to values that are within the saturation limits [16].

In the case of the liquid level control system to be designed, input saturations can be introduced into the system by using a DC motor to pump the water since the DC motor has a minimum and maximum rate at which it can pump water from the reservoir. To incorporate output saturation, an unrestricted outflow pipe near the top of the tank can be included in the design to ensure that the water level cannot exceed a certain value.

2.1.3 Dead zone

Dead zone is a type of hard nonlinearity that creates a region in which the output does not respond to the input applied to the system. Figure 2.3 graphically illustrates the dead zone nonlinearity.

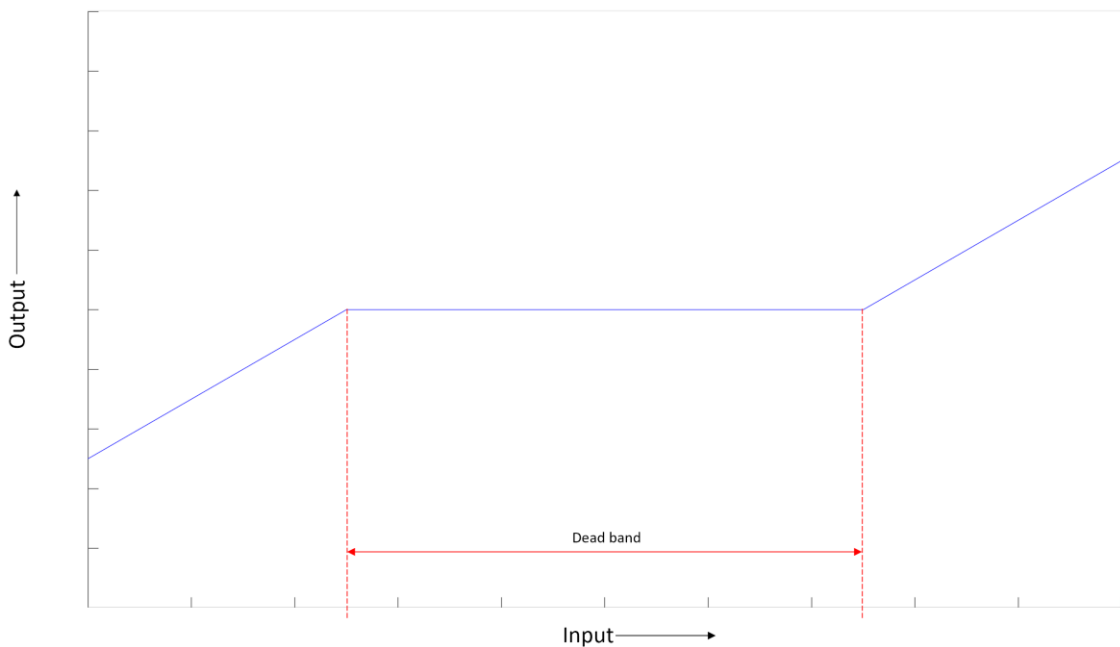


Figure 2.3 Deadzone nonlinearity as it typically appears in DC motors and other actuators

Dead zone is a common nonlinearity in mechanical systems and is usually brought about by static friction and gear backlash in systems involving motors. Unlike saturation where the maximum and minimum values are typically known before hand, dead zone parameters are typically unknown and are sometimes estimated as a form of compensating for this non-linearity [18]. Without compensation, system performance can be degraded and tracking inaccuracy, oscillations as well as instability are often consequences of this nonlinearity. Other forms of compensation that have been used to compensate for dead zone is the use of adaptive dead zone

inverse controllers [19] which seek to ‘cancel out’ the nonlinear relationship shown in figure 2.3. The exact inverse of the nonlinearity shown in figure 2.3 is shown in figure 2.4.

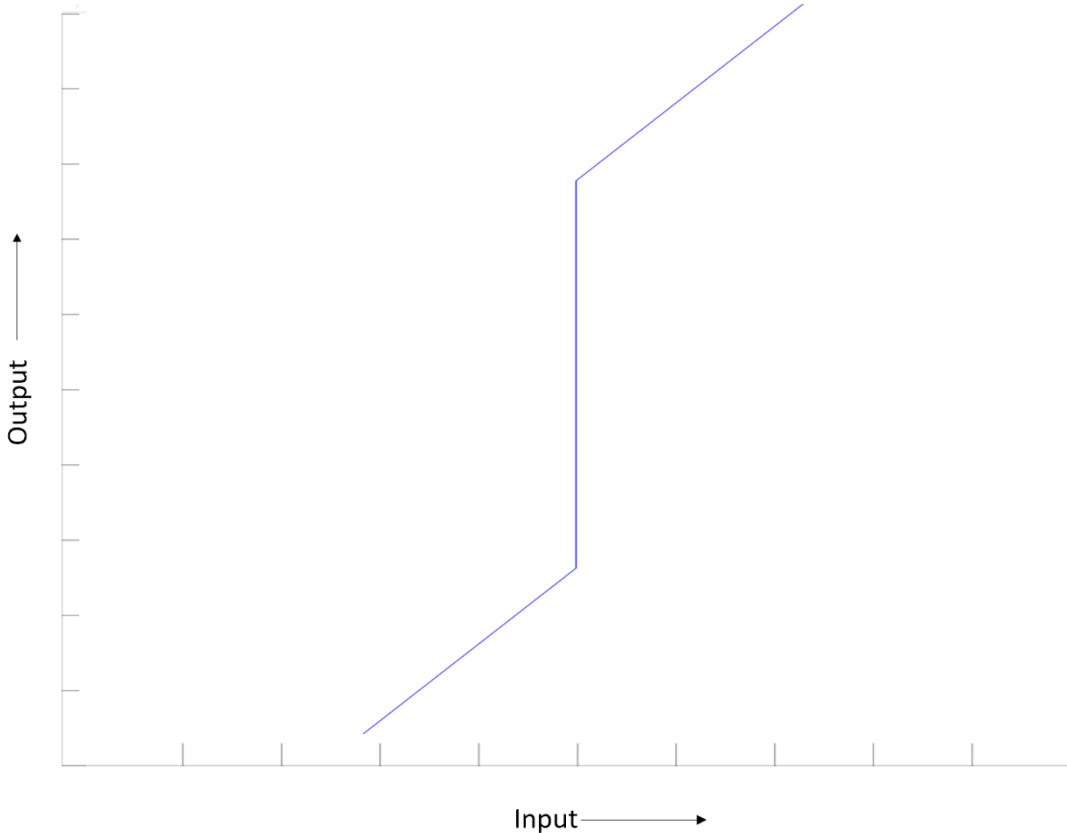


Figure 2.4 Inverse nonlinearity of the deadzone show in figure 2.3

The product of the nonlinearity and the inverse nonlinearity each shown in figure 2.3 and 2.4 respectively is unity and ideally, this would cancel out the non-linearity. Adaptive inverse controllers seek to change the shape of the inverse nonlinearity in response to changing parameters of the dead zone nonlinearity since these can be changed by factors such as wear, temperature, and corrosion[18].

To incorporate dead zone into the design of the liquid level control system, the actuators used in the system must be deliberately chosen to be non-ideal and have dead zone characteristics – this is typical of DC motors.

2.1.4 Non-linear and Linear regions of operation

A linear plant is much easier to control than a non-linear plant – linear controllers have been widely used in industrial applications and most of the linear control problems have been addressed by extensive research in the field. However, practical systems are rarely ever linear in nature and engineers also need to be able to deal with nonlinear systems and their control.

A linear controller is typically designed under the assumption that the system can be linearised and this works for most cases except for when hard nonlinearities are involved. Hard nonlinearities are discontinuous nonlinearities that typically arise because of saturation and dead zones. These nonlinearities typically cause instability in systems as well as self-excited oscillations or limit cycles – therefore, the effects of these nonlinearities need to be compensated for and linear controllers are not capable of handling this [20]. Various approaches exist in the literature to deal with nonlinear systems and their control with the most popular one being the linearisation of the plant at a specified operating point. However, this approach has its downfalls with the main one being the obscuring of important system dynamics that only manifest when the controller is tested on the complete non-linear plant. Nevertheless, the design of non-linear controllers is mathematically

intensive and the effort in designing these is rarely ever justified [20]. Furthermore, linear control typically requires the use of high-quality actuators as well as sensors when used to operate at a specified operating range – this typically increases the cost of the control system whereas nonlinear controllers provide satisfactory performance with less expensive components. Another interesting phenomenon that occurs in strongly nonlinear systems is chaos – this is where the output of the system is unpredictable as it is extremely sensitive to the initial conditions of the system[20]. This is unique to nonlinear systems – a linear system that is being driven by an arbitrary sinusoidal waveform will always produce a sinusoid with the same frequency. However, a chaotic nonlinear system may display other unexpected results such as nonperiodic sinusoids of varying frequency – the exact output depends on the initial conditions and can rarely ever be predicted. It is therefore imperative that nonlinear control techniques are studied carefully and applied to achieve satisfactory performance when controlling nonlinear systems.

The laboratory rig to be designed will need to show both linear and nonlinear characteristics in its response to allow its users to implement controllers that can deal with both characteristics. To achieve this, the tanks in which the water level will be controlled will need to have a nonlinear shape such as a hemisphere or cone shaped base as well as a cylindrical upper half. In addition, the inclusion of saturation and dead zone in the system.

2.1.5 Multivariable coupling

PID loops are one of the most popular single variable control schemes used to control systems in which there is a single variable of interest. The PID controller works by measuring and feeding back the variable of interest (usually the output) and comparing it to the reference value being provided at its input – should the variable of interest not fall within an acceptable range; the controller takes corrective action to rectify the error. This process of checking whether the output falls within acceptable ranges repeats and ideally, the system tracks the reference value accurately. Single variable controllers can also be used in systems with multiple variables of interest if such variables can be manipulated independently.

In industrial applications where various systems interact, there is a need to control more than one variable. Looking at a distillation column as an example of an industrial process, there is need to coordinate pressure, liquid flow rate and temperature to obtain the best quality product. However, affecting one variable such as pressure also influences the temperature according to the ideal gas law. The interaction that pressure and temperature have in this distillation column example is what is known as multivariable coupling[21]. This phenomenon complicates the control of these multiple input multiple output (MIMO) systems because single variable controllers such as PID controllers are not able to account for cross coupling effects and as a result, they are not able to meet the desired system objectives whilst also minimising the control effort as efficiently as multivariable controllers.

Controlling the liquid level in a single tank will be a relatively trivial task that can be completed using simple PID controllers. However, to incorporate multivariable coupling, the liquid level should also be affected by the process that occurs in the other tank. Therefore, by using two tanks and making the outflow pipe of one tank feed the inlet pipe of the other tank with a valve controlling when water can flow, multivariable coupling can be introduced in the system. When the valve is closed, the system can behave as a single input, single output system. However, when the valve is open, the multivariable nature of this plant will become apparent and other controller configurations can be used to control the plant.

2.1.6 Second order dynamics

A second order system has a response that is more complex than that of a first order system. Second order systems are oscillatory in nature whilst first order responses cannot oscillate. This makes the mathematical model used to describe second order models more complex as it depends on more than just the gain (k) and time constant to produce the model – it also depends on the damping coefficient ζ and the undamped natural frequency ω_n . The general form of a second order system is given as:

$$G(s) = \frac{k\omega_n^2}{s^2 + 2\zeta\omega_n s + \omega_n^2}$$

The damping coefficient dictates the degree of overshoot in the system – systems that overshoot the final value are said to be underdamped and this is typically undesirable as oscillations could be dangerous in applications that require high tracking accuracy. Whilst first order systems can typically be controlled using proportional control, second order systems require a bit more intensive controller design methods that make use of pole and zero placement approaches to achieve the desired system response.

The motor pump and tank combination will dictate the transfer function of the system. DC motors are a popular pump choice due to their ease of control and these will likely be used as a pump in the system. The schematic of a DC motor is shown in figure 2.5.

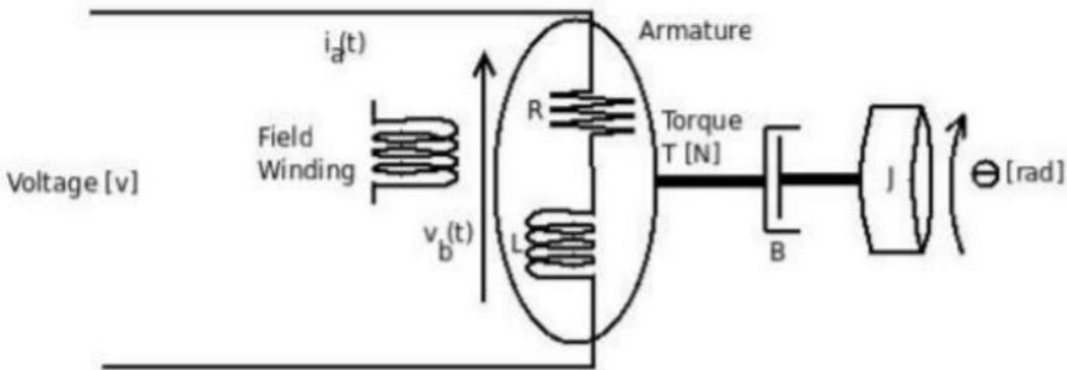


Figure 2.5 Schematic of a typical DC motor.

The torque of the motor, T , is directly proportional to the armature current. The constant of proportionality will be a constant factor labelled K_t . Mathematically:

$$T = K_t i_a \quad (1)$$

The back emf, $V_b(t)$ is a function of the constant factor K_f and the angular velocity. Mathematically:

$$V_b(t) = K_f \omega(t) = K_f \frac{d\theta}{dt} \quad (2)$$

Newton's law as well as Kirchhoff's law can be applied to the schematic in figure 2.5 and we obtain the following equations:

$$\frac{Jd^2\theta}{dt^2} + \frac{bd\theta}{dt} = K_t i \quad (3)$$

$$L \frac{di}{dt} + Ri = V - \frac{K_f d\theta}{dt} \quad (4)$$

In control systems, differential equations are more useful if taken into the Laplace domain. The Laplace transform of equation 3 and 4 are represented below by equations 5 and 6, respectively.

$$Js^2\theta(s) + bs\theta(s) = K_t I(s) \quad (5)$$

$$LsI(s) + RI(s) = V(s) - K_f s\theta(s) \quad (6)$$

From equation 6, we can make $I(s)$ the subject of the formula and substitute that into equation 5. This produces:

$$Js^2\theta(s) + bs\theta(s) = \frac{K_t(V(s) - K_f s\theta(s))}{R + Ls} \quad (7)$$

We can find the transfer function between the input voltage and the speed of the DC motor and we obtain the following expression after ignoring the winding inductance which is negligible and noting that $\omega(s) = s\theta(s)$:

$$Ga(s) = \frac{\omega(s)}{V(s)} = \frac{K_t}{[(R)(Js + b) + KtKf]} \quad (8)$$

The flow rate of the system, f is directly proportional to the motor speed.

$$f(s) = kw(s) \quad (9)$$

In the linear region of the tank with uniform cross sectional area A , the flow rate is given by :

$$f(t) = \frac{dh(t)}{dt} A \quad (10)$$

Taking the Laplace transform on both sides and substituting (10) into (9) and making $\omega(s)$ the subject of the formula, we obtain:

$$\omega(s) = \frac{sA}{k} h(s)$$

Substituting the above expression into (8), and leaving only $\frac{h(s)}{V(s)}$ on the left-hand side of the equation we obtain:

$$Ga(s) = \frac{h(s)}{V(s)} = \frac{kK_t}{sA[(R)(Js + b) + KtKf]}$$

As can be seen by the above expression, this system with a DC motor and linear tank is both second order and includes an integrator. This is only true when the outflow of the tank is allowed to drain which was an assumption made during the derivation of this transfer function.

2.2 Component choices

To include the system dynamics mentioned in section 2.1, a few different components that exhibit the desired characteristics need to be used in the system. Each of these components shall now be discussed below.

2.2.1 Valves

Valves are devices that can regulate the flow of fluid or air through a transportation medium such as a pipe or a duct. They achieve this by opening or obstructing passageways in which the fluid or gas is flowing. There are mainly 5 different valve types, namely:

- Hydraulic
- Pneumatic
- Manual
- Solenoid
- Motor

Each of these valve types shall now be discussed in turn with the focus being on flow control valves. Manual valves will not be discussed as they require manual operation of the valve and thus cannot be used in a control system.

Hydraulic valve

There are three primary types of hydraulic valves namely hydraulic pressure control valves, hydraulic flow control valves and hydraulic directional control valves but this discussion will focus only on hydraulic flow control valves since the valve to be used in the system will need to be regulating fluid flow rate. Unlike other valve types, hydraulic valves use liquid pressure to actuate the opening and closing of the valve. These valves are usually constructed using high strength metals such as iron and steel because they need to continuously operate whilst withstanding high pressure from the liquid used to actuate the valve. These high strength metals make them heavier when compared to non-pressurised valves.

Pneumatic valve

Pneumatics is the use of pressurised air to perform a mechanical operation. In the case of a pneumatic fluid flow control valve, the pressurised air is used as a control medium whose role is to send signals to the pneumatic actuator to either open or close flow as required. This type of device is sometimes referred to as a pneumatically actuated valve. As with hydraulic valves, pneumatic valves also need to be constructed from high strength materials to allow for operation under high pressure conditions. Pneumatic valves are therefore typically bulky as well as heavier.

Solenoid valve

This electrically controlled valve uses a solenoid – an electrical coil that produces a magnetic field around it when charge is passed through it. In addition, it features a movable plunger which is made of ferromagnetic material and in its rest position, the plunger closes off the orifice that allows water to flow through the valve for a normally closed valve. When the solenoid is excited, an upward magnetic force is exerted on the ferromagnetic plunger the orifice is opened – allowing free flow of fluid through the orifice of the valve.

Motor valve

A motor valve seeks to overcome the limitations of a manual valve by using an electric motor with a gear train system to open and close the orifice within the valve rather than an operator manually turning the gear. The

internal physical characteristics of the motor valve and the manual valve are identical with the only difference being the inclusion of an electric motor to open and close the valve as needed. The inclusion of this allows for the motor valve to be used in process loops because it can be controlled by inputs from an automated system.

Comparison of valves

As mentioned earlier, the hydraulic and pneumatic valves are typically rated to operate at very high pressures and are therefore made from strong, heavy metals. For a low cost and portable application, using these valves would only add unnecessary complexities to the operation of the system due to all the pressure systems that would need to be designed to operate the valves. Furthermore, their bulky and heavy nature would unnecessarily increase the weight of the set up. Since manual valves need manual manipulation of the valves position by turning the hand-lever or handwheel, the manual valve is not suitable for this application.

The solenoid and motor valves are both better suited for this application compared to the valve types mentioned earlier in this subsection. However, motor valves typically open and close much slower when compared to solenoid valves which would make it perfect for introducing dead time in the system. However, motorised valves are more popular and readily available for tubing with larger diameters from local electronic components suppliers.

2.2.2 Water pump

A pump will be needed to displace water from the different containers. A pump converts the mechanical power provided by a prime mover into pressurised fluid power and this can be achieved in various ways – for example, using fuel powered engines or an electric motor in the case of electro-hydraulic pumps which are more suited for this application. Different pump types exist in the electro-hydraulic pump domain but DC motor pumps are typically used in industry due to their much simpler speed control and good transient response.

Hydraulic pumps are either centrifugal in nature or positive displacement. Centrifugal pumps use a rotating device called an impeller which transfers its rotational energy to the fluid and subsequently, the fluid velocity and pressure increase. The fluid is then forced to exit through an outlet port whilst more liquid is brought into the impellers chamber where the process repeats itself. A down-side of this kind of pump is that it has very minimal suction power which means it cannot be used to lift water from one container to another unless it is submerged in the liquid, or it has been primed. Forgetting to prime the pump before operation would most certainly damage the delicate motor components as this causes overheating.

Positive displacement pumps can create suction using a piston, plunger, or a flexible membrane (diaphragm) – these pumps use a concept known as reciprocation. In the first stroke of the reciprocation cycle, a vacuum is created by either the piston, plunger or diaphragm and the outlet valve is closed – this sucks water into the vacuum chamber. In the second and final stroke of the cycle, the motion of the pump reverses which closes the inlet valve due to pressure build-up and the outlet flow then opens which allows fluid to get discharged. Other positive displacement pumps use rotating gears to transfer liquid by using a liquid seal developed in the pump casing to create suction at the inlet. By rotating the gears, the fluid can then be expelled out of the pump. Positive displacement pumps have moving parts which are more prone to mechanical wear and tear compared to centrifugal pumps. Furthermore, they typically cannot generate high flow rates like those seen in centrifugal pumps.

2.2.3 Water level sensors

There are two main classes of water level sensors – point level measurement and continuous level measurement sensors. Point level measurement sensors are ideally used as indicators of whether fluid is present at a discrete point in space. Continuous level measurement sensors on the other hand, can provide information about the level of fluid in a container as it rises and falls in the container with only a single sensor.

The continuous level measuring sensors that are readily available are :

1. Ultrasonic sensor
2. Radar(microwave) sensor
3. Optical (time-of-flight) sensor

In a water level control system, it is vital to have continuous readings of the water level. This allows water level setpoints to be chosen arbitrarily (within the physical limits of the tanks) and for better controller performance since any tracking errors will be compensated for in real time. As such, only the continuous level sensors will be discussed in this report.

The way ultrasonic, radar, and optical time-of-flight level sensors operate is based off the same principle – the sensor transmits waves towards the water and these waves are reflected towards the receiver that is typically fitted in the sensor housing. The time it takes for the waves to propagate and get reflected can then be used to determine the distance of the water from the sensor. With an ultrasonic sensor, ultrasonic waves are used whilst in a radar sensor, microwaves are used. The optical sensor typically uses infrared beams to detect objects. Given a continuous level sensor at an unknown height h_w above the surface level of water and is mounted at a constant height h_b above the bottom of the container as shown in the figure 2.6, the height of water in the container - h , can be computed as follows:

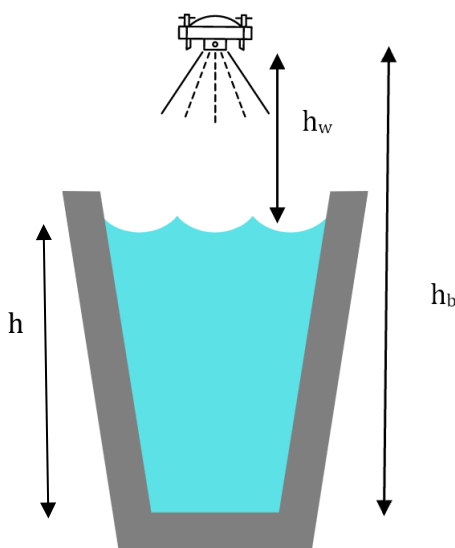


Figure 2.6 Water level can be determined by knowing the values shown in the figure

$$h = h_b - h_w$$

Since the height of the sensor above the container is a fixed constant, only h_w affects the h value. The waves propagated by the sensor need to travel to the water surface and get reflected towards the sensors' fixed receiver so the wave travels a total distance of $2h_w$. If this wave travels at a speed v_s and it takes t seconds between transmitting and receiving the wave, then the distance h_w is given by:

$$h_w = \frac{t * v_s}{2}$$

Substituting this expression of h_w into the equation for h , we obtain the following:

$$h = h_b - \frac{t * v_s}{2}$$

In the above equation, h_b depends on the experimental set up, v_s depends on the type of sensor being used – ultrasonic waves travel at the speed of sound – 343m/s whilst microwaves and light travel at the speed of light – 3×10^8 m/s. Therefore, by measuring the time taken (t) between transmitting waves and receiving them back, the height of water in the cup can be calculated.

Figure 2.6 also illustrates some rippling within the water which is something that needs to be considered and accounted for when taking level readings. These ripples could potentially cause incorrect sensor readings that fluctuate – especially when water is being pumped into the tanks as vibrations from the pumps running will also add to the rippling effect. In cases where water level readings are needed for use immediately (for example in the control loops), a low pass filter can be designed which will remove high frequency noise caused by the vibrations.

2.2.4 Flow rate sensors

Mechanical sensors

Mechanical flow rate sensors use a rotating paddle wheel that is free to rotate on a bearing in the flow path of the liquid. As the liquid flows through the device and the paddle rotates, the speed of rotation of the paddle wheel can be quantified using the Hall effect or an infrared sensor. Typically, the flow rate is measured in volume per unit time and modern-day sensors have electronics that convert the paddle rotational speed into the desired volume per unit time measurement.

The mechanical structure of the device means that the rotating parts are subject to wear over time – which can affect the operation of the device. Furthermore, contaminated liquids could affect the operation and accuracy of the device. Nevertheless, these devices operate on a simple principle and their cost-effective nature makes them an attractive choice of sensor in most applications.

Electromagnetic sensors

In electromagnetic flow rate sensors, Faraday's law of induction is used to determine flow rate. Faraday's law of induction states that the voltage induced in a circuit is directly proportional to the rate of change of the magnetic flux through that circuit. By inducing a magnetic field in the liquid through an excitation coil, when the liquid flows, it induces a voltage in nearby electrodes that are placed within the device on the flow path. Since the voltage induced in the coils is directly proportional to the velocity of the fluid, the volumetric flow rate can be calculated using the velocity measurement and the dimensions of the pipe in which the fluid is flowing.

The fluid flowing through the sensor needs to be conductive for this sensor to work. As such, not all liquids are compatible for use with this sensor. Nevertheless, fluids with some contamination tend to not affect the operation of electromagnetic flow sensors. However, it requires external power to excite the coil which induces the magnetic field in the liquid.

Ultrasonic sensors

Ultrasonic flow rate sensors use the Doppler effect to measure flow rate. The Doppler effect is a change in frequency of a wave when there is a relative speed greater than zero between the source and the receiver. An ultrasonic transducer transmits ultrasonic waves into the fluid and these waves get reflected towards a fixed receiver. Because the fluid is in motion, a frequency shift that is proportional to the fluid velocity occurs. This shift in frequency can be used to compute the flow rate. If the fluid is not in motion, then the relative speed between the receiver and the fluid is zero and there is no frequency shift.

The ultrasonic sensor overcomes some of the limitations of the mechanical and electromagnetic sensors. Firstly, it can be used with both conductive and nonconductive liquids unlike the electromagnetic sensor. Secondly, it can be installed externally to the pipe so it can be used in conditions that would otherwise be corrosive to the mechanical as well as electromagnetic sensors. However, air bubbles within the liquid and certain pipe materials can interfere with the readings of the ultrasonic sensor.

2.3 Laboratory rig control

With all the aforementioned system dynamics in mind, the choice of controller used will determine the performance of the system. Each controller type that can be used in this system shall now be discussed in turn.

2.3.1 Model Predictive Control (MPC) vs PID control

Model Predictive control is a control algorithm that uses the plant model to predict the future response of the system (over the prediction horizon), using the current state of the plant as an initial condition[12]. The objective in MPC is to select a control action (over the control horizon) that optimises an objective function. The quadratic objective function is typically used in MPC and it takes the form shown below:

$$J = Q \sum_{i=1}^P (r_{k+i} - \hat{y}_{k+i})^2 + R \sum_{i=0}^{M-1} \Delta u_{k+i}^2$$

In the equation above, Q is a matrix containing weights for the output or controlled variable y whilst R is a matrix containing weights for the control action or the manipulated variable, u. The reference or setpoint is given by r. P is the prediction horizon whilst M is the control horizon.

PID controllers are the most widely used controllers in industry. PID stands for proportional-integral-derivative and each of these 3 terms fulfil different control requirements. The proportional (P) part of the controller aims to output a control action that is proportional to the difference between the setpoint and the process variable (the error). However, the error term is always present and it cannot be eliminated purely by the proportional term alone. The speed of the system is directly proportional to the proportional gain value. The integral (I) term integrates the error over time when tracking a constant setpoint and it allows error free tracking (as demonstrated by the final value theorem). However, the speed of the response is inversely proportional to the value of the integral gain value. Furthermore, constant disturbances are well rejected when using an integral controller. Lastly, the derivative (D) term seeks to anticipate future behaviour of the error term. This is because its output is directly proportional to the rate of change of the error[22].

As discussed earlier in the literature review, system dynamics imposed by a hard nonlinearity such as saturation and system deadtime can quickly deteriorate system performance. Unlike PID control, MPC allows for constraints handling which results in the most efficient control action being taken and avoiding saturation as well as other system constraints. Work done by Pushpavani et al [12] showed that a PID controller implementation was a superior control technique to MPC when controlling liquid level in a conical tank. Although the MPC algorithm they implemented had no oscillations compared to the Ziegler-Nichols closed loop tuning method PID implementation which had approximately 50% overshoot, the Chien et al method 2

regulator obtained using PID controller tuning rules given in [23] resulted in no oscillations. Typically, PID controllers require tuning – which can be mathematically intensive as well as time consuming. Nevertheless, adequately tuned PID controllers give a much better system response. However, PID controllers did not accurately track the reference point with all controllers obtained from the different tuning rules exhibiting at least a 5% tracking error for a step input. Nevertheless, the PID controllers all gave faster settling times that were less than half the settling time provided by the MPC implementation. MPC can be used in the control of unstable systems which can be useful in certain applications.

2.4 Controller implementation

Controllers that are designed to control the level in the coupled water tank system will need to be physically realisable and there are 2 main ways of realising a controller. Controllers can either be of analogue form or digital. Each of these controller types shall be discussed in turn

2.4.1 Analogue controllers

An analogue controller can be made from a combination of passive components such as resistors, capacitors, and inductors. Active components such as operational amplifiers along with the passive components can be configured in a way that implements pure gains (proportional control), integration(for integral control) and differentiation (for derivative control). An obvious limitation of analogue controllers is that they can only implement classical controllers such as PID controllers – MPC and other advanced control techniques heavily rely on the advancements in digital computers and they cannot be implemented using analogue components. Furthermore, tuning of controller parameters requires modification of the analogue controller typically through rewiring and replacement of components which is very time consuming

2.4.2 Digital controllers

The advancements in digital computers have allowed for controllers to be implemented on digital, reprogrammable computers rather than on electronic boards with discrete components. The implementation of controllers using only a computer and a programming language will require the use of an external digital to analogue converter (DAC) to convert the digital output of the computer into analogue signals that can be passed on to actuators in the system. Furthermore, an external analogue to digital converter (ADC) will be required to convert the analogue output of sensors in the system into a digital sequence that the computer can understand.

Nevertheless, microcontrollers such as Arduino's and Raspberry Pi's have become popular implementation platforms for digital controllers as mentioned in [6], [7] and [8]. These devices have built in DACs as well as ADC's making them an attractive alternative to using a computer with a DAC and an ADC since they provide more functionality for roughly the same cost as buying a dedicated DAC and ADC for use with a computer. Furthermore, the limitations of analogue controllers are easily overcome by implementing controllers on a digital platform. A limitation of using a microcontroller to implement these digital controllers is that MPC cannot be implemented on the smaller 8-bit microcontrollers due to the computational effort required to perform that type of control. However, software frameworks such as the ACADO toolkit and Simulink with the Arduino Hardware Support Package toolkit make it possible to implement MPC.

Simulation packages

There are multiple software packages available to interface the computer with the microcontroller and the attached hardware. Python and MATLAB (Simulink) stand out as great options for integrating between hardware on the microcontroller and software written on a computer but they both have their pros and cons. The table below compares these two popular software packages.

Python	MATLAB/Simulink
Pros	
The software and its packages are free to use.	Provides better debugging functionality.
It is open-source software.	Simulink allows for rapid development when working with hardware prototypes using block models.
Python code tends to be simpler and more readable	Toolboxes are professionally developed with specific applications in mind.
Popular software with large online community support platforms	
Cons	
Lacks a graphical interface to build block models as in Simulink	Licenced software with money required for toolboxes on certain licences.
Slower programme execution time	Steeper learning curve when compared to Python.

Table 2-1Pro's and cons of different software frameworks available to use in this project

Popular microcontrollers that are typically used in projects of this size are the Raspberry PI (which uses Python as its programming language) and Arduino microcontrollers (which uses C++ as its programming language). Both microcontrollers can integrate easily with MATLAB and the Arduino can also be programmed using Python through the use of Pyfirmata[24].

3. Research Design

This section of the report aims to detail the procedures and methods that were followed to achieve the research objectives laid out in chapter 1 of this report. Furthermore, ideas and concepts explored in the preceding literature review section will form the backbone that will guide research design decisions to be documented in this section of the report. Details that are included in this section will fundamentally guide all design decisions made in subsequent chapters.

3.1 Design Process

The research objectives of this project do not have a clear solution. As such, it is essential that there is room for revising the exact details of how the solution will be implemented. The agile project management methodology is perfect for use in this project as it requires frequent testing, reassessment, and adaptation of the project - ensuring that there is room for any changes to be made to the project. Work to be done in each of the agile development cycles will be taken from the Gantt chart and a Trello board will be used to keep track of progress made in accomplishing the tasks. In addition to the agile methodology, the Verification and Validation model (V-model) will be used due to its prioritisation of testing and verification of tasks completed at each stage in the development lifecycle. The V model is shown in figure 3.1.

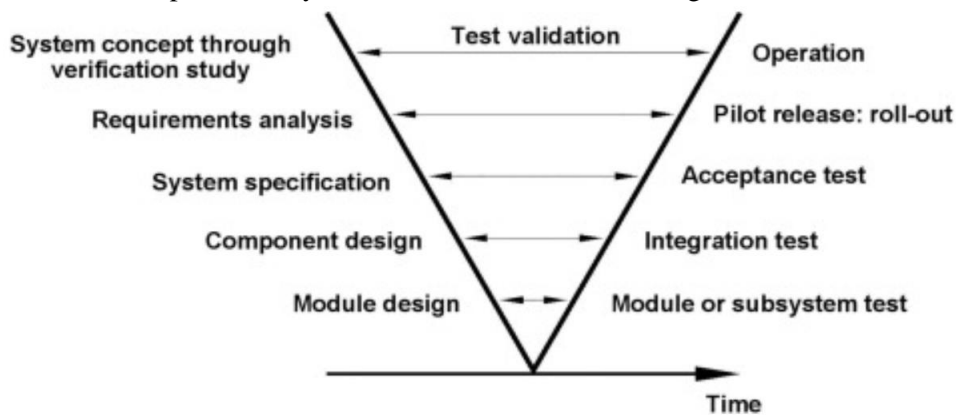


Figure 3.1 V model approach that will be used as the project management methodology [25]

3.2 System Requirements Analysis

The laboratory rig to be designed can be thought of as a system that can be broken up into different subsystems. These subsystems will each in turn work to achieve the broader set of system requirements that were briefly mentioned in the introduction chapter. Before proceeding with designing the system, it is vital that the system requirements are precisely defined at a high level (as user requirements) and at a low level (as technical specifications and acceptance test procedures). The following subsections detail the system requirements at a high and low level.

3.2.1 User Requirements

Table 3-1 specifies the user requirements for the system. Each user requirement will be assigned a code in the form “UR_X” where ‘UR’ stands for user requirement and ‘X’ is a number identifying which entry in the user requirements table. This naming convention will make referencing these system requirements in later sections of the report easier and it will also be adopted in the technical requirements table as well as the acceptance test procedures table.

User Requirement ID	Requirement Description
UR_1	The system should be portable.

UR_2	The system should cost less than R5000.
UR_3	The system should be ready to use as a practical tool for teaching Control Systems engineering.
UR_4	The results of operating the rig should be displayed in real time.
UR_5	Different controllers should be easy to implement on the system.

Table 3-1 User requirements tracking table

3.2.2 Technical Requirements

The user requirements mentioned in section 3.2.1 are high level requirements of the system and from these, technical specifications of the system can be drawn out. Table 3-2 specifies the technical specifications for the system. Each technical specification will be derived from one or more of the user requirements in table 3-1. Each technical requirement will be assigned a code in the form “TR_X” where ‘UR’ stands for technical requirement and ‘X’ is a number identifying which entry in the technical requirements table. Since these technical requirements will be derived from user requirements, the user requirement ID from which the technical specification was derived from will also be included in the table.

Technical specification ID	Requirement Description	Derived From
TR_1	Subsystem components should be made from devices or materials that are lightweight and compact.	UR_1
TR_2	Components should be chosen with cost as a limiting constraint.	UR_2
TR_3	The system should exhibit a dead-time or delay characteristic in its response.	UR_3
TR_4	The system should exhibit second order integrating dynamics.	UR_3
TR_5	The system should have linear as well as nonlinear regions of operation.	UR_3
TR_6	The system should exhibit time-varying dynamics.	UR_3
TR_7	The system should have hard nonlinearities (dead zone and saturation)	UR_3
TR_8	The system should exhibit multi-variable coupling	UR_3
TR_9	The resulting plant should be stable or can at least be made stable using a pre stabilising controller.	UR_3, UR_5
TR_10	A software framework should allow for integration with the hardware and display the data in real time	UR_4

Table 3-2 Technical requirements tracking table

To meet the above technical requirements, components that make up the system will have to be carefully chosen such that they exhibit the desired characteristics. As shown in figure 3.1, component and module design should succeed the system requirements specification stage. Details of the design of components as well as modules will be discussed in the design chapter.

3.3 Testing

The V-model requires that a testing phase happens in parallel to each development phase. As such, there is a need to develop broad and testable criteria that confirm whether the user and technical requirements discussed earlier in this chapter have been met and that the functionality of subsystems or components is as expected. There are 3 main testing phases which occur in the following order:

1. Module/Subsystem testing – validates module design
2. Integration testing – validates component design
3. Acceptance testing – validates the system specifications

The order of testing in this case is essential as it proactively tracks defects which allows for any issues to be identified and rectified early. Each of these stages and details of how testing will be implemented shall now be discussed.

3.3.1 Module testing

There are 4 main submodules in this system. Each of these submodules will now be broken down into their individual components and details of how they will be tested will be explained below.

Instrumentation subsystem

There are 2 different sensor types that will be used – water level sensors and flow rate sensors. Each of these will need to be thoroughly tested since their outputs are what drives the system in the control loops. It is vital that the correct values are measured by the sensor and this can be ensured by correctly calibrating the devices.

For the water level sensor, linearity cannot be assumed for the full operating range of the device. A calibration curve will need to be generated and the calibration process is as follows – firstly, the maximum and minimum output that the sensor will produce when it is being used in the tank needs to be recorded by varying the water level in the container from the minimum level (no water in the tank) up to the maximum level (where the water level begins to overflow into the saturation pipe). The level sensor will be mounted in a fixed position. The water level will then be varied across the operating range of the tank (from minimum water level to maximum water level) and outputs of the sensors will be recorded along with analogue readings of the same measurand. A graph will then be plotted of the sensor outputs and the corresponding analogue readings and the sensor readings will be adjusted accordingly by multiplying them by a suitable gain until they are within 5% of the analogue readings.

Having calibrated the level sensor, the flow rate sensor can then be calibrated. The water flowing through the flow sensor will be pumped by a motor whose output flow rate depends on the voltage across its terminals. Alternatively, should a combination of a pump and a valve be used to control the flow rate, then the pump will supply a constant flow rate to the system and the valve will be partially opened as needed to achieve different flow rates. To calibrate the flow sensor, the water level is made to lie within the linear region of the tank before the calibration begins. The water level will then be incremented or lowered by pumping water into the tank or out of the tank respectively. This will be done at a constant flow rate by applying constant voltage to the actuators. The height of the water will always be kept within the linear region of operation during this procedure. The change in height reported by the level sensor is recorded along with the time taken for the water level to change. Since this calibration is done in the linear region, the rate of change in volume of water in the tank (the flow rate) will simply be:

$$\text{flow rate} = \frac{\Delta V}{t} = \frac{\pi R^2 \Delta h}{t}$$

where R is the radius of the container in the linear region and Δh is the change in height as noted by the level sensor and t is the time taken for the water level to change. In addition to the readings obtained from the level

sensor, the output of the flow rate sensor is also recorded over the same period. A graph will then be plotted of the flow rate obtained from the flow sensor output and the flow rate determined using the level sensor readings. The output of the flow rate sensor will be adjusted accordingly should its readings not fall within 5% of the flow rate determined using the level sensor by multiplying the flow sensor values by an appropriate gain. To ensure that the change in height is due to the water flowing into the tank only, the outflow path of the tank will be closed when performing calibration for the flow rate sensor attached to the inflow pipe. Similarly, when the flow rate sensor on the outflow pipe is being calibrated, the inflow pipe will be closed so that no water comes into the system during the test. The sensor readings required will be processed in Python 3.8 to produce a .csv file that will be processed in Microsoft Excel 2018 to obtain the calibration curves.

Actuation subsystem

The actuators that will be used in this system will consist of pumps and/or valves. During the calibration of the flow rate sensor, different flow rates will be obtained by varying the voltage across the motor which directly influences the flow rate. Alternatively, by partially opening valves that are being fed by a constant flow rate from a pump, different flow rates can also be achieved. During the flow rate sensor calibration, the voltages applied to the pumps/valves will also be recorded. A graph will then be plotted which will have the voltage applied to the pump/valve on the x axis, and the flow rate that was obtained from the level sensors will be plotted on the y axis.

Microcontroller subsystem

The microcontroller will be responsible for collecting data and implementing controllers for the plant. However, it needs to sample the sensors fast enough and be used to digitally filter any measurement noise due to vibrations in the system. To pick an appropriate sampling rate for the microcontroller, the time it takes to fill up the tank from being empty with the pump working at maximum flow will be recorded. To allow the system to have adequate time to respond to this extreme condition, the microcontroller should be able to sample the sensors at least 50 times between the transition from the tank being empty to being full. The sampling frequency to be used will be the reciprocal of the time taken to fill up the tank, divided by 50.

Noise generated from mechanical vibrations of the motor will need to be filtered out. To design the digital filter and implement it, the cut-off frequency of the filter will need to be determined. By recording audio clips of when the motor is turned on, the spectrogram of the audio clip can then be obtained using the FFT function in MATLAB 2021b. Using the spectrogram, an appropriate cut-off frequency for the low pass filter will be determined and the digital implementation of that filter will be implemented on the microcontroller.

Tank subsystem

Saturation of the output is an essential dynamic property to have in the system. To test that this dynamic is included in the system, the calibrated water level sensor will be used to keep track of water level in the tank. Next, water will be continuously pumped into the tank and the water level recorded along with the total volume of water that has been pumped into the tank. If saturation is indeed present in the system, it is expected that the water level will increase up to a maximum value after which it will not increase any more despite an increase in water volume being fed into the tank.

3.3.2 System Integration testing

The system integration testing phase seeks to validate the component design. The components chosen to meet the functional requirements of the system need to exhibit the desired system dynamics such as the order of the system, dead-time and the other dynamics mentioned in section 1.2.2 of this report. Performing system

identification on the system will allow the model of the plant to be obtained, and this will give insight into the dynamics of the system. To perform system identification, each of the two tanks would need to be tested separately. For the first tank that is fed directly from the reservoir and feeds the second tank through a motor or valve, the tank will need to be divided into its linear and nonlinear regions of operation. For the nonlinear region, a transfer function cannot be obtained since it is nonlinear in nature - so the model for this section of the tanks will be derived from physical principles to form the governing differential equation rather than performing system identification through experimental analysis. The pipe resistance (k_v) is one quantity that will be required to form the governing equation of the system and that requires experimental analysis to quantify it. The equation linking the output flow rate of the first tank(Q_o) to the height of water in the first tank (h_1) is given as:

$$Q_o = k_v h_1$$

To measure the pipe resistance, the output flow rate and height of liquid in the tank need to be known for different corresponding values. To get these values, the water in both tank 1 and tank 2 will be put in the linear region of operation. The outflow rate will be measured by finding the rate of change of volume of liquid in the second tank – the same equation used to find the flow rate when calibrating the flow sensor in section 3.4.1 will be used to find the flow rate. The output of the second tank will be closed throughout this experiment to ensure that no water leaves the second tank. For every flow rate that is calculated, the height of liquid in the first tank will also be recorded using the level sensor. By plotting a curve of h_1 on the x axis and Q_o on the y axis, the gradient of that curve will be equal to the pipe resistance k_v . The calibrated flow rate sensor can also be used to calculate the output flow directly provided that the chosen flow sensor is sensitive enough. Should this be the case, the flow rate sensor will be used rather than the indirect method of finding flow rate through water level readings in the second tank.

For the linear region of the tank, the water level will be made to remain constant by matching the inflow rate with the outflow rate. Having obtained this state of equilibrium, the voltage across the terminals of the motor will then be stepped and the water level is expected to respond. The measurements of the water level in response to the step input is the step response of the system, and this experiment will be repeated with different step sizes and quantities such as the gain and time constant of the system will be averaged out across the different experimental results and an experimental model of the linear region of operation of the tank can then be obtained. By analysing the response of the system and comparing it to the expected output – which is a second order response with some dead time, the integration test of the system will be complete.

3.3.3 Acceptance test procedures

The V-model that is being used to design this system requires that the testing phase happens in parallel to each development phase. As such, there is a need to develop broad and testable criteria that confirm whether the user and technical requirements discussed earlier in this chapter have been met. However, acceptance testing is usually performed by the end user and as such, details of acceptance test procedures will be omitted from this report.

4. Design

4.1 System Design

The water level control system to be designed will consist of 2 tanks that are coupled through a pipe that flows from the outflow of the first tank into the inflow of the second tank. In between these two tanks, a valve or motor will be used to regulate the rate of flow from the first tank into the second tank. The piping and instrumentation diagram (P&ID) below shows the system and how it will be interconnected.

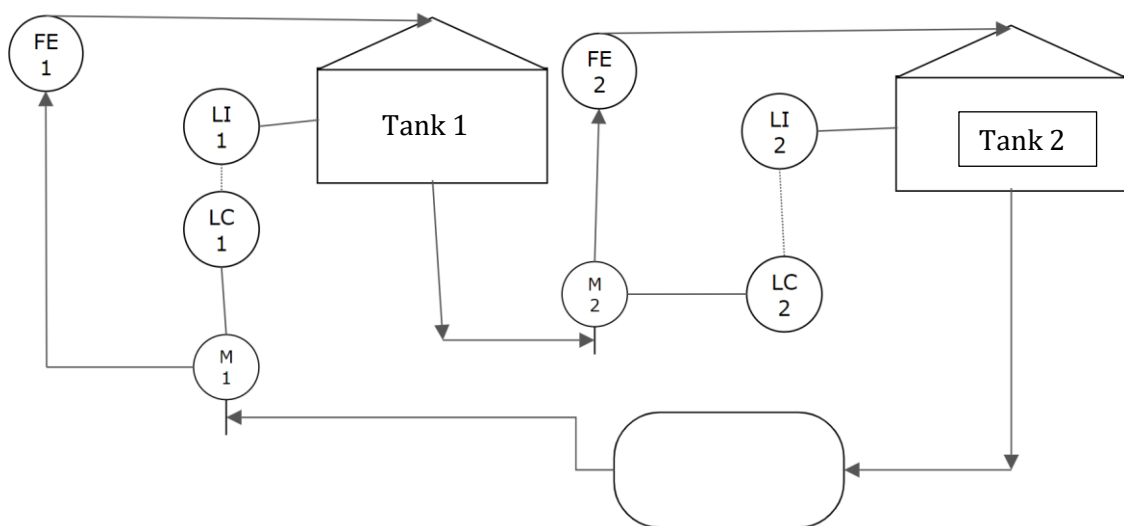


Figure 4.1 Piping and instrumentation diagram of the system

The reasons why certain components were chosen over others to implement the system shown in the figure will be explained in chapter 4.2 which deals with hardware design. The P&ID diagram is great at showing how different components are connected in the system, but it does not offer a visual representation of what the prototype will look like. To alleviate this, SOLIDWORKS models of the system were made with the assistance of a colleague - Koshesai Khosa, to create the following computer aided design (CAD) system models.

4.1.1 Model 1

Figure 4.2 shows the first CAD iteration of the system

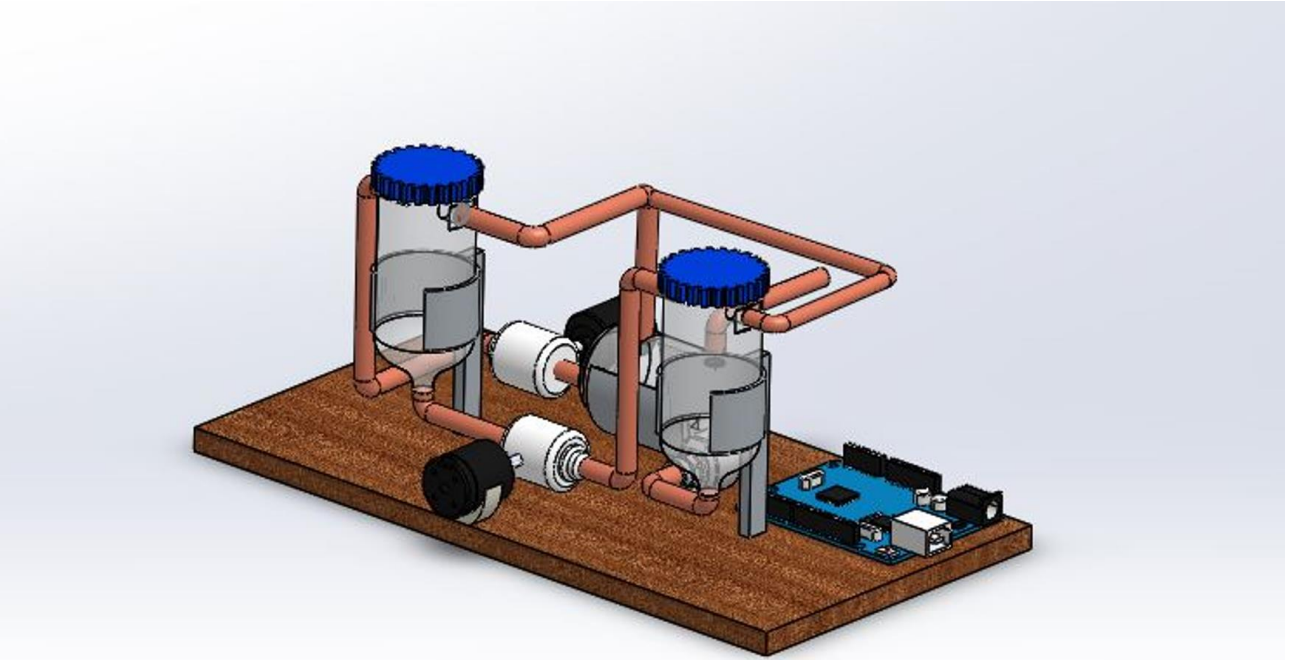


Figure 4.2 First iteration of the CAD design.

Should this design be chosen for prototyping, the left most tank would be elevated higher than the second tank to allow for water to flow from that tank into the tank on the right without providing actuation to the motor or normally open valve that connects the two tanks. The level sensors will be mounted on the blue lids and they will be connected to the microcontroller along with the other sensors and actuators in the system.

4.1.2 Model 2

Figure 4.3 shows the second CAD iteration of the system.

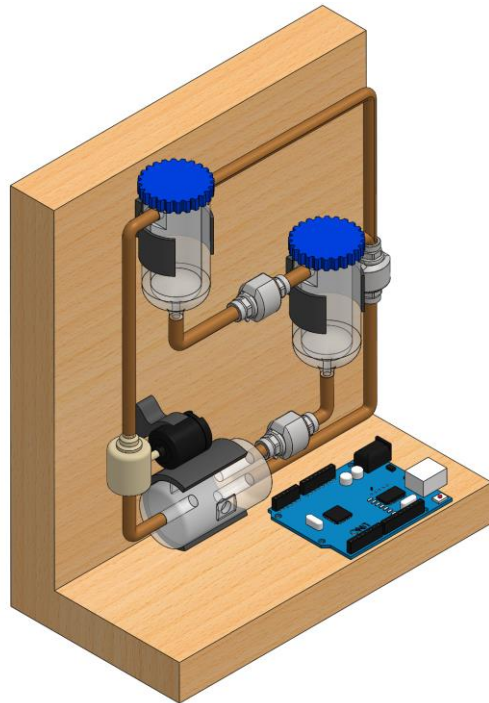


Figure 4.3 Second iteration of the system with improvements made

This design is ready to prototype as it appears in the figure and the placement of pipes and sensors will be done according to the spatial constraints on the prototypes frame.

The second design was chosen over the first design because there is greater flexibility of where to place components should the need arise. Pipes, motors, and sensors can be moved to the back of the frame if certain components are bigger than the system was designed for, and everything will not fit in the front.

4.2 Hardware Design

This section of the report will delve into the justifications behind choosing hardware components to meet the set of technical requirements. Details of key considerations will also be given along with details of the final device that was chosen.

4.2.1 Microcontroller

Due to the size constraint of the system, a microcontroller was chosen as the best way to handle the data acquisition as well as control of the system whilst keeping the cost of the system low. Nevertheless, the device will still need to be programmed on a computer to access the data but once programmed, it can perform control operations as a standalone unit – if it is powered. The microcontroller selection was based on the need to meet the following requirements:

1. Light weight
2. Low cost
3. Hardware interfacing capabilities with actuators, flow sensors and level sensors
4. Ease of integration with software tools for data display

In addition to the above, controllers will also be implemented on the microcontroller. Since the system will include a delay and a Pade approximation will be used to characterise that delay in the transfer function, it is important that the system samples the output values fast enough since the Pade approximation becomes less accurate the lower the sampling rate.

With these requirements in mind, the Arduino Mega 2560 and the Raspberry Pi Zero W met the criteria. The Arduino Mega 2560 was chosen over the Raspberry Pi for the following reasons:

1. The Arduino Mega 2560 was R110 cheaper than the Raspberry Pi Zero W.
2. The Arduino Mega has analogue input pins which makes it compatible with more sensors compared to the Raspberry Pi.
3. Individual I/O pins on the Arduino can drive more current (150mA) compared to the Raspberry Pi which can output a maximum of 50mA. The Arduino can therefore be used to drive power hungry components that may be used in the system.

The Raspberry Pi has its own advantages over the Arduino such as its smaller footprint and it uses Python as a programming language unlike the Arduino which uses C++. The advantage of using Python over C++ and many other programming languages is to do with code readability and ease of learning the language as was mentioned in the literature review. Nevertheless, C++ is also open source just like Python and a plethora of resources are available on the internet to learn the language. The Arduino can also be programmed in Python using Pyfirmata [24].

4.2.2 Flow rate sensor

The flow rate sensor offers a way to measure liquid level in the tank if it is calibrated accurately. The flow sensor selection was based on the need to meet the following requirements:

1. Low cost
2. Interface capability with the chosen microcontroller
3. Portability

The YF-S201 and the Adafruit 5066 flow rate sensors were identified as meeting the above requirements. Although the Adafruit sensor offered better precision – especially at low flow rates for roughly the same cost as the other sensor, the YF-S201 was chosen because of the project time constraints. The lead time of 2 weeks would have jeopardised the project timeline and the YF-S201 was already in stock at the University of Cape Town and careful calibration would improve its accuracy at low flow rates.

4.2.3 Level sensor

The water level is the output of the system and it will dictate the control actions taken by the controller. The water level sensor needs to meet the following requirements:

1. Provide continuous readings of water level in both the linear and nonlinear region of the tank.
2. The sensor should be able to provide readings at the sampling rate of the system or higher in order to obtain real time readings.
3. The sensor should be compact enough to be fixed on the tank lid.
4. The sensor should be low cost.

Two sensors were identified as being potentially compatible with the system – the HC-SR04 Ultrasonic sensor and the VL53L0X Time-of-Flight (ToF) sensor. Although the ultrasonic sensor is cheaper and provides a longer range to obtain readings, the cone shape of the bottom half of the tank could be problematic because the 30-degree wide beam angle produced by the ultrasonic transducer may get reflected by the walls of the conic region of the tank and get reflected to the detector and thus give incorrect readings. The ToF sensor on the other hand, uses a narrow laser beam and this can be placed directly above the narrowest portion of the conic tank region resulting in accurate level readings for the full length of the tank. The ToF sensor has a beam width of 25 degrees, and this would potentially work better for this application. As a result of this difference in beam widths, the ToF sensor was chosen over the cheaper ultrasonic sensor.

4.2.4 Actuators (Pumps/Valves)

Actuators will be needed to transport water between the tanks in the system. Ideally, a single pump will be needed to fill up the left most tank shown in model 2 (section 4.1.2) and a valve would be used to regulate flow from the pump filled tank into the second tank. The actuators in the system need to be able to provide the following functionality:

1. Variable flow capability
2. Compact and low cost
3. Integration capabilities with the microcontroller
4. Good energy efficiency

Of all the valve types that were discussed in the literature review, only the solenoid valve was available at local component suppliers and would integrate easily with the microcontroller. However, this BMT G1/2IN water flow solenoid requires at least 0.02 MPa to operate which translates to 2.04m of water being required to operate such a valve. This is impractical and leads to the system requiring a substantially larger tank than necessary to

allow the valve to operate. It was therefore decided to use a pump between the first tank and the reservoir tank, as well as between the first and second tank.

There were a variety of pumps that could meet the requirements and were available at local electronics suppliers. These pumps fell into two main categories – non-submersible diaphragm pumps and submersible DC motor pumps. The submersible DC motor pump was not considered for use in this project due to the electromagnetic interference they are known to cause – especially the low-cost ones since they typically do not involve complex noise filtering equipment. Although this interference can be minimised using a capacitor across the leads of the motor, it cannot be eliminated, and this will likely lead to inaccurate readings from the flow sensor since it operates based on the Hall effect. The non-submersible motor pumps that were available were all diaphragm pumps and these are much less noisy and do not have their electromagnetic interference amplified by the water since they do not sit inside the water reservoir. Two pumps from different manufacturers with different characteristics were chosen mainly because of their ability to meet the component functional requirements and because they were the most affordable option. The key specifications of the pumps chosen are summarised in the table below

	Pump 1	Pump 2 (for tank 1 to tank 2)
Operating voltage	6V-12V	4V-12V
Current draw	0.5A-0.7A	0.8A
Other important features	Positive displacement pump	Centrifugal pump

Table 4-1 Summary of key motor specifications

The pumps can work up to a maximum of 12V and yet the microcontroller can provide only a maximum of 5V. The Arduino comes with multiple add on attachments that can be connected to pins on top of the board to achieve a certain function. One such add-on is the FundoMoto L298 Motor driver board which allows for speed control of the pumps through pulse width modulation (which in turn determines the flow rate). This motor driver circuit is a plug and play device, and no additional circuitry needs to be designed to integrate with the motors. In addition, the motor driver includes a buzzer which can be used to audibly alert the user when the system is in operation.

From the power requirements of the motors, an external power supply that can supply a maximum of 12V and 1.5A needs to be designed. The L298 motor driver features connection ports to connect an external power supply and this will be able to handle the switching on and off of power to the motors as required. To provide the necessary power, using a 12V rechargeable battery was considered as well as purchasing a generic power supply that can supply at least 12V and 1.5A and then adapting it as needed for the project. However, high capacity 12V batteries will be needed and these are typically bulky. Furthermore, the voltage characteristics of batteries change as the state of charge on the battery decreases and this could cause model changes which would unnecessarily complicate the controller design. It is for this reason that a generic 12V, 2A switching power supply was used and it was obtained from Takealot. The end connector will be cut off to reveal the cables inside which will then be connected to the motor driver

4.2.5 Water tank

The water tanks in which level control will be done are important to the system and their shape is crucial to making sure the desired system dynamics are present. The tank needs to exhibit the following characteristics:

1. Both linear and non-linear regions.
2. Water level should not increase beyond a predefined point to protect the level sensors from water damage and for saturation.
3. The tank should be compact and made from lightweight material.

Due to the custom shape needed for the tanks, it was better to 3D print the tanks since no off the shelf alternative that met the compact and light weight criteria was available. 2 tank designs were made in SOLIDWORKS and their dimensions are summarised in table 4-2.

	Design 1	Design 2
Diameter at the top	9cm	9cm
Diameter at the bottom (outflow diameter)	1.27cm	1.27cm
Length of linear region	10cm	7cm
Length of nonlinear region	4cm	7cm
Total length	14cm	14cm
Inflow diameter	0.6cm	0.6cm
Saturation pipe diameter	3cm	3cm

Table 4-2 Tank dimensions in the different CAD designs

Note that the saturation pipe diameter is larger than the inflow diameter. This was a deliberate design choice made to ensure that the tank can release water quicker than it comes in through the inflow pipe if saturation occurs. Each of these tank designs shall now be discussed in turn along with visual representations of each of the tanks.

Design 1

This design features a hemisphere bottom along with connectors for the inflow, outflow, as well as saturation pipes. The 3-dimensional view of the tank designed in SOLIDWORKS is shown in figure 4.4.

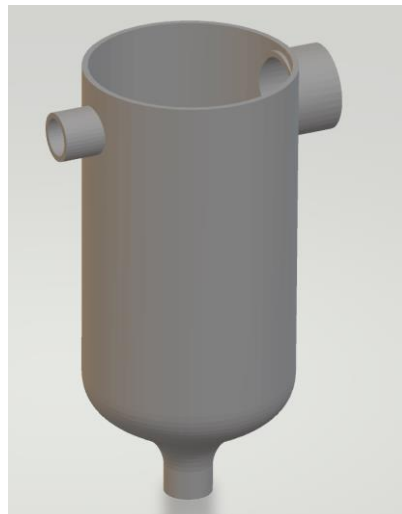


Figure 4.4 Hemisphere bottom shaped tank for the first tank design

Although this design would be optimal, the Prusa Mini 3D printers available at the University of Cape Town would take approximately 13 hours to print the above design and the hemisphere region was too steep to 3D print without a tremendous amount of support material being required to 3D print the tank.

Design 2

To improve on the short comings of the above design, it was decided to make the base cone shaped rather than hemisphere shaped in the hopes of reducing wasting printing filament on generating support material. Furthermore, the protrusions at the top of the tank were also removed for the same reason. Figure 4.5 shows the second iteration of the design. It was also generated using SOLIDWORKS.

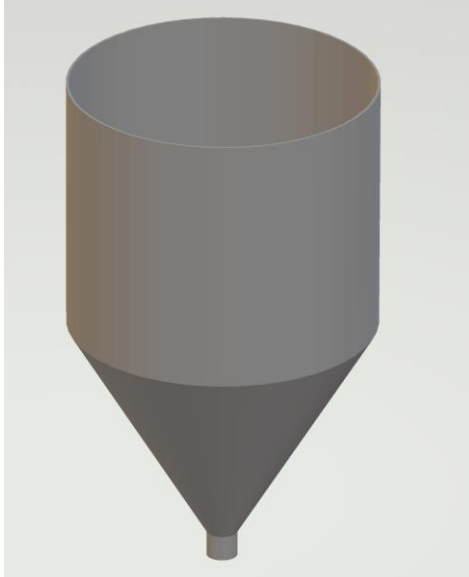


Figure 4.5 Cone bottom tank for the second design

The above design takes 9 hours to print on the Prusa Mini 3D printer compared to the first designs 13-hour print time. However, manual modifications will need to be made to the tanks to include inflow and saturation paths.

Reservoir Design

Design 1 will hold more liquid volume than the design 2 tank. The total volume of the design 1 tank ignoring the existence of the saturation outflow pipe is given by the following expression:

$$\begin{aligned} \text{Total Volume} &= \text{Volume of hemisphere} + \text{volume of cylinder} \\ V &= \frac{2}{3}\pi r^3 + \pi r^2 h \end{aligned}$$

In the above equation, r is the radius of the cylindrical region – which also happens to be the radius of the hemisphere. Although this hemisphere is not precisely a hemisphere, it can be approximated as such, and this leads to an overestimate of the volume which results in the reservoir having more water than the system needs – this is in no way detrimental to the system and the approximation is therefore justified. Using the above equation, the volume of the tank 1 design is 827cm^3 . With two tanks, it means the reservoir needs to have a volume of at least 1654cm^3 or 1.654 litres.

The figure 4.6 shows the 3-dimensional view of the storage tank. It was designed in SOLIDWORKS with the aim of 3D printing it.

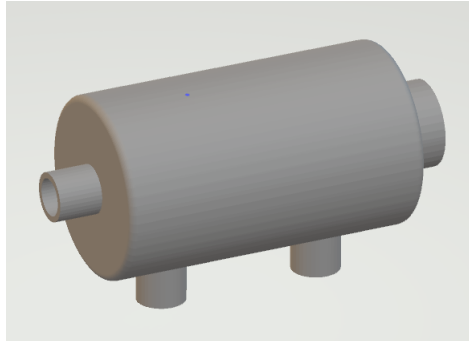


Figure 4.6 Reservoir tank design with multiple inlet and outlet pipes

The tank has a radius of 7cm and a length of 11cm and a volume of 1693cm^3 - this is more than enough for the system.

4.3 Software Design

The data being produced by the sensors needs to be processed by the microcontroller first before it is useful. The details of how each hardware component was interfaced with the microcontroller through software shall now be discussed below. This section mainly deals with algorithms that will be implemented in code. To access the code that implements these algorithms, please refer to the code in the GitHub repository linked in the appendix.

4.3.1 Flow rate sensor

The flow rate sensor chosen produces 4.5 pulses for every litre of water that flows through it. To detect flow rate, an interrupt needs to be set up on one of the Arduino's GPIO pins that have interrupt capabilities. The flow chart in figure 4.7 illustrates how the algorithm for calculating flow rate will be implemented in the Arduino.

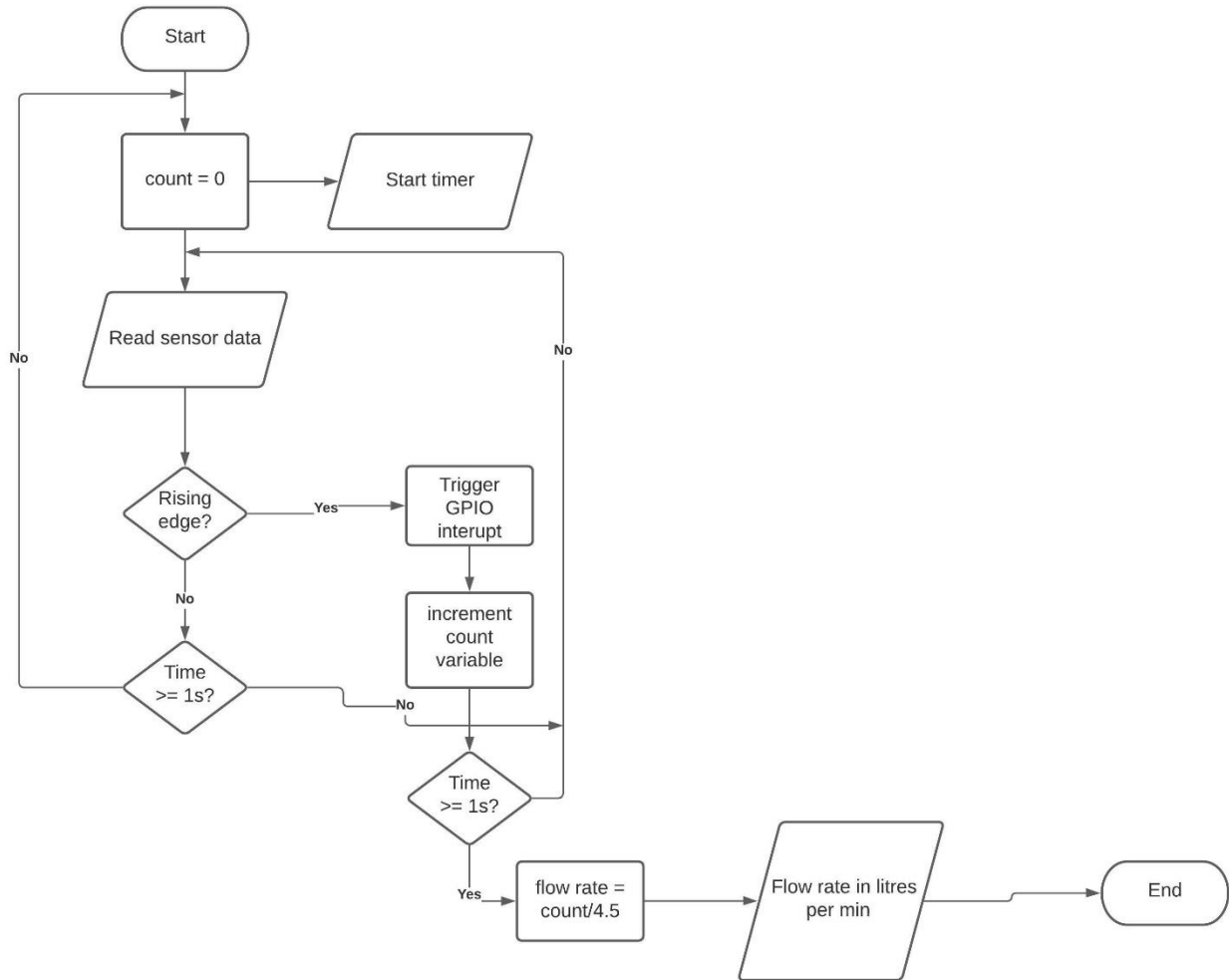


Figure 4.7 Flow chart for reading and processing flow sensor readings

4.3.2 Level sensor

The level sensor is an I²C smart sensor. Since two level sensors will be used, the sensors need to have different addresses to read from them at the same time. The flow chart in figure 4.8 shows how these sensors will be initialised as well as read from.

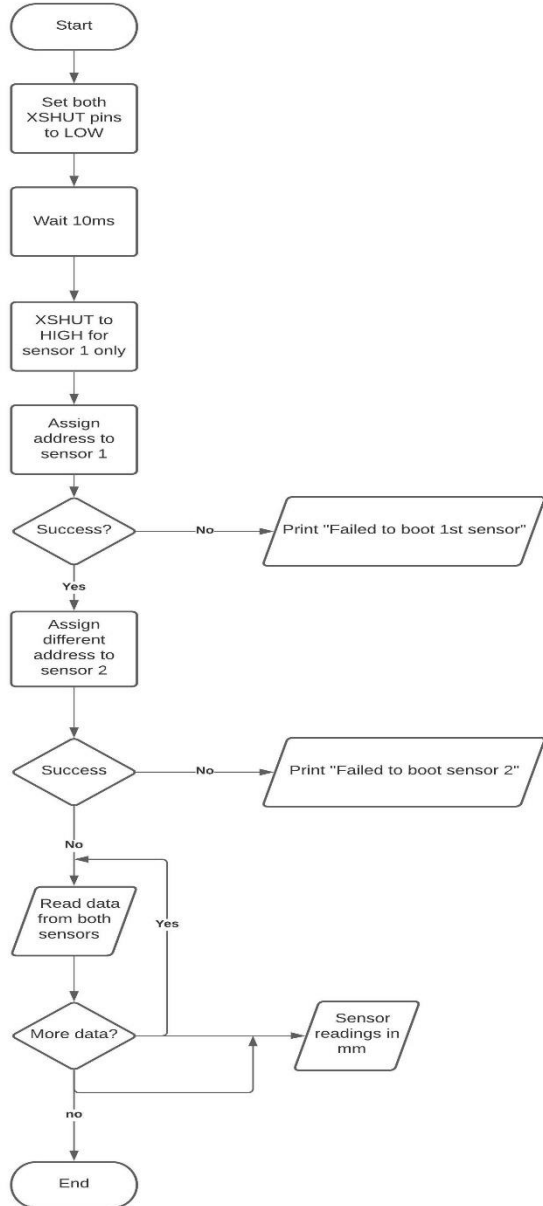


Figure 4.8 Flow chart for successfully using two I2C VL53L0X level sensors

There is a library that is pre-made for use with the VL53L0X sensor. This library can be accessed through the Arduino library manager and it is authored by Adafruit. The library name is ‘Adafruit_VL53L0X’ and version 1.1.1 of that library was used and modified for the purposes of this project.

4.3.3 Software Packages

The Arduino was programmed in C++. To generate the graphs used in the results section, Microsoft Excel 2018 using pre-processed data that was captured from the serial data output of the Arduino will be used. For controller implementation and certain component tests, this will be done in Simulink in MATLAB 2021b with the Arduino Support Package version 20.0.2.

The Arduino was programmed using Arduino IDE version 1.8.16. This was run on an HP Spectre with a Core i7 8th generation CPU with 8GB of RAM.

4.4 Implementation

This section of the report details how the system prototype was built.

4.4.1 Laboratory rig

To achieve a stable frame that is also resistant to water, the second design discussed in section 4.1.2 was modified to be made from aluminium. This required rethinking how the L shape of the design could be achieved. Figure 4.9 shows the dimensions of the final prototype design

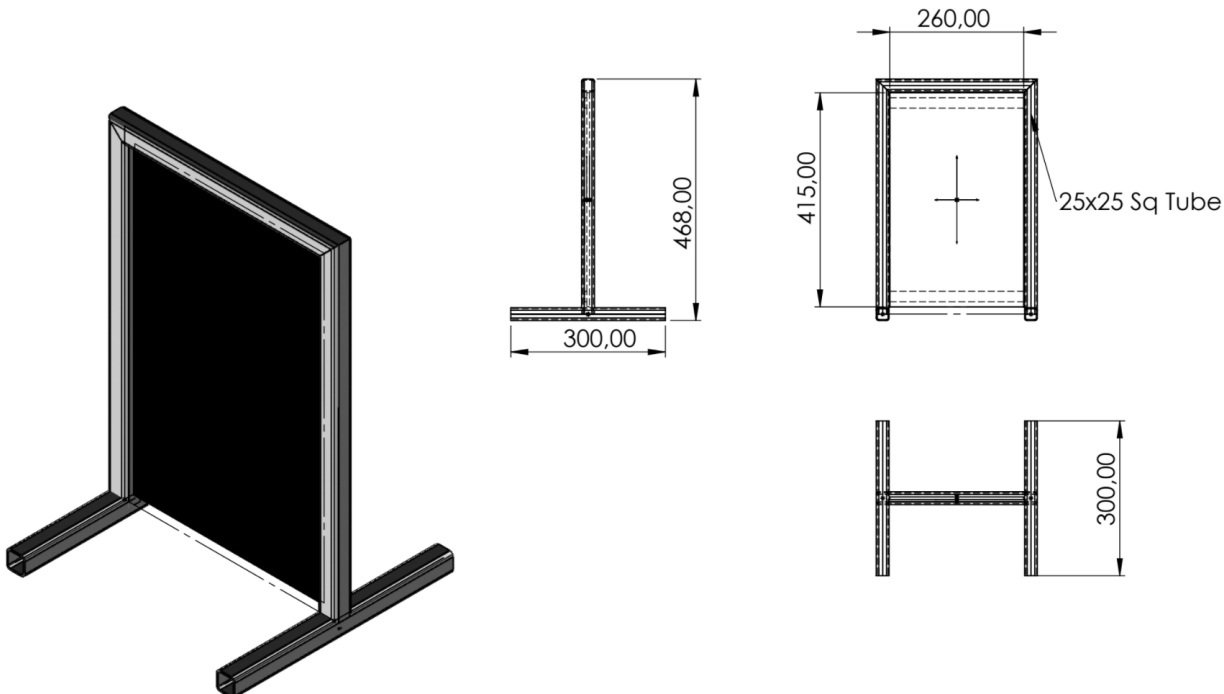


Figure 4.9 CAD design of the final laboratory rig to be prototyped aswell as the dimensions in mm

As can be seen from the dimensions of the rig, the system is quite compact. Welding of the frame according to the above specifications was done with the help of Nwabisa Mtyhulubi in the Department of Mechanical Engineering at UCT. However, 3D printing of the tanks discussed in section 4.2.5 was not done due to the unavailability of the 3D printers which would have added an extra 2 week waiting period to the project timeline. This could not have been done since prototyping was on the critical path and any delays would have jeopardised the project. To make the tanks, a 9cm diameter, 500ml cylinder container was attached to a cone shaped rain gauge that was cut at a height with roughly the same diameter as the cylinder. The two were joined by first sanding the sides of the containers that would need to be joined to ensure better adhesion and then the two were bonded together using a waterproof epoxy adhesive. The joint was also sealed using a silicone sealant to ensure the tank was leak proof. Due to the 3D printing setback having occurred after the laboratory rig frame was already constructed according to the above figures' dimensions, component placing on the rig had to also be changed to ensure they were protected from any water damage should any of the adhesives that held the tanks together failed. Components were therefore placed at the back panel of the laboratory rig and a Coca Cola bottle with holes made for the pipes that take water in and out of the system was stuck onto the feet of the frame - this will be used as the water reservoir in the system.

The cylindrical container had a lid and a hole was made directly above the outflow hole of the make-shift tank that was constructed. This hole was made big enough for the time-of-flight sensors transmitter and receiver to have unimpeded 'view' of the tank. Inflow, outflow, and saturation connectors for the tank were made from sawed pipe connectors that were glued in place after melting off the plastic on the tank using a soldering iron. The full implementation is shown in figures 4.10 and 4.11.

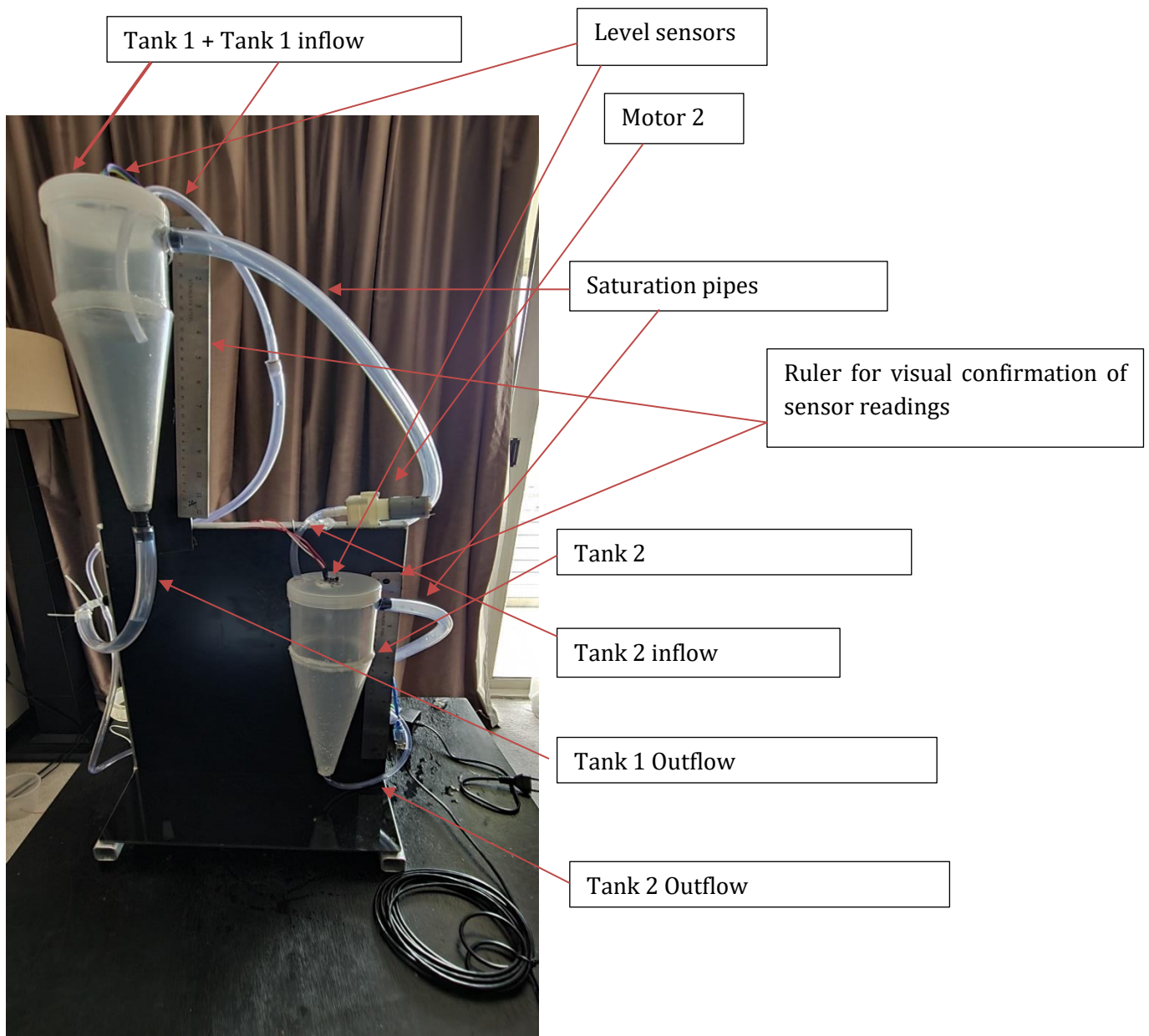


Figure 4.10 Practical implementation of the designed system (front view)

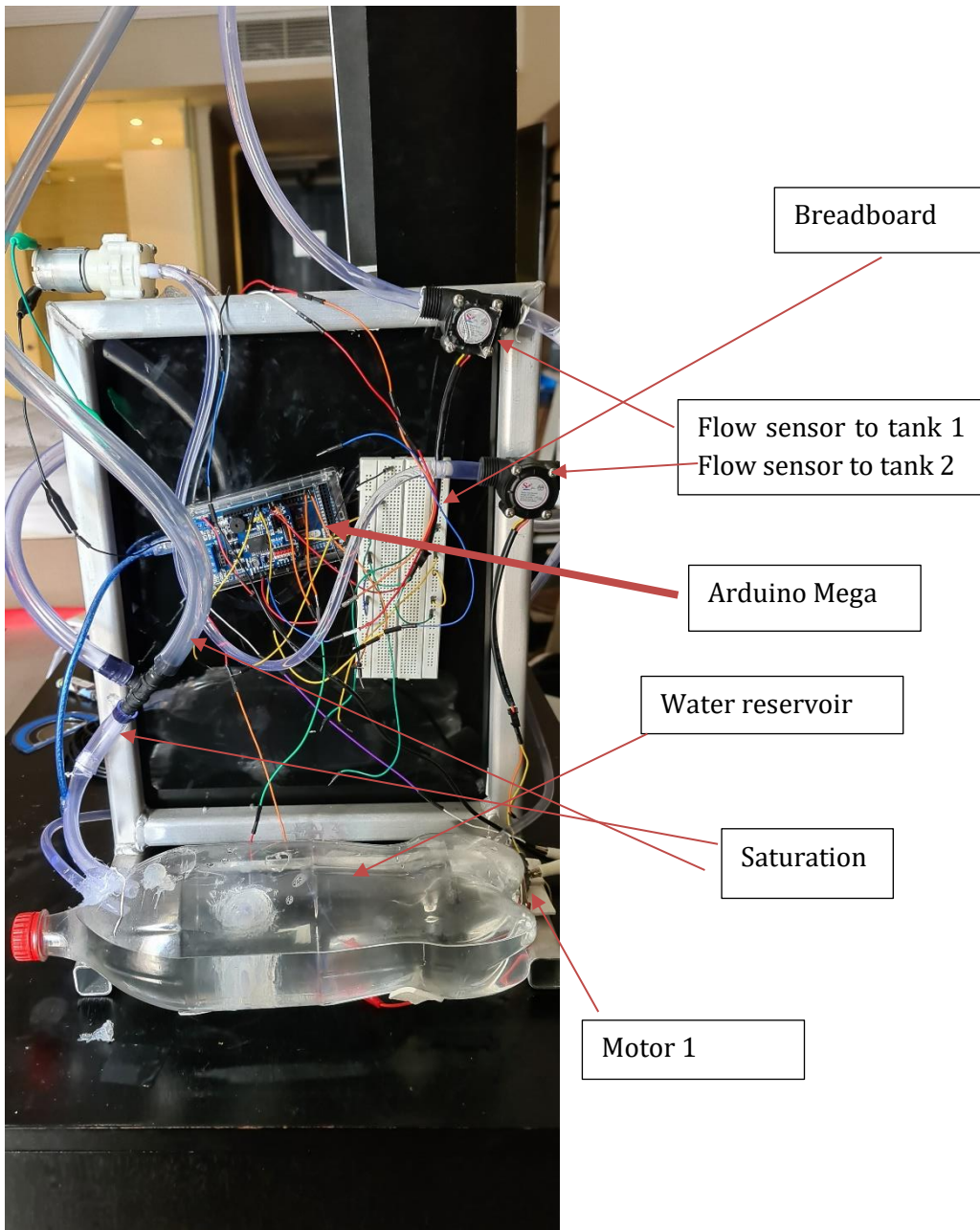


Figure 4.11 Practical implementation of the designed system (back view)

Most of the electronic components were placed at the back of the laboratory rig to ensure that if any failure were to happen and tanks were to leak, the electronics would not be water damaged.

4.4.2 Hardware integration

The practical implementation pictures show how the system is built but the connections of different sensors with the microcontroller are not obvious from the pictures. The fritzing diagram in figure 4.12 illustrates how the sensors and actuators were connected to the breadboard and the microcontroller in a visual manner than is more practical to work with compared to a schematic.

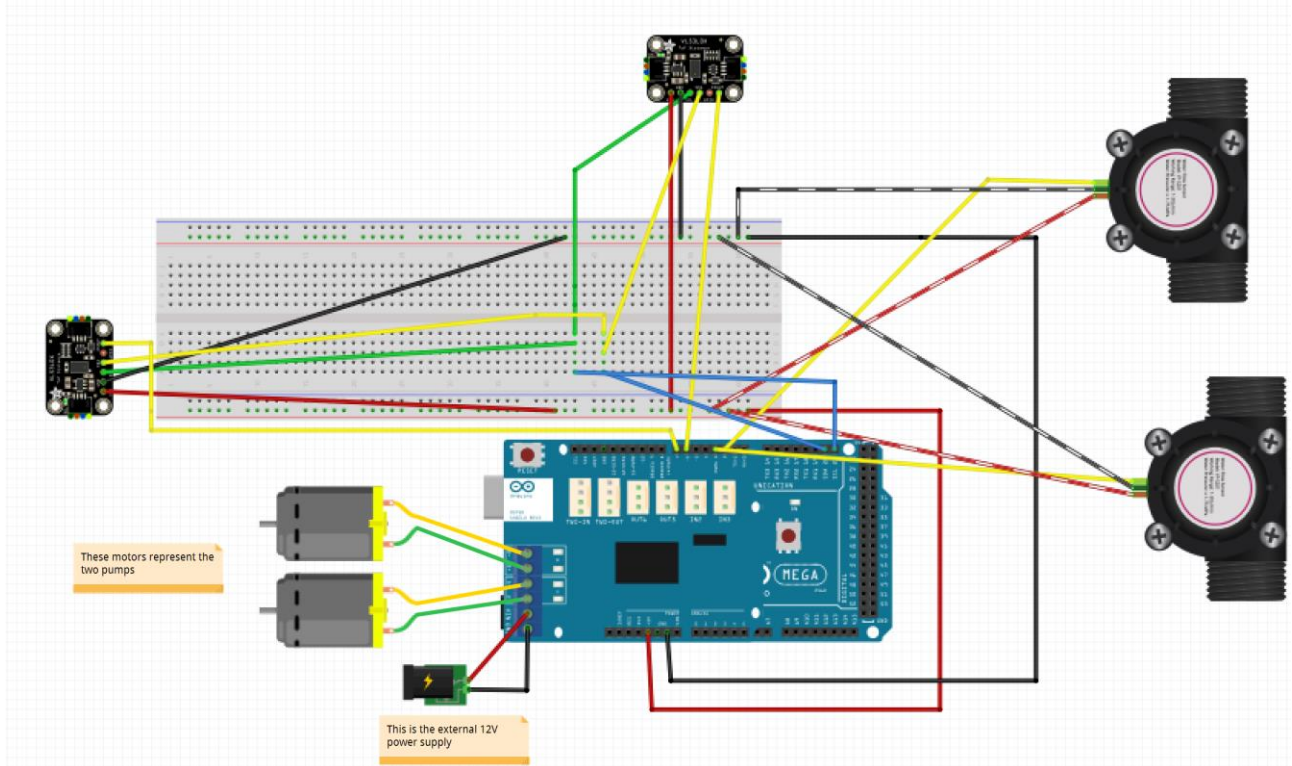


Figure 4.12 Fritzing diagram of the hardware illustrating how it is integrated

In addition to figure 4.12, a schematic of the system is illustrated in figure 4.13.

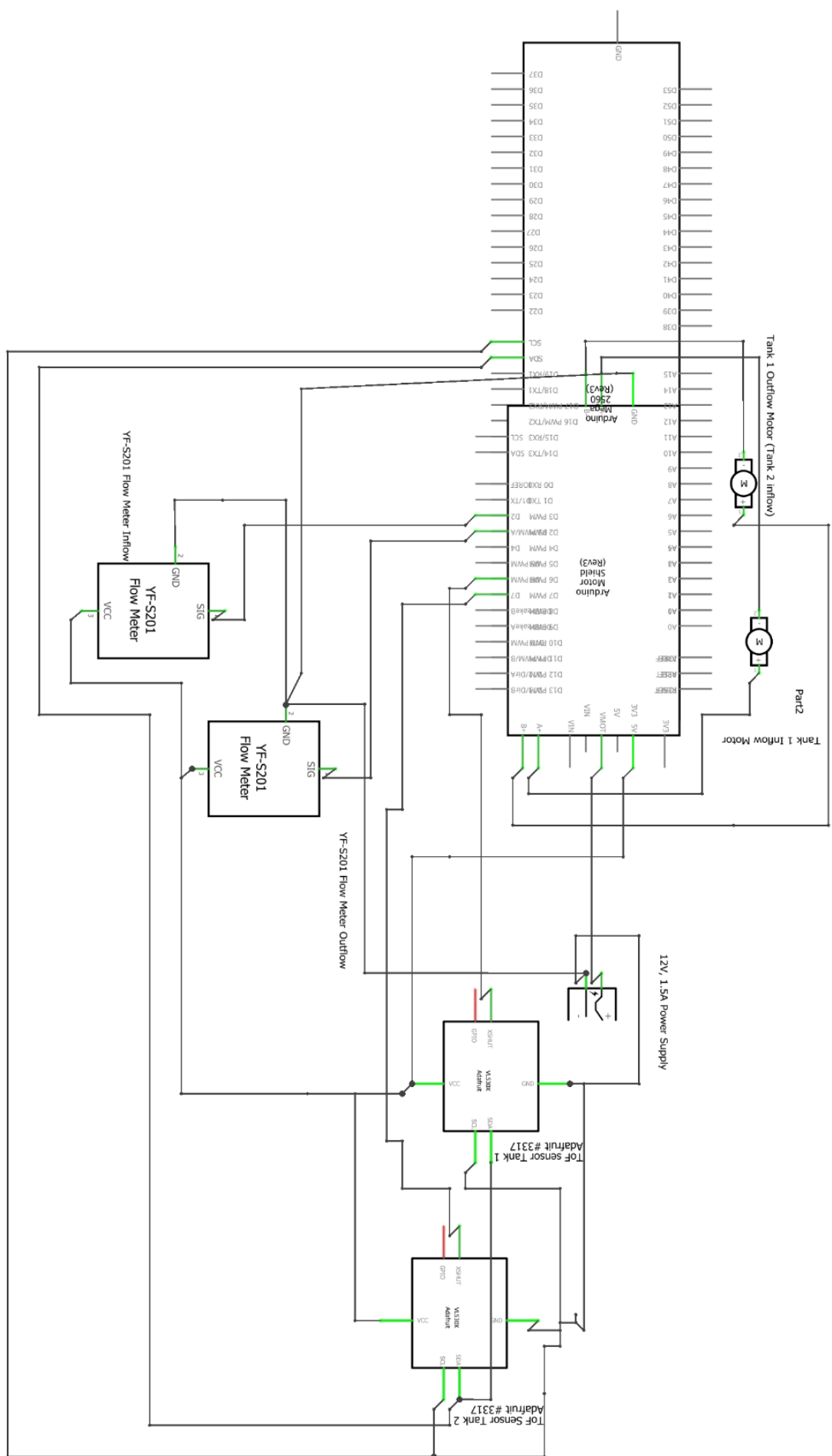


Figure 4.13 Schematic of the hardware showing connection points.

4.4.3 Bill of materials

The bill of materials is shown in table 4-3.

Component	Cost
2 x Tanks (rain gauge + cylindrical container)	R120.00
2 x VL53LOX	R448.80
2 x YSF201	R147.82
Arduino Mega 2560	R276.00
L289P Motor Driver Shield	R178.45
Motor 1 (BMT Mini Water/Air pump)	R85.00
Motor 2 (HKD Mini Reversb water pump)	R82.61
2 x Ruler	R74.00
Aluminium frame	R829.90
12.7mm tubing(1 meter)	R16.00
6mm tubing (1 meter)	R45.00
PTFE Tape	R10.00
Jumper cables	R57.99
Crocodile clips	R82.14
Double sided tape	R40.00
Epoxy Adhesive	R55.00
Silicone sealant	R75.00
USB Extension	R59.00
12V Switching Power supply	R145.00
TOTAL	R2 823

Table 4-3 Bill of materials for the laboratory rig prototype

The total cost of the system was below the R5 000 budget that was allocated to this project.

5. Results and Data Analysis

The results of performing the testing procedures described in section 3.4.1 will be presented in this section of the report. In addition, controllers that were designed to demonstrate the controllability of the system were also implemented and the results of that will be presented in this chapter. A complete set of the data that was generated during the testing and controller implementation stages can be found in the GitHub repository whose link is provided in the appendix.

5.1 Level sensor calibration

Following the level sensor calibration steps laid out in chapter 3.4.1, the results obtained for the level sensor calibration are presented here.

5.1.1 Tank 1 level sensor

Figure 5.1 shows the results of the level sensor calibration in the first tank.

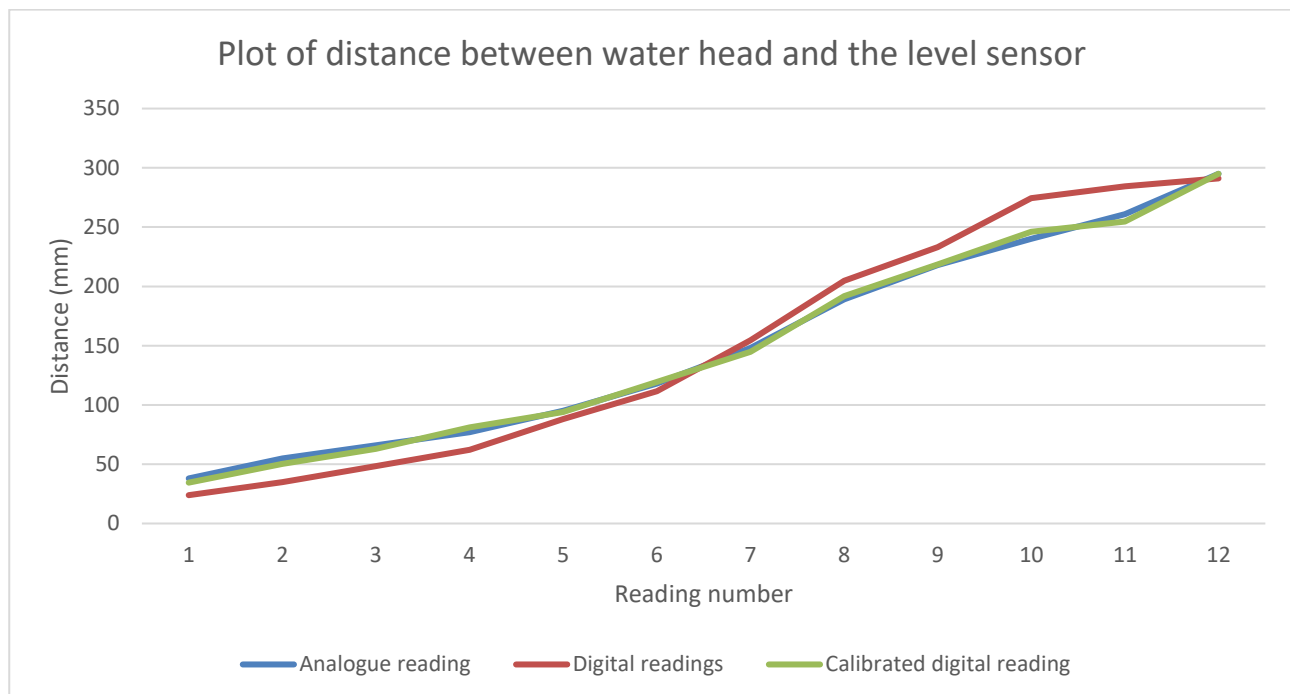


Figure 5.1 Calibration of the level sensor in tank 1 using analogue readings from a meter rule.

As evident in the above graph, the digital readings did not follow a linear path as the water level was changed. The digital readings were much lower than the measured analogue values and this trend seemed to reverse at 125mm, which is in the conic region on the tank. It appears the narrowing of the tank affected readings since the digital readings became much larger than the analogue readings even though the experimental set up was the same and the only difference was the region of operation in the tank. Gains were calculated to make the digital readings be within 5% of the analogue readings. These gains were found by averaging the gains in regions where the digital readings follow a straight line. The gains that were calculated and the regions in which they apply are shown in table 5-1.

Distance range	Gain
60mm to 80mm	1.30
80mm to 120mm	1.07
120mm to 240mm	0.937
240mm to 260mm	0.90
260mm to 290mm	0.97

Table 5-1 Calibration gains for the level sensor over different regions

5.1.2 Tank 2 level sensor

Figure 5.2 shows the level sensor calibration results for the sensor in tank 2.

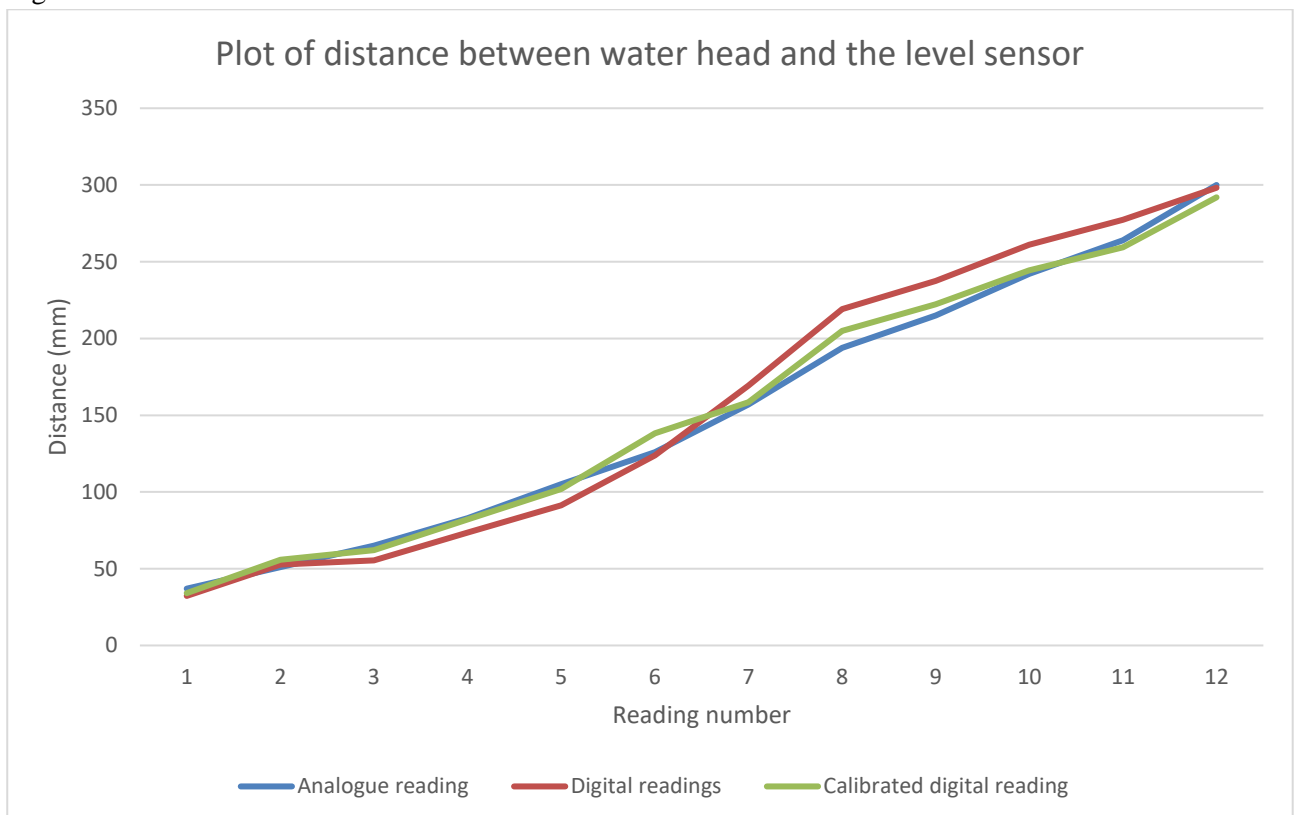


Figure 5.2 Calibration of the level sensor in tank 2 using analogue readings from a meter rule.

The same trend that was noted when calibrating the first level sensor was evident when calibrating the sensor for the second tank – sensor readings followed a different linear path in the different tank regions. The same procedure was used for calibration of the second level sensor and the gains used for this purpose are shown in table 5-2.

Distance range	Gain
30mm to 60mm	1.06
60mm to 130mm	1.12
130mm to 270mm	0.936
270mm to 300mm	0.979

Table 5-2 Calibration gains for the level sensor in tank 2 over different regions

The minimum measurable distance the sensors were calibrated for was different because the tanks have different dimensions and their saturation levels are also different.

5.2 Flow sensor calibration

Having calibrated the level sensors, it was now possible to also calibrate the flow sensor given that the rate of change in volume in the tank can be used as a benchmark to which the flow sensor could be calibrated to. The results of the flow sensor calibration tests will now be presented.

5.2.1 Input flow rate sensor

Figure 5.3 shows the results of calibrating the input flow rate sensor.

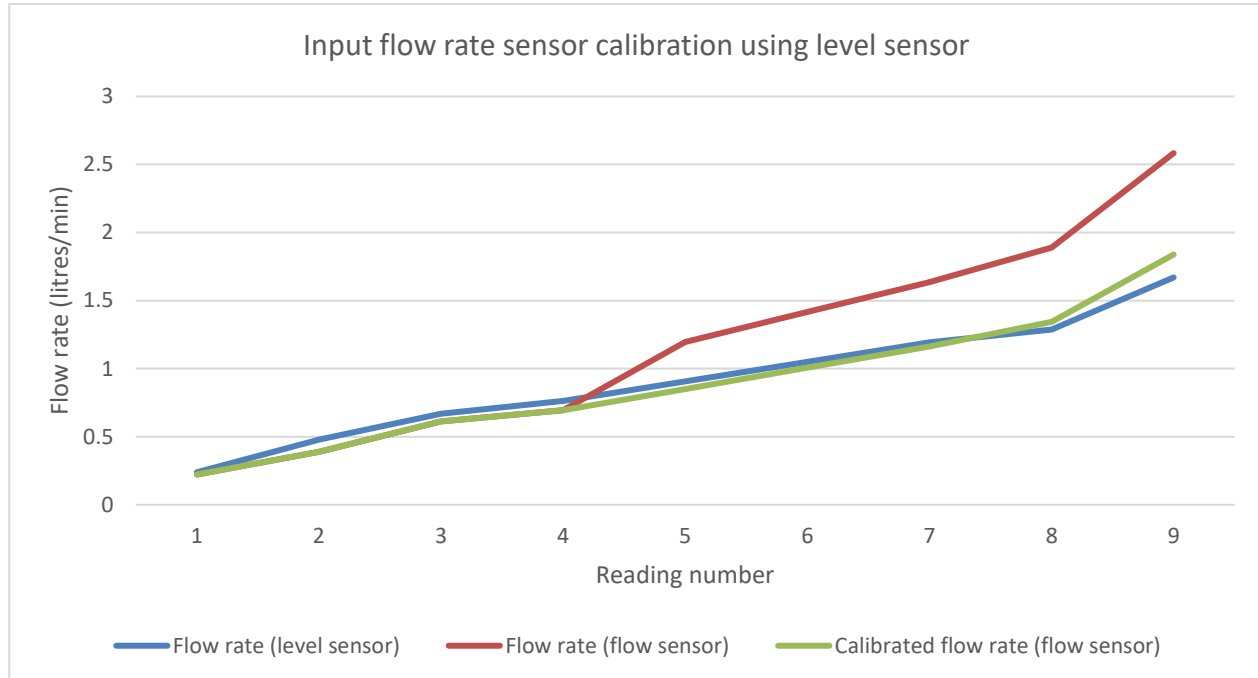


Figure 5.3 Calibration curve for the flow rate sensor on the inflow of tank 1

As can be seen from the figure above, the flow rate sensor readings and the flow rate obtained from the level sensor readings were within 5% of each other up until the flow rate became larger than 0.7 litres per minute. Both graphs were linear so a gain can be used to scale the readings from the flow sensor. The gain between flow sensor readings and flow rates calculated using the flow rate sensor was averaged out for all readings between the 4th to the 9th reading. This gain that needs to be applied to the flow rate sensor readings was calculated to be 0.71 and it put the calibrated flow rate readings within the 5% tolerance range.

5.2.2 Output flow rate sensor

Figure 5.4 shows the results of calibrating the output flow rate sensor.

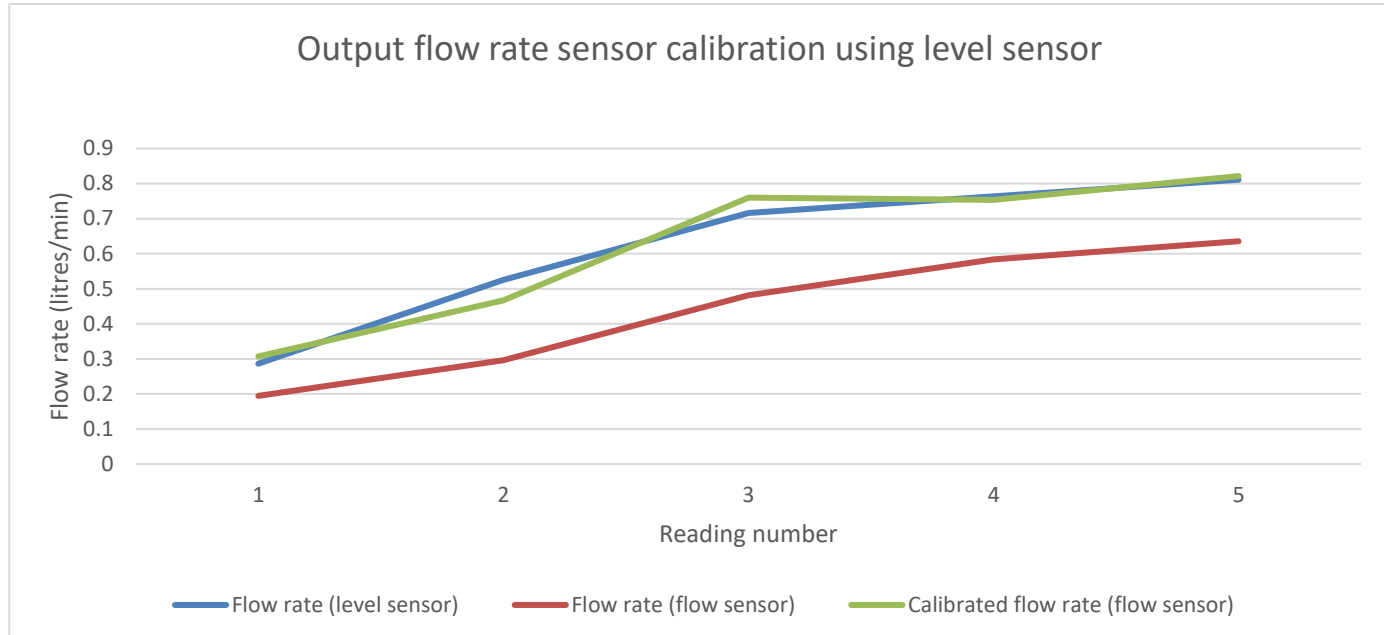


Figure 5.4 Calibration of the flow sensor on the outflow of tank 1 which is the inflow of tank 2

As can be seen from the figure, the output flow sensor appears to be underestimating the fluid flow rate. The flow rate sensor being calibrated is known to be more accurate at higher flow rates, but because all readings were less than 1 litre per minute, it appears the flow rate sensor was under reporting the flow rate. Fortunately, both curves (flow rate from the level sensor and flow rate from the flow rate sensor) were linear so a gain can be applied to scale the flow sensor readings until they agree with the level sensor readings which are presumed to be more accurate. Table 5-3 summarises the gains that led to the calibrated flow rate curve which is within 5% of the more accurate readings provided by the level sensor.

Flow rate sensor range (litres/min)	Gain
0.25 to 0.70	1.58
0.70 to 0.85	1.29

Table 5-3 Calibration gains for the flow sensor over different flow rates

The dependency of this calibration on the level sensors precision could have caused inaccurate calibration for both sensors. However, both sensors will now be in agreement when being used to measure flow rate.

5.3 Motor testing

The motors were supposed to exhibit dead-zone characteristics. Figures 5.5 and 5.6 illustrate the results of testing both motors in the system.

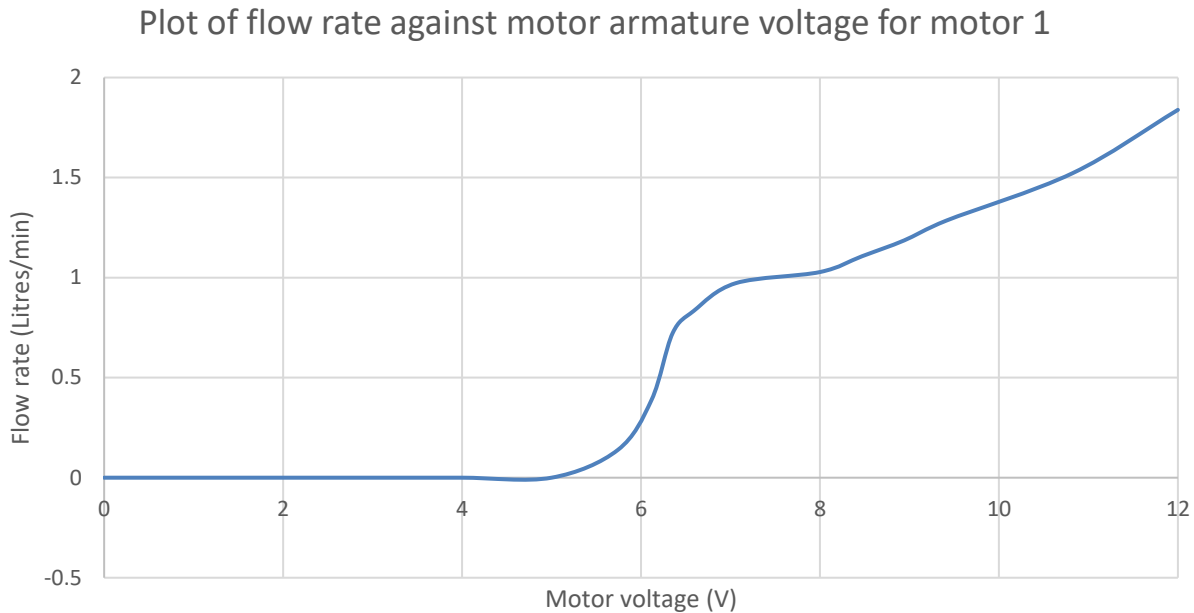


Figure 5.5 Plot of measured fluid flow rate for different armature voltage values on motor 1.

As can be seen from the plot, the first motor displays deadzone characteristics between 0 to 5V. Above 5V though, the motor flow rate appears to not be linear at its lower operating voltages of 5 to 7V. However, beyond 8V, the motor behaves linearly up to its maximum operating value of 12V. Figure 5.6 shows the experimental results for the second motor.

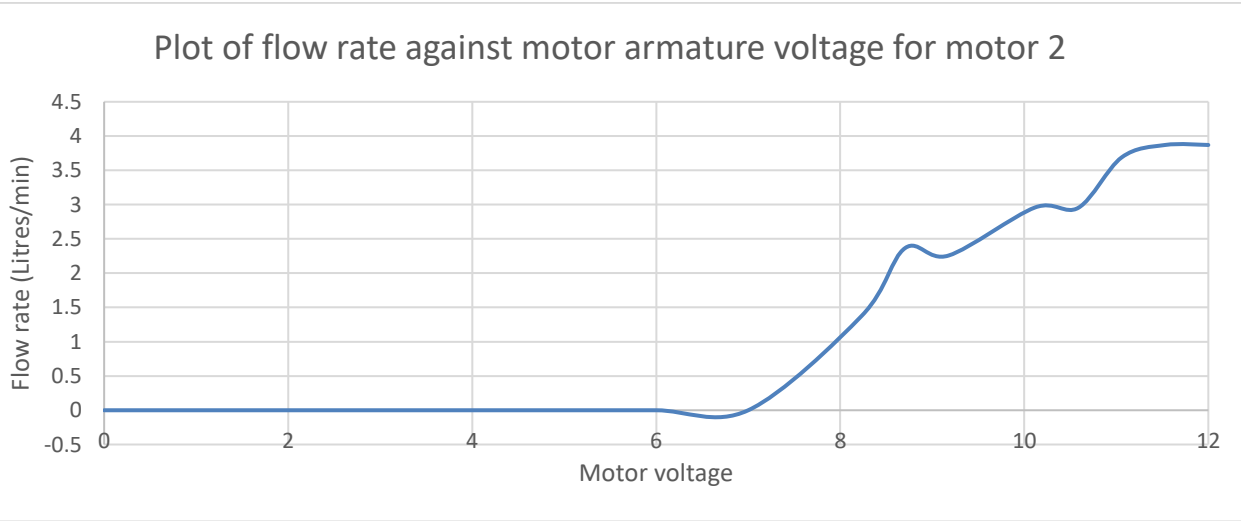


Figure 5.6 Plot of measured fluid flow rate for different armature voltage values on motor 2.

Motor 2 has a deadzone between 0 to 7V and then a linear region between 7 to 9V. Beyond 9V, the flow rate does not increase linearly with armature voltage on the motor and the flow saturates at a flow rate of 3.9litres/min beyond 11V to 12V.

As evident from the figures, both motors display input saturation as well as deadzone characteristics.

5.4 Noise filter testing

The tank was noted to fill up from being initially empty within 30 seconds. To obtain enough readings that allow the system controller to be able to respond quickly to sudden changes in water height, it was chosen to sample the sensors at 2Hz – this gives 60 level readings before the tank fills. Noise from the vibrations of the motor could also interfere with sensor readings and as such a low pass filter was designed. Figure 5.7 shows the frequency spectrum of both motors operating together.

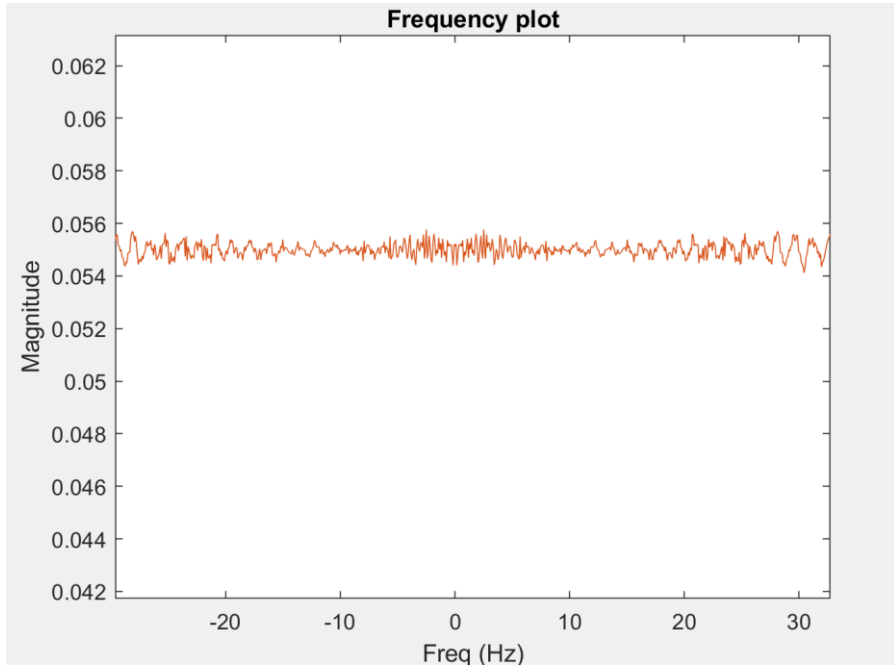


Figure 5.7 Frequency spectrum of motors obtained by performing an FFT on an audio recording of the motors both operating at maximum flow rate. This was zoomed into the frequency region of interest

As evident in the spectrum, there does not appear to be much low frequency noise in the spectrum of the motors. A low pass filter with a cut-off of 1Hz was designed to remove measurement noise from the 2Hz sampling rate as well as the low amplitude noise the motors could generate. The filter transfer function is given as:

$$H_{LP}(s) = \frac{2\pi}{s + 2\pi}$$

This was discretised using the backward difference method and the Bode plot of the controller is shown in figure 5.8.

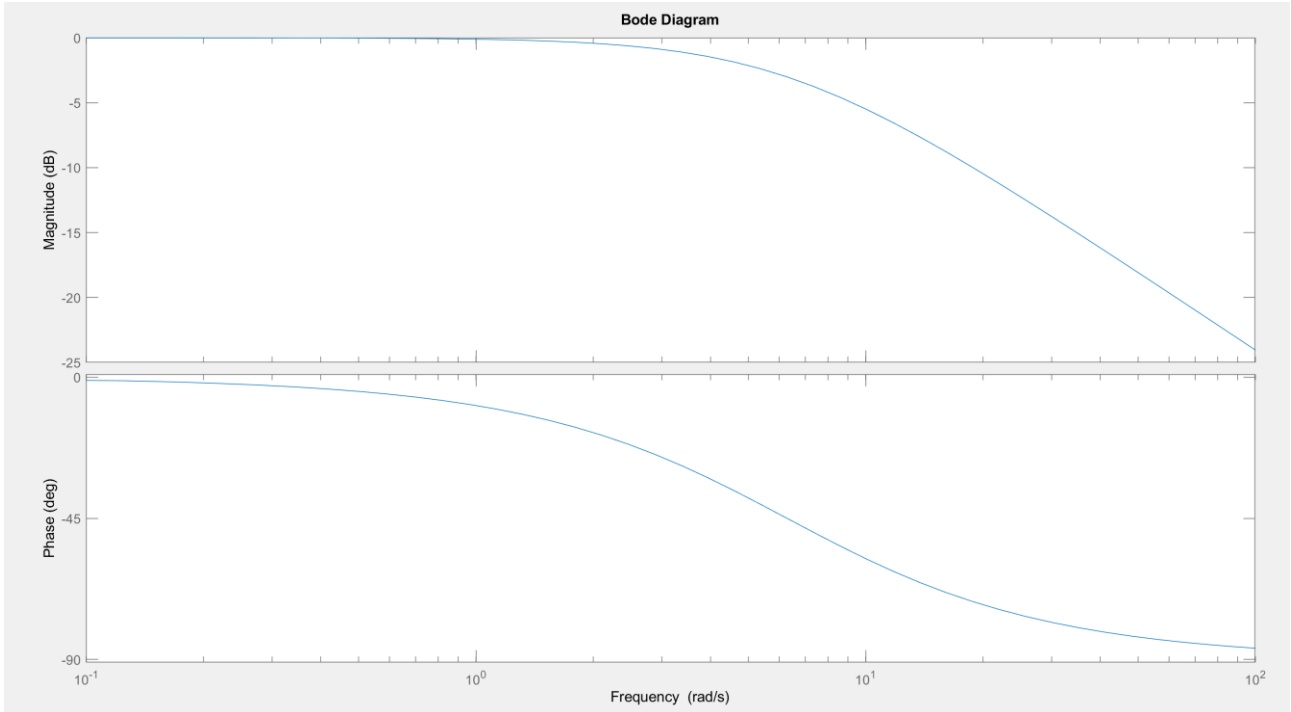


Figure 5.5 Bode plot of the low pass filter with a 1Hz cut-off

Using a test 2Hz sine wave with 50Hz noise, the performance of the filter was verified in simulation. Figure 5.9 below show the results.

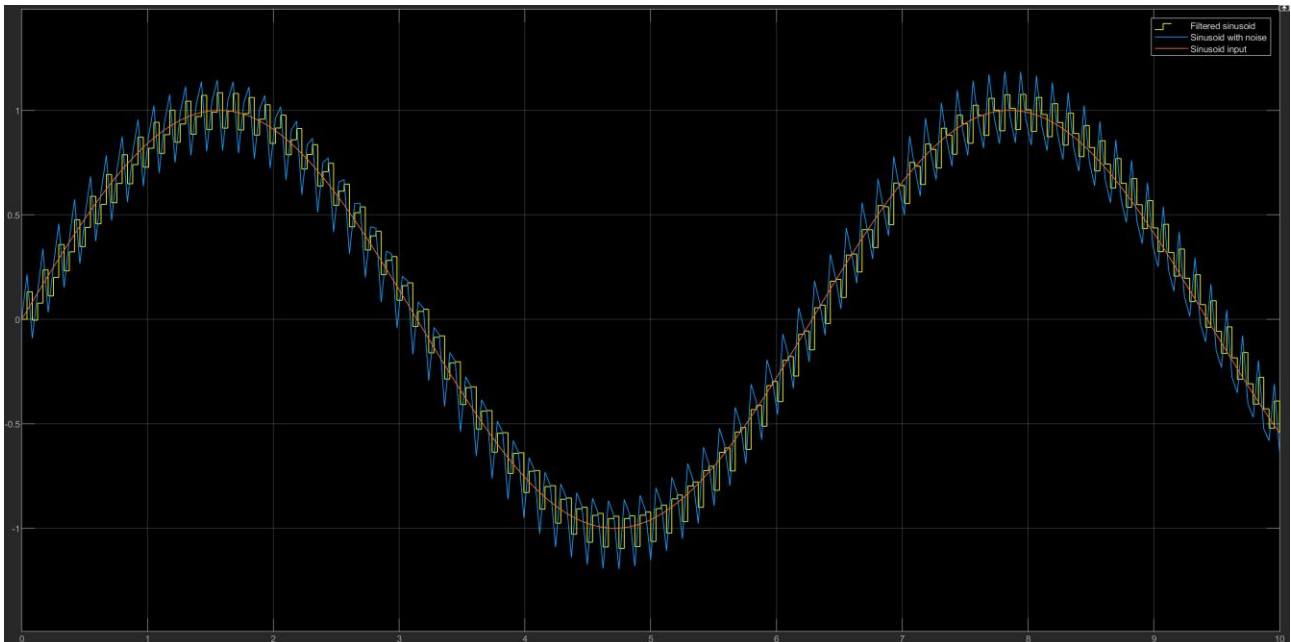


Figure 5.9 Filter performance verification using MATLAB Simulink

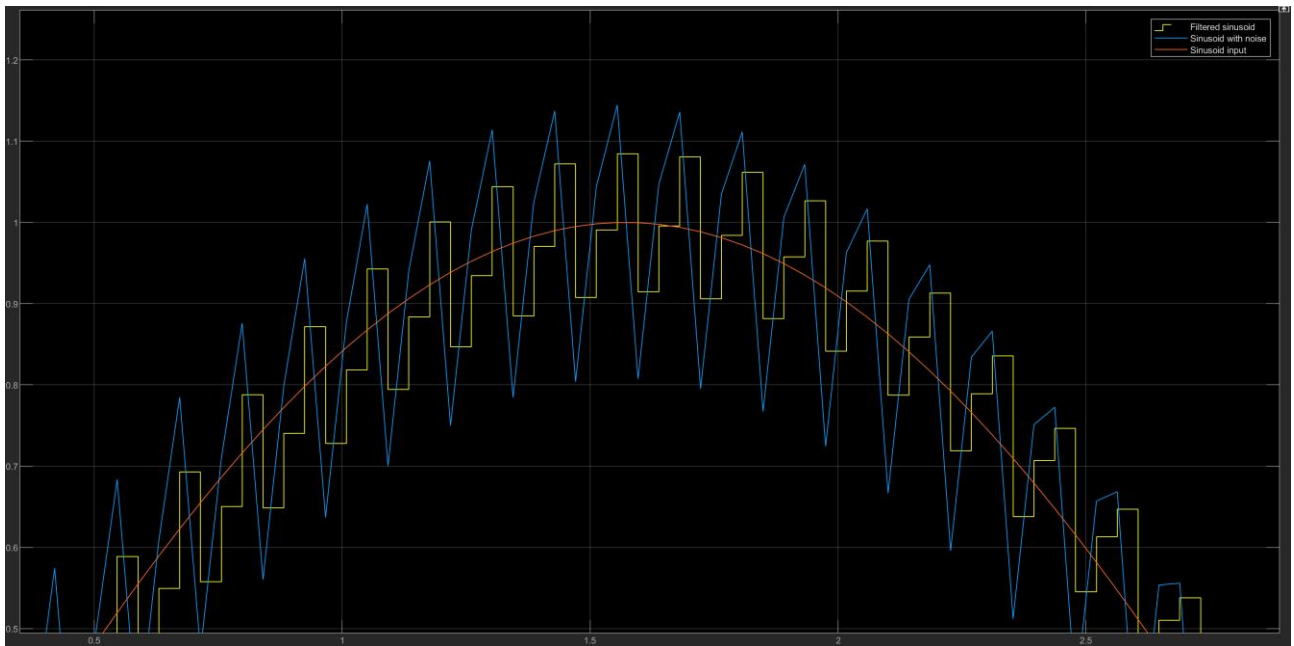


Figure 5.10 Filter performance zoomed in at the peak of the sinusoid

As seen in the above figures, the filter does a good job at reducing some of the 50Hz noise. The amplitudes of the noise were reduced by about 50% which should be sufficient for the purpose of this system.

5.5 System testing

5.5.1 Tank testing

The tanks are each supposed to have a nonlinear and linear region of operation as well as saturation. Figure 5.11 shows the results of testing tank 1 for these characteristics.

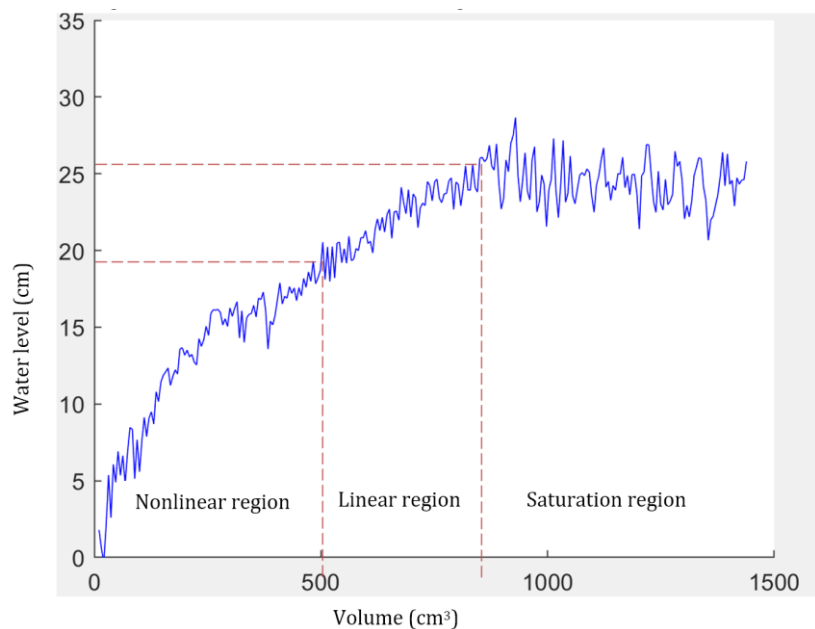


Figure 5.11 Testing of tank 1 using a constant flow rate into the tank with the outflow closed

As illustrated by the water level readings in the figure, the tank clearly exhibits a nonlinear region starting from 0cm to 19cm of the tank, a linear region from 19cm to 26 cm as well as a saturation region at 26 cm. Figure 5.12 shows the results of testing tank 2.

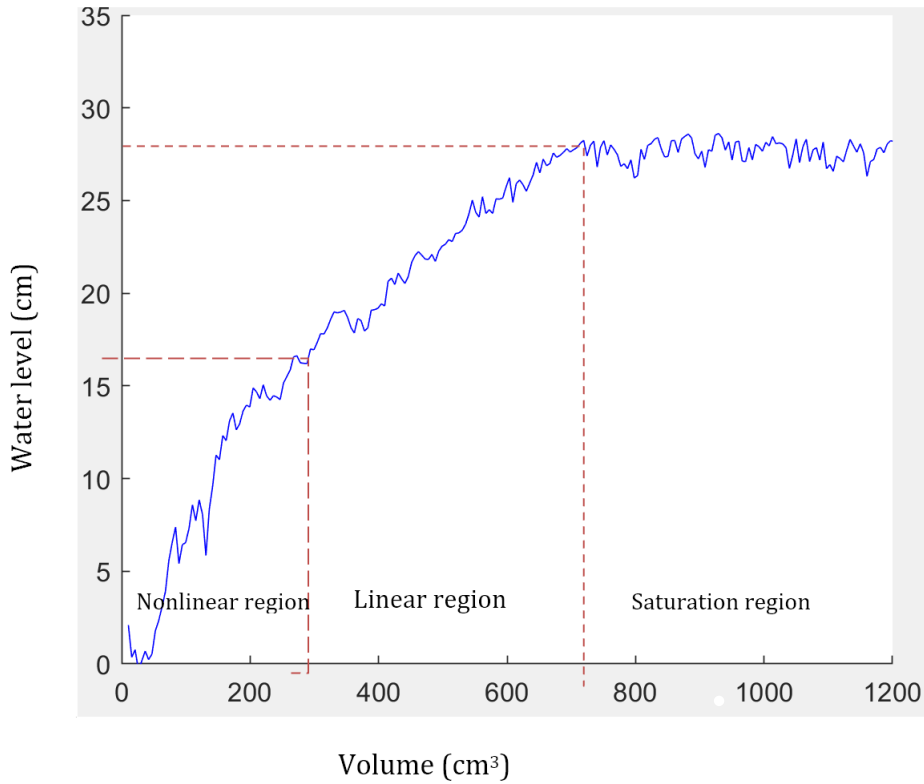


Figure 5.6 Testing of tank 2 using a constant flow rate whilst the outflow was closed

As can be seen in the figure, tank 2 also exhibited all the desired tank characteristics. The nonlinear region for tank 2 is from 0cm to 17 cm whilst the linear region is from 17cm to 27 cm. The water level readings saturate at 27cm. The water level readings in the second tank appear steadier compared to those of tank 1. Unlike tank 2, tank 1 was not stuck onto the rigs frame but it was rather attached to a metal sheet attached to the frame because of size constraints. It appears the vibrations from the motor cause noise in the readings to be more pronounced since it was not firmly attached to the frame which offers some damping to the vibrations. The water was rippling much more in tank 1 compared to tank 2. In addition, in the saturation region, both tanks' water level readings appear to slightly oscillate. It was observed that that when water would exit the saturation pipes, bubbles would get form in the water which most likely gave incorrect water readings as what is being observed in both tanks' saturation regions.

It is also evident that both tanks add an integrator term to the system response when the outflow is blocked as seen by the linear increase of water level in the linear region when constant flow rate is being provided into the tanks.

5.5.2 Multivariable coupling

Figure 5.13 graphically illustrates the water level in both tanks during the testing for multivariable coupling

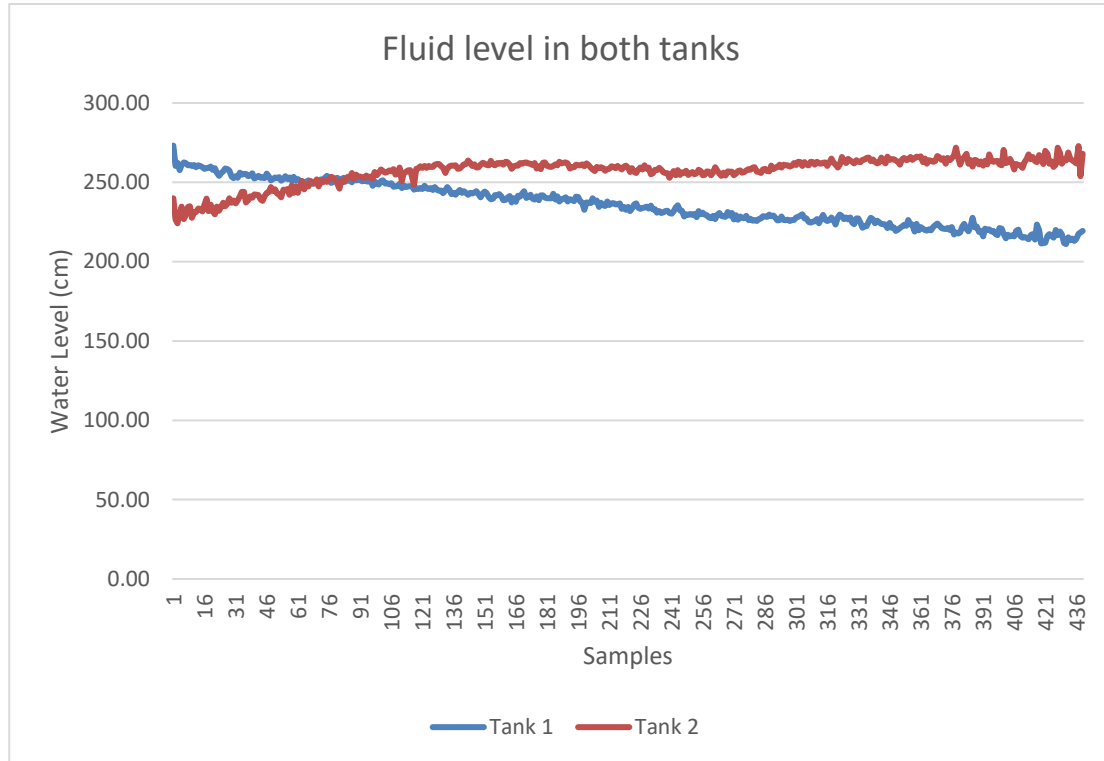


Figure 5.13 Multivariable coupling test done by providing 4V to the motor connecting outflow of tank 1 to the inflow of tank 2 .Both tanks were in the linear region of operation. Outflow of tank 2 was closed during this test aswell as the inflow of tank 1.

As can be seen from the graph above, providing voltage to the motor between the tanks causes the water level in tank 2 to rise whilst the water level in tank 1 falls. This illustrates the multivariable nature of the system. The water level in tank 2 increased by the same level that tank 1's level dropped by which supports the hypothesis that the water level in both tanks is coupled. The level sensor in tank 1 appears to be more finely calibrated as can be seen its textbook linear shape. The readings from tank 2 follow a more curved path but it can still be approximated as being linear over the experimental range since the water level rise in tank 2 is equal to the water level drop in tank 1.

The same experimental setup was then used to find the discharge coefficient without any actuation provided to the motors. Figure 5.14 summarises the results.

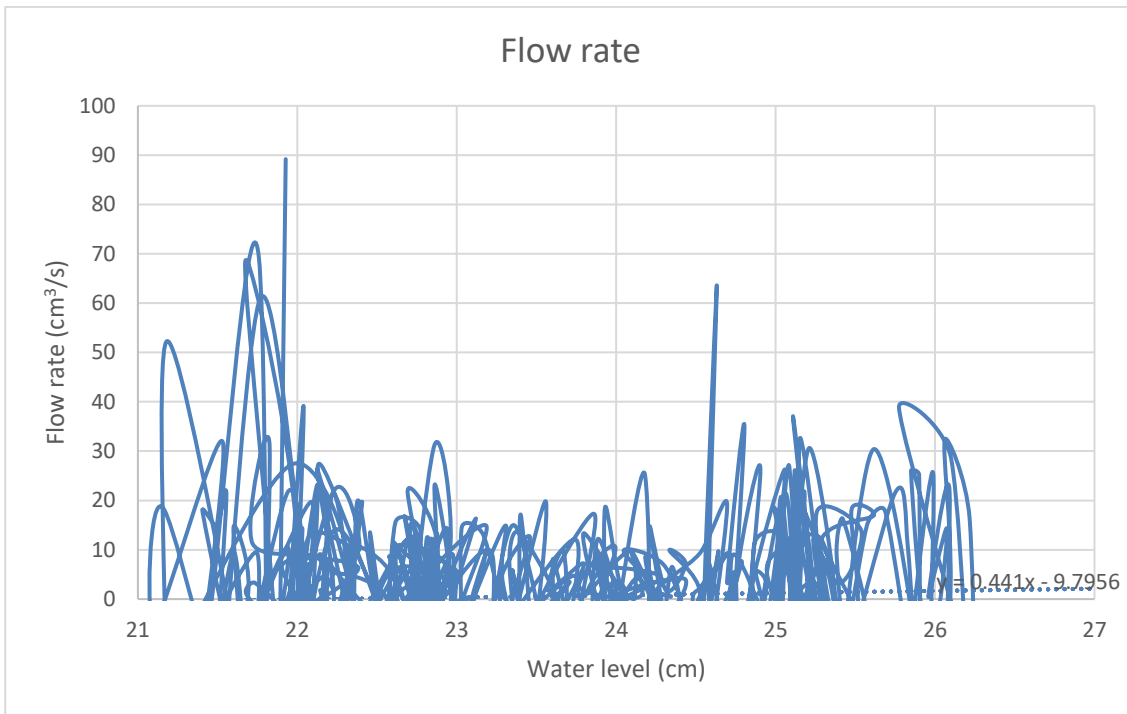


Figure 5.14 Experimental results of measuring pipe resistance. No actuation was provided to the motor joining the outflow of tank 1 with the inflow of tank 2.

As the figure shows, the water level readings were very chaotic and did not follow a linear path as would have been expected for this experiment. Although the sensor was calibrated and its output was also filtered, it seems not to be precise enough as required to conduct this experiment. Nevertheless, a linear trend line was fit to the data and a pipe resistance of 0.441 was found to be the gradient of this graph. This value however is likely to be far from the true value and a more sensitive way of measuring liquid level would yield better results. The same experiment could be done for the outflow of tank 2 but this was omitted from the report due to the poor results of this first experiment.

5.5.3 System identification

Tank 1

The first tank was provided with a step input and its step response is shown in figure 5.15.

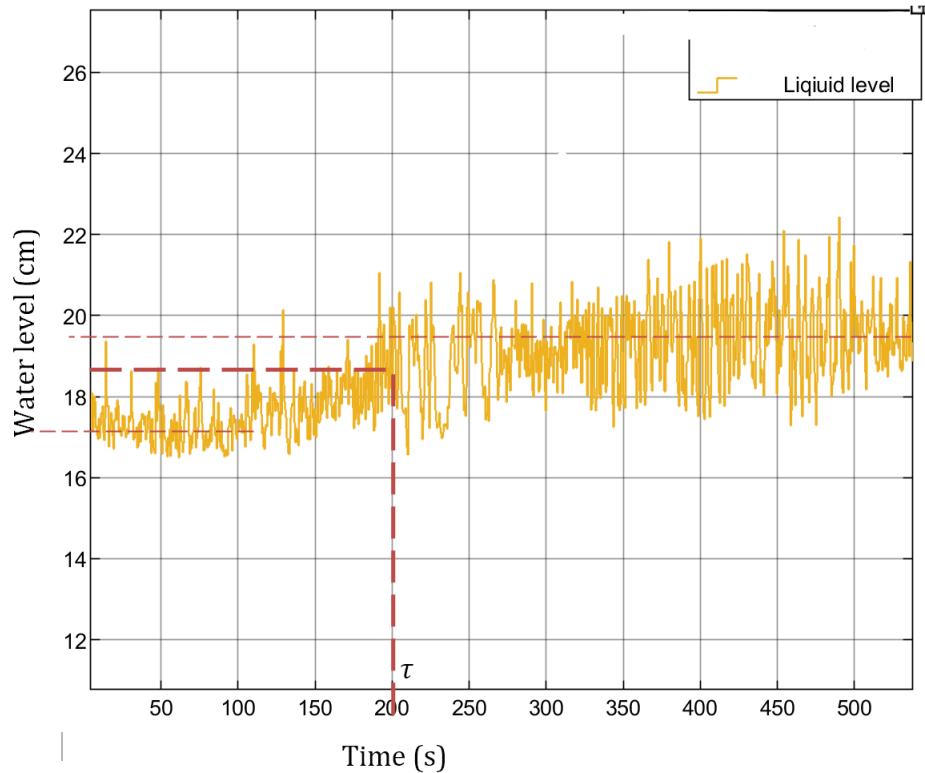


Figure 5.15 Step response of motor. Voltage of the motor was stepped from 4.2V to 4.42V

The step response of the first tank is very noisy as seen from the figure. Small steps had to be provided to the system because the systems gain was quite high. Stepping from 4.2V to 4.47V quickly caused saturation whilst stepping to 4.42V did not cause saturation. Unfortunately, smaller steps caused very small step responses that were hard to analyse whilst larger steps caused saturation. Only one step response that could be graphically analysed was obtained and that is what is shown in the figure. The gain of the system is:

$$Gain = \frac{\Delta y}{\Delta V} = \frac{19.5 - 17}{4.42 - 4.2} = 11.36$$

The time constant is the time it takes the tank to reach 63.3% of its final value. This value from which the time constant can be found is calculated as:

$$\text{water level at time constant} = 17 + 0.633 * (19.5 - 17) = 18.58\text{cm}$$

The step was applied at the 30s mark and hence from the above figure, the time constant is 170 seconds. This gives a combined transfer function of:

$$G_{11} = \frac{11.36}{170s + 1}$$

Tank 2

The step response of the system was obtained by stepping the voltage of the motor from one value to another with the outflow of the tank allowed to drain normally whilst the inflow water was being drained through the outflow of tank 1 through the motor joining the two tanks. The figures that will follow show different step responses of the tank.

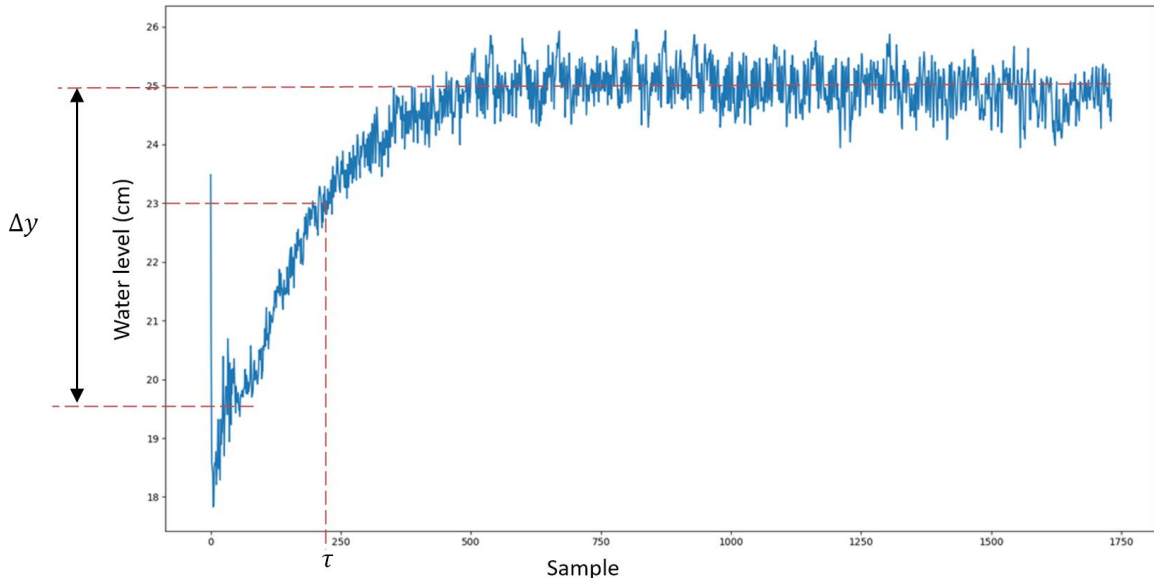


Figure 5.16 Step response of tank with motor voltage stepped from 7.5V to 8V

From the step response shown in figure 5.16, it is evident the response is first order. The system gain and time constant were calculated as shown below. The variable y represents the water level whilst V represents the motor voltage which was recorded manually during the experiment.

$$Gain = \frac{\Delta y}{\Delta V} = \frac{25 - 19.5}{8 - 7.529} = 11.68$$

The time constant is the time it takes the tank to reach 63.3% of its final value. This value from which the time constant can be found is calculated as:

$$\text{water level at time constant} = 19.5 + 0.633 * (25 - 19.5) = 23\text{cm}$$

The time constant was reached after approximately 220 samples. A sampling rate of 2Hz was used and the step was applied during the 40th sample during each of the step tests. Therefore, the time constant was after 180 samples in the case shown in figure 5.17 which is approximately 90 seconds. The same procedure was followed for the step responses shown in the figures below to calculate the gains and the time constants. Figure 5.17 shows another step response.

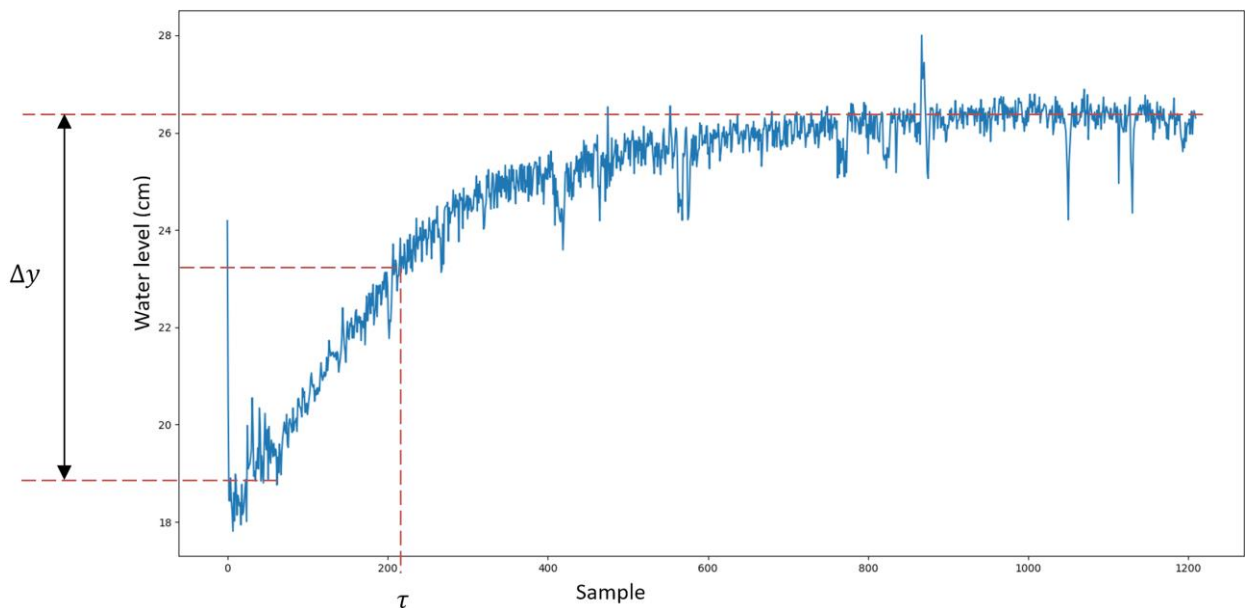


Figure 5.17 Step response of tank with motor voltage stepped from 7.52V to 8.47V

From figure 5.17, we can deduce the following:

$$\text{Gain} = \frac{26.25 - 19}{8.47 - 7.52} = 7.70$$

$$\text{water level at time constant} = 19 + 0.633(26.25 - 19) = 23.59\text{cm}$$

$$\tau = (210 \text{ samples} - 40 \text{ samples}) * \frac{0.5\text{sec}}{1 \text{ sample}} = 92.55 \text{ sec}$$

Below is the third and final step test performed on tank 2.

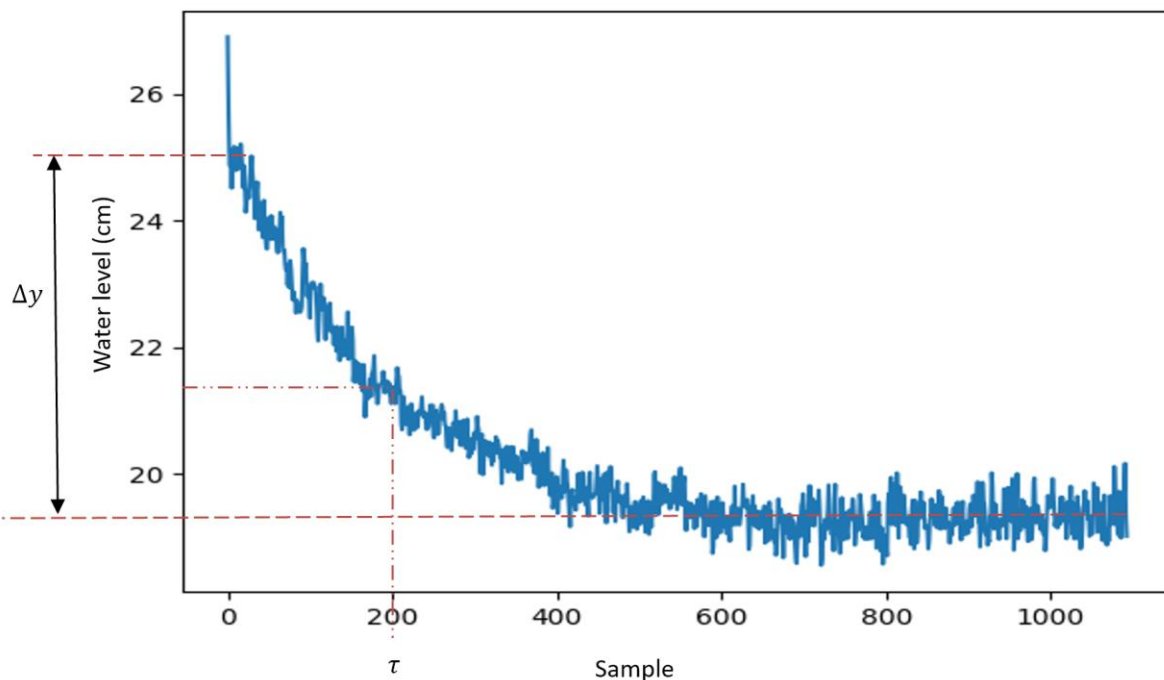


Figure 5.18 Step response of tank after voltage was stepped from 8V to 7.5V

From figure 5.18, we can deduce the following:

$$\text{Gain} = \frac{25 - 19.5}{7.522 - 8} = 12.55$$

$$\text{water level at time constant} = 25 + 0.633(19.5 - 25) = 21.52\text{cm}$$

$$\tau = (200 \text{ samples} - 40 \text{ samples}) * \frac{0.5\text{sec}}{1 \text{ sample}} = 92.55 \text{ sec}$$

With these three readings, a nominal model of the plant can be obtained by averaging these three gain values. The table below summarises the results

Step test	1	2	3	Average
Gain (cm/V)	11.68	7.70	12.55	10.6 ± 4.5
Time constant (s)	90	92.55	92.55	91.70 ± 1.4

Table 5-4 Summary of step test results on tank 2

The transfer function of the linear region of tank 2 is therefore given by

$$G_{22}(s) = \frac{10.64}{91.7s + 1}$$

The effects of time delay were neglected in producing the $G_{11}(s)$ and $G_{22}(s)$ transfer functions. Time delays between turning on the pump and water entering the tank were recorded by noting time differences between stepping the motor voltage and when the level sensor begins noting a rising water level. The figures below show plots of water level as the motor is stepped. The time delays were also recorded manually by timing how long fluid takes to flow from the pump into the tank.

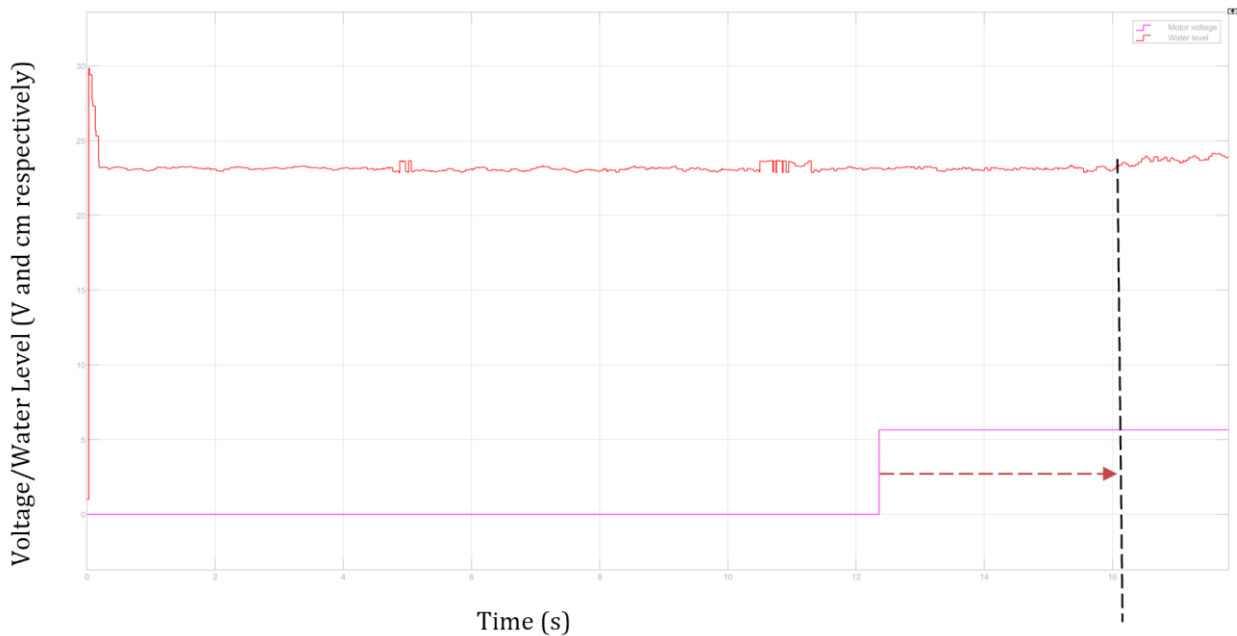


Figure 5.19 Stepping voltage from 0V to 5.65V and noting the time delay it takes for water level to increase

From figure 5.16, there appears to be a 4.2 second input delay in the system. Using a timer, this delay was noted to be 5.18 seconds.

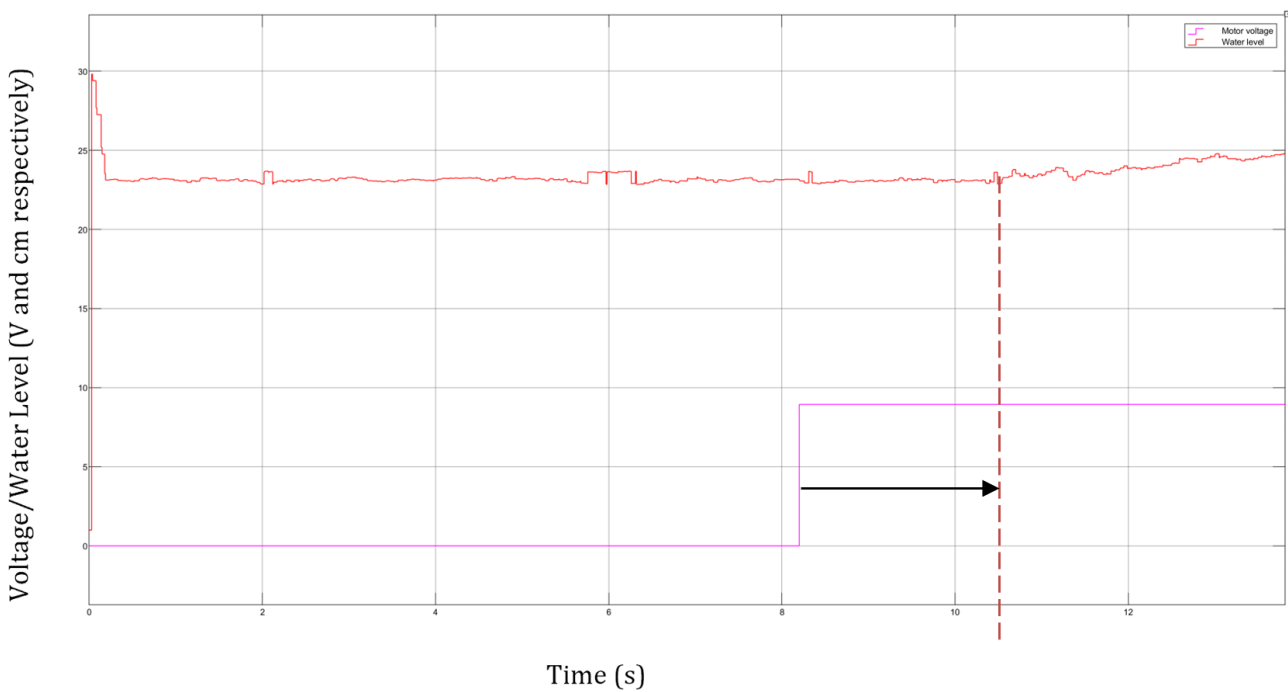


Figure 5.20 Stepping pump voltage from 0V to 8.5V and noting the input delay

From figure 5.17, the time delay was noted to be 2.1 seconds for an 8.5V input to the pump. This is expected since the flow rate increases proportionally with the motor voltage. The time noted from using a timer was 3.4 seconds. The motor voltage was then stepped to its maximum value to get maximum flow.

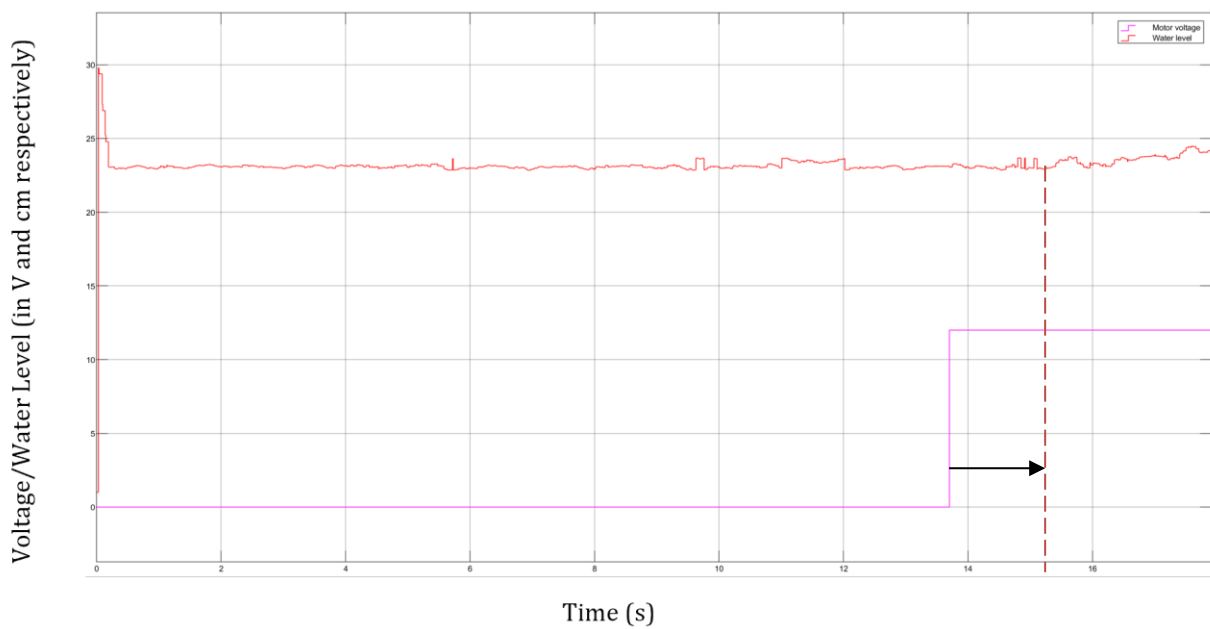


Figure 5.21 Stepping pump voltage from 0V to 12V and noting the input delay

Figure 5.18 shows the input delay at the maximum flow rate the pump can deliver. As expected, this delay was relatively small and was approximately 1.6 seconds. The time delay noted using a timer was 3.4 seconds. The average delay across the pumps' operation range using these values is therefore 2.6 ± 1.3 seconds and can be included in the transfer function as shown below. The time sensor readings were used over the manual readings due to the influence of human reaction time in operating the stopwatch. A first order Pade approximation was then used to produce the following second order system model which cooperates the systems dead time characteristic:

$$G_{22}(s) = \frac{10.64}{91.7s + 1} e^{2.6s}$$

$$G_{22}(s) = \frac{10.64(1 - \frac{2.6s}{2})}{(91.7s + 1)(1 + \frac{2.6s}{2})}$$

$$G_{22}(s) = \frac{10.64 - 13.832s}{119s^2 + 93s + 1}$$

Using the delay obtained from these tests, $G_{11}(s)$ can also be approximated as second order using the Pade approximation used for $G_{22}(s)$ since the time delays were roughly identical for both motors. The equation becomes:

$$G_{11}(s) = \frac{11.36 - 14.77s}{221s^2 + 171.3s + 1}$$

The derivation of these transfer functions confirms not only the presence of deadtime in the system but also the second order nature of the plant – which satisfies some of the research objectives.

5.5.4 Controller testing

The response of the water level in the first tank was very unstable as was discussed earlier and it was decided to use the second tank to test the controllability of the tanks. The controller designed for testing this system was not designed to meet any predefined performance specifications but it was designed for the sole purpose of testing.

The system will be controlled in a negative feedback configuration as shown in figure 5.22.

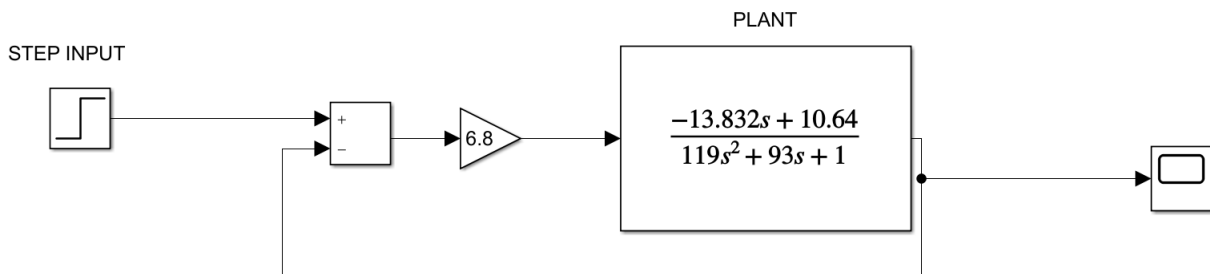


Figure 5.22 The plant to be controlled in negative feedback

In the appendix (section 10.3), a screenshot of how this controller was implemented with the Arduino in Simulink is shown.

Using Simulink, the Bode plot of the $G_{21}(s)$ transfer function was obtained and it is shown in figure 5.23.

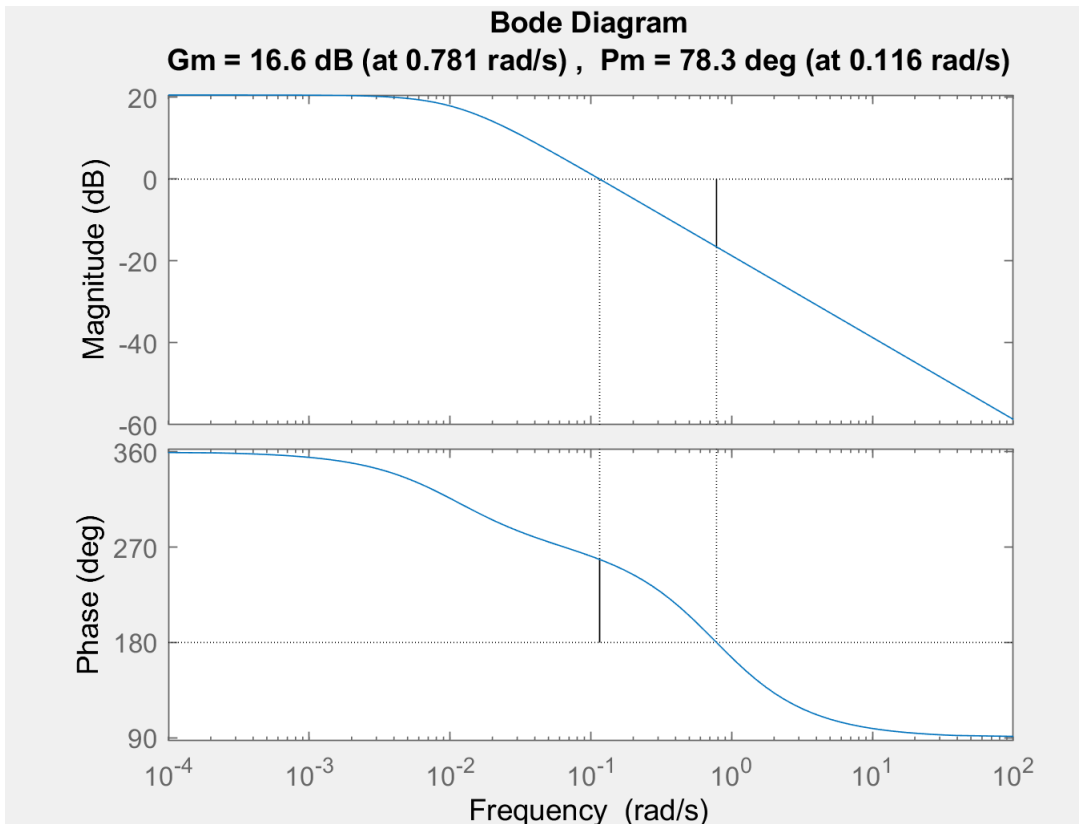


Figure 5.23 Bode plot of the system

The frequency response of the system had good phase and gain margins. It was decided to use the Zeigler-Nicolls PID tuning rules in [23] to come up with a suitable PID controller. The ultimate gain of the system was found to be 6.8 in simulation with a neutral stability oscillation period of 8.07s as shown in figure 5.21.

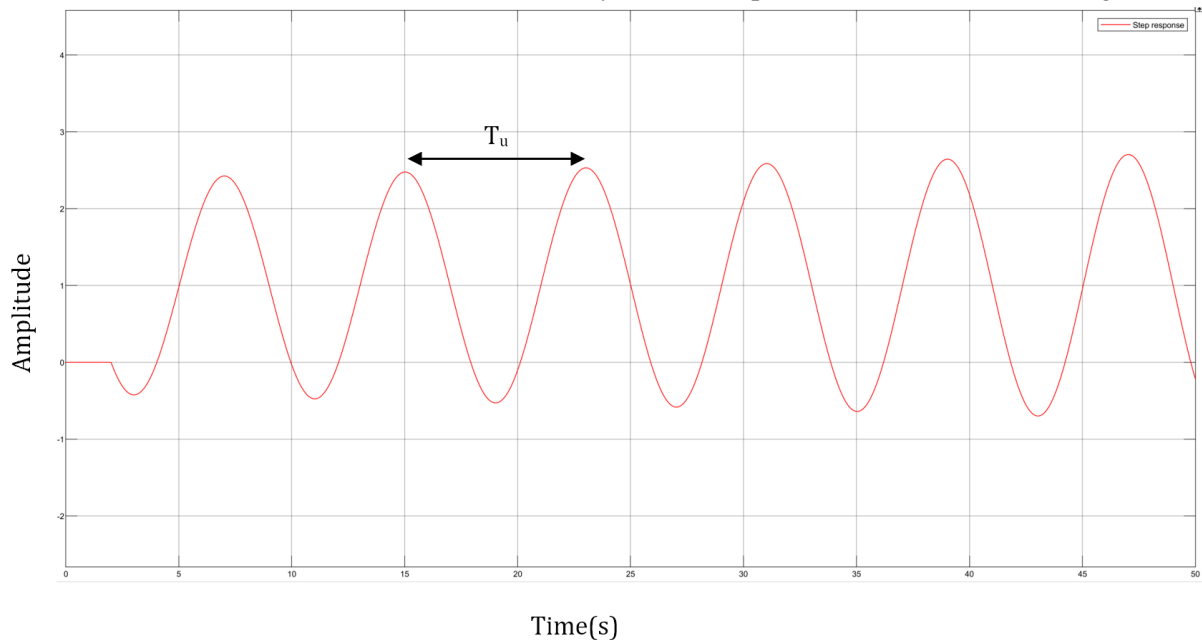


Figure 5.24 Response of the system at the ultimate gain

The period of oscillation at the ultimate gain, T_u was measured to be 8.07s as shown in figure 5.24. Using the PID with no overshoot tuning rule, the following system response was obtained after tuning the values. All step responses were first validated in simulation and those plots can be found in the appendix.

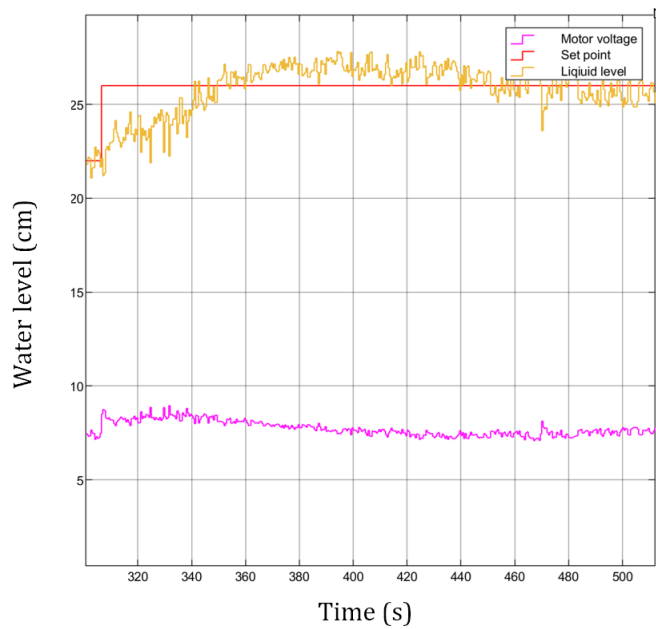


Figure 5.25 System response with the control action shown

The system response is stable with a control action that does not exhibit bang-bang behaviour. Figure 5.26 below shows only the liquid level and set point.

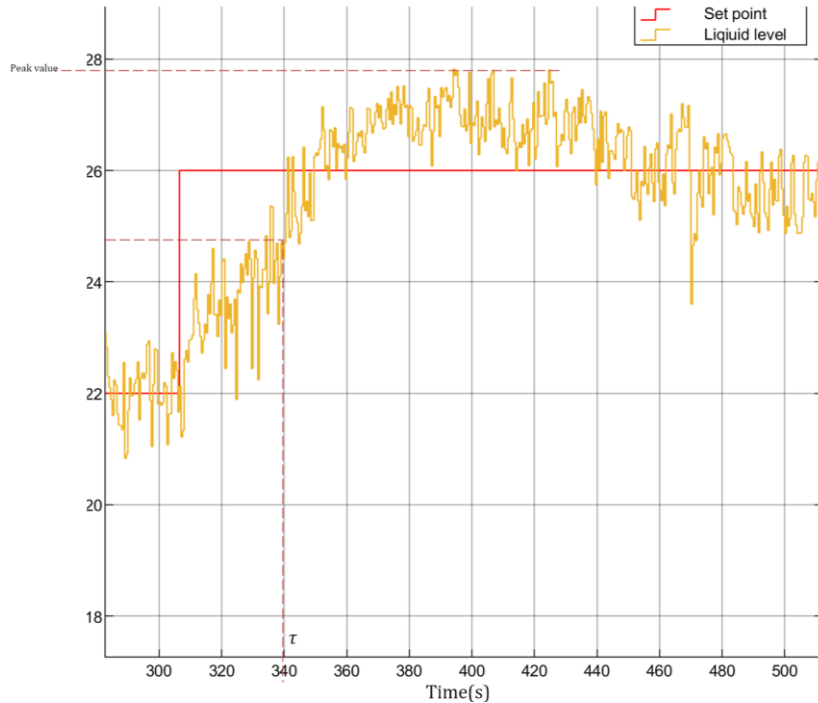


Figure 5.26 Step response of system with Ziegler-Nichols tuned PID controller. $K_p = 1.481$, $K_i = 0.07148$, $K_d=2.108$

The time constant of the plant's response was found to be 35 seconds after the step input was applied at 305 seconds as shown in the graph – 38% of the uncompensated plants time constant. The step response also has a peak overshoot of 7.31%. This tuned PID controller provided satisfactory performance and hence tank 2 can be controlled in the nonlinear region with a finely tuned PID controller.

Another controller with different gain combinations obtained from the PID (some overshoot) tuning rule was also implemented to test different controller configurations. The step response is shown below along with a plot of the control action magnitude

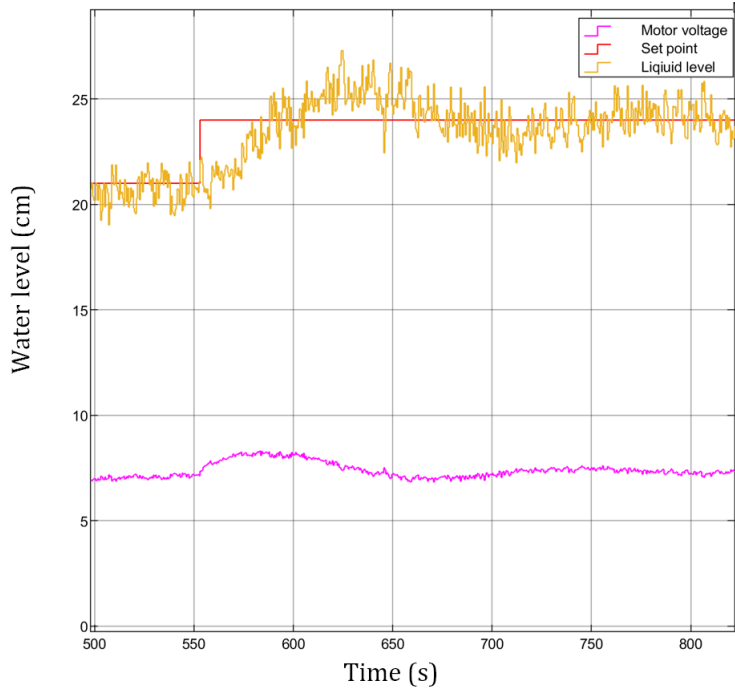


Figure 5.27 Step response of tuned PID controller along with the control action

This PID controller also has a smooth control action profile throughout the systems response. The step response alone is shown in figure 5.28.

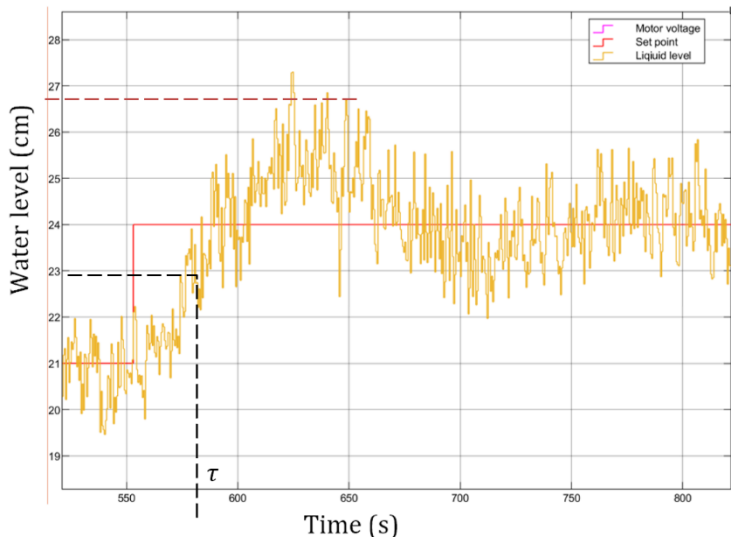


Figure 5.28 Step response of the PID controller with $K_p = 0.9138$, $K_i = 0.1$, $K_d = -1.917$

The time constant of the response was found to be 25 seconds (27% of the uncompensated plants' time constant) – and this is faster than the step response in figure 5.23, however, the overshoot was 11.7% which is larger than that same step responses overshoot. Depending on the user's needs, each of these controllers could potentially be used to satisfy those users performance requirements.

6. Discussion

The results clearly indicate that the design proposed suffices as a proof of concept for the laboratory rig. However, some short comings were noted and these will be discussed below.

6.1 Water Level Readings

The water level readings were very susceptible to noise from any external disturbances such as vibrations from the motor, bubbles in the liquid and touching the lab rig frame or the table on which it was placed. The sensor was placed directly above the outflow pipe so that the sensor can measure water level throughout the tank but this also proved to be troublesome because the turbulent flow of liquid in the tank created a ‘tornado’ looking bubble within the water which made readings very noisy. This is shown in figure 6.1.

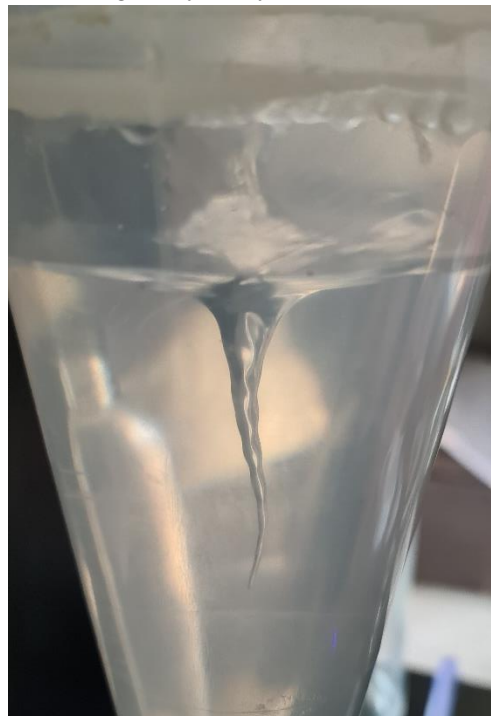


Figure 6.1 'Tornado' bubble caused by turbulent flow in the tank when water was pumped in with the outflow open

A lower flow rate reduced the size of this but the effects of turbulent flow could never be eliminated.

6.2 Tank 1 outflow

Tank 1 proved to be challenging to work with in the proposed design. Solenoid valves that are readily available needed at least 0.02MPa of pressure to operate and a motor was used in-between tank 1 and tank 2 to try overcome this since 0.02MPa of pressure required at least 2.14m of water in tank 1 to achieve such a pressure. Without providing actuation to motor 2, water did not easily flow between the two tanks and it would take about 3 minutes for tank 1 to drain completely into tank 2. This made system identification and control of tank 1 very challenging as the system had a very unstable response that would cause saturation for extremely small step inputs. Had there been more time such that the project timeline would not have been jeopardised waiting for components to arrive from overseas, a 12V motorised valve such as [26] would have been a better pick over the motor that was used as a compromise after not finding such a valve locally.

7. Conclusions

This report has detailed the design and implementation of a laboratory rig that can be used for control systems teaching. Looking back at the initial aims of the project, the following conclusions can be drawn out from the results obtained in the testing of the laboratory rig.

The system was able to exhibit deadtime from the motor delays as shown in section 5.3. The motors also showed input saturation characteristics as well as deadzone – also shown in section 5.3. The response of the tanks to a constant inflow with their outflow blocked confirmed the non-linear as well as linear nature of the different regions of the tank (as shown in section 5.5.1) – which was to be expected given the design of the tanks. The output saturation was clearly shown for both tanks as was noted in the results given in section 5.5.1. The tanks were interactive and multivariable coupling was shown to exist as shown by the results in section 5.5.2. System identification yielded a transfer function of both tanks which not only confirmed that the tanks could be approximated as second order, but that they had time varying dynamics and an integrator when the outflow was closed – this was supported by the testing done on the tank in section 5.5.1. Analysis on the nonlinear region of the tank was however not fruitful due to the noisy sensor readings when trying to experimentally determine the pipe resistances in both tanks.

A PID controller was used to improve the performance of the plant (tank 2) as a means of testing the integration of the hardware components and this resulted in a 75% reduction in the settling time of the plant showing that the system can indeed be controlled with satisfactory results. A Simulink model was used to send commands and read sensor data in real-time – one of the research aims.

The laboratory rig was weighed and weighed a total of 4.34kgs with the 2-litre reservoir filled. The laboratory rig by itself therefore weighed 2.34kgs - the weight of 2 standard 13-inch laptops and it is therefore lightweight in relative terms. The original design idea was supposed to have dimensions of 26cm x 30cm x 48cm however the height had to be increased by 30cm to accommodate the first tank making it have a total height of 78cm instead. Had the tanks been 3D printed, the original frame dimensions would have been used making it more compact than it ended up being. Finally, the cost of the overall frame came to a total of R2823 – only 56.5% of the R5 000 budget. Although most of the research objectives were met, the first tank was difficult to work with due to the restricted outflow path and hence the whole system was not able to be tested due to the time constraints of the project.

8. Recommendations

Certain aspects of the project were not investigated due to the time constraints of the project. Below are some recommendations for further investigations that can be done in future adaptations of this work to come up with a robust laboratory rig.

1. The water level sensor proved to be problematic. Using a water level sensor that uses pressure instead of time of flight could potentially reduce the effect of the disturbances that were noted with a ToF sensor since its readings are based on the pressure of water which should be constant despite vibrational disturbances to the water. Filtering out errors from the pressure sensor should be easier than with the level sensor that was used.
2. A more detailed user interface which can provide graphical readings on water level in the tanks should also be developed. This would allow remote control of the water level in the tanks without the need to physically be present to ensure the tank is not too full or too low.
3. The nonlinear region of the tank needs to have its mathematical model developed properly by using a very sensitive flow rate meter on the outflow pipe to quantify the pipe resistance. Using level readings to experimentally quantify this value proved to be very challenging and the same could apply with other indirect ways of measuring the outflow flow rate.
4. Having done recommendation 3, a simple controller for the nonlinear region should be designed to demonstrate that the nonlinear region of the tank can be controlled. A feedback linearisation control scheme is one way to complete this task aswell as adaptive control.
5. It would be interesting to see what difference using modern control techniques to control the liquid level would have on the performance compared to the PID controller implemented in this report
6. The project used only a portion of the budget. Using higher quality pumps as well as sensors could be investigated as a way of removing a lot of the measurement noise as well as sensor issues encountered throughout this project.
7. The cross-coupling effect of the tanks were not quantified in the project and hence multivariable control of level in both tanks was not investigated. This could be improved on in future projects to demonstrate that multivariable control is possible with this system.

9. List of References

- [1] L. Feisel and A. Rosa, "The Role of the Laboratory in Undergraduate Engineering Education", *Journal of Engineering Education*, vol. 94, no. 1, pp. 121-130, 2005. Available: 10.1002/j.2168-9830.2005.tb00833.x [Accessed 30 September 2021].
- [2] ECSA, Qualification Standard for Bachelor of Science in Engineering (BSc (Eng))/ Bachelor of Engineering (BEng): NQF Level 8, 6th ed. 2021, pp. 18-22.
- [3] W. Powers, "The Tank That Filled Itself", in Control Systems Group Conference, Manchester, 2010.
- [4] M. Khalifa, A. Amhedb and M. Al Sharqawi, "Position Control of Real Time DC Motor Using LabVIEW", Journal of Robotics and Control (JRC), vol. 2, no. 5, 2021. Available: 10.18196/jrc.25104 [Accessed 15 August 2021].
- [5] Iswanto, N. Raharja, A. Ma'arif, Y. Ramadhan and P. Rosyady, "Pole Placement Based State Feedback for DC Motor Position Control", Journal of Physics: Conference Series, vol. 1783, p. 012057, 2021. Available: 10.1088/1742-6596/1783/1/012057 [Accessed 15 August 2021].
- [6] J. Kocijan, J. O'Reilly and W. E. Leithead, "An integrated undergraduate teaching laboratory approach to multivariable control," in IEEE Transactions on Education, vol. 40, no. 4, pp. 266-272, Nov. 1997, doi: 10.1109/13.650839.
- [7] R. Reck, "BYOE: Affordable and Portable Laboratory Kit for Controls Courses", in ASEE Annual Conference and Exposition, Seattle, 2015.
- [8] R. Kadhim, A. Raheem and S. Gitaffa, "Implementing of liquid tank level control using Arduino-Labview interfaceing with ultrasonic sensor", Kufa Journal of Engineering, vol. 8, no. 2, pp. 29-41, 2017.
- [9] K. H. Johansson, A. Horch, O. Wijk and A. Hansson, "Teaching multivariable control using the quadruple-tank process," Proceedings of the 38th IEEE Conference on Decision and Control (Cat. No.99CH36304), 1999, pp. 807-812 vol.1, doi: 10.1109/CDC.1999.832889.
- [10] K. H. Johansson, "The quadruple-tank process: a multivariable laboratory process with an adjustable zero," in IEEE Transactions on Control Systems Technology, vol. 8, no. 3, pp. 456-465, May 2000, doi: 10.1109/87.845876.
- [11] C. Urrea and F. Páez, "Design and Comparison of Strategies for Level Control in a Nonlinear Tank," Processes, vol. 9, no. 5, p. 735, 2021.
- [12] T. Pushpavani, S. Srinivasulu Raju, N. Archana and M. Chandana, "Modeling and Controlling of Conical tank system using adaptive controllers and performance comparison with conventional PID", International Journal of Scientific & Engineering Research, vol. 4, no. 5, p. 629, 2013. [Accessed 16 August 2021].
- [13] R. Hedjar and M. Bounkhel, "Wireless model predictive control: Application to water-level system," Advances in Mechanical Engineering, vol. 8, no. 4, pp. 1–13, 2016.
- [14] S. Frank, "Time Delays", *Control Theory Tutorial*, pp. 95-102, 2018. Available: 10.1007/978-3-319-91707-8_13 [Accessed 26 October 2021].
- [15] J. Richard, "Time-delay systems: an overview of some recent advances and open problems", Automatica, vol. 39, no. 10, pp. 1667-1694, 2003. Available: 10.1016/s0005-1098(03)00167-5 [Accessed 21 September 2021].
- [16] T. Hu and Z. Lin, "Control Systems with Actuator Saturation", 2001. Available: 10.1007/978-1-4612-0205-9 [Accessed 21 September 2021].
- [17] D. Limon, J. Gomesda Silva, T. Alamo and E. Camacho, "Improved MPC Design based on Saturating Control Laws*", European Journal of Control, vol. 11, no. 2, pp. 112-122, 2005. Available: 10.3166/ejc.11.112-122 [Accessed 21 September 2021].
- [18] J. Lentz, "PARAMETER ESTIMATION OF SYSTEMS WITH DEADZONE AND DEADBAND AND EMULATION USING xPC TARGET", Masters, Missouri University of Science and Technology, 2008.

- [19] A. Taware, Gang Tao and C. Teolis, "An adaptive dead-zone inverse controller for systems with sandwiched dead-zones," Proceedings of the 2001 American Control Conference. (Cat. No.01CH37148), 2001, pp. 2456-2461 vol.3, doi: 10.1109/ACC.2001.946121.
- [20] J. Slotine and W. Li, *Applied nonlinear control*. Taipei, Taiwan: Pearson Education Taiwan, 2005, pp. 4-14.
- [21] J. Kocijan, J. O'Reilly and W. Leithead, "An integrated undergraduate teaching laboratory approach to multivariable control", *IEEE Transactions on Education*, vol. 40, no. 4, pp. 266-272, 1997. Available: 10.1109/13.650839 [Accessed 24 September 2021].
- [22] "PID control", *IEEE Control Systems*, vol. 26, no. 1, pp. 30-31, 2006. Available: 10.1109/mcs.2006.1580151 [Accessed 27 September 2021].
- [23] A. O'Dwyer, *Handbook of PI and PID controller tuning rules*. London: Imperial College Press, 2009, p. 78.
- [24]"pyFirmata", PyPI, 2021. [Online]. Available: <https://pypi.org/project/pyFirmata/#:~:text=pyFirmata%20is%20a%20Python%20interface,Python%202.7%2C%203.3%20and%203.4>. [Accessed: 25- Oct- 2021].
- [25] P. Childs, "Design", *Mechanical Design Engineering Handbook*, pp. 1-47, 2019. Available: 10.1016/b978-0-08-102367-9.00001-9 [Accessed 13 October 2021].
- [26] Amazon.com, 2021. [Online]. Available: <https://www.amazon.com/engineering-DC12V-SS304-Motorized-Electrical/dp/B00OUTP6D8>. [Accessed: 06- Nov- 2021].

10. Appendices

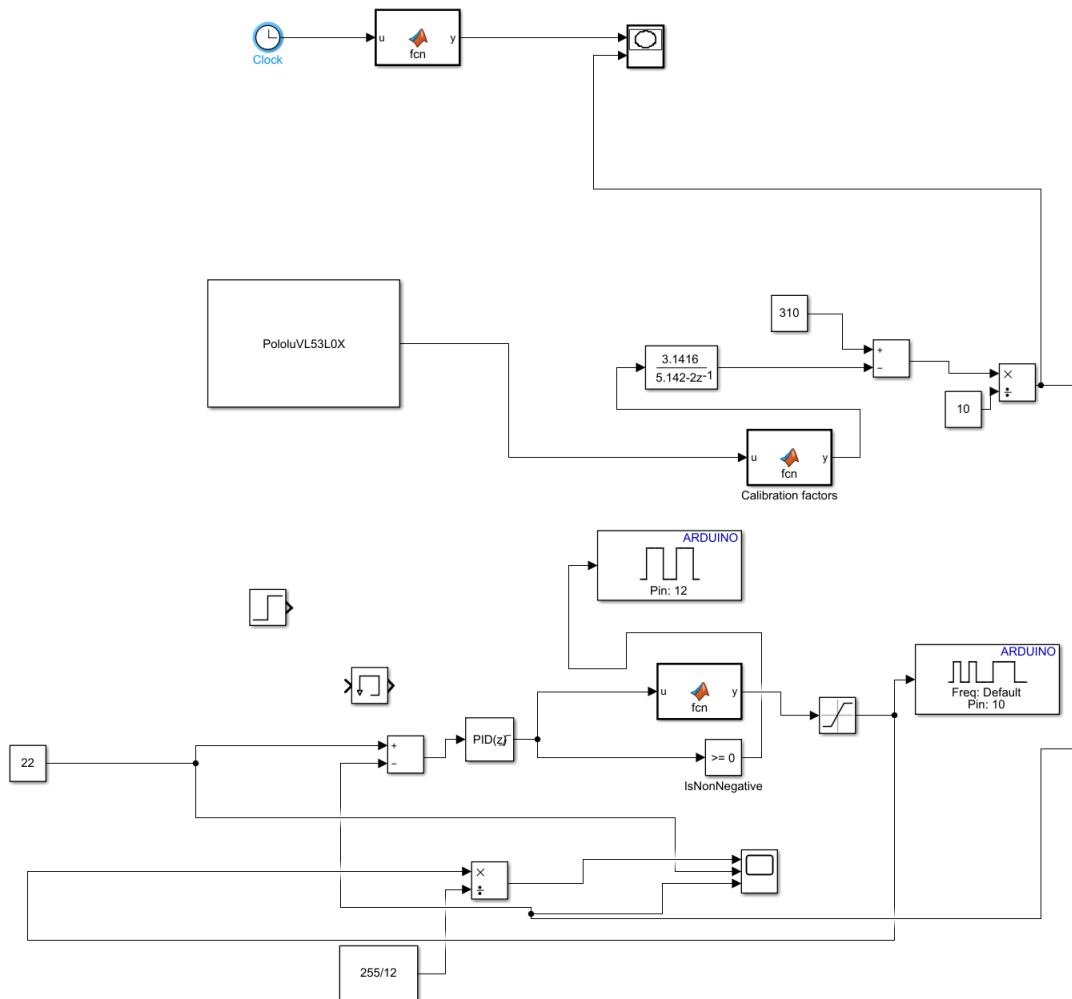
10.1 Quote for the Quanser double tank

Quotation		Date: 2021/08/18	TDAQ00327	Page 1 of 1
	Test Dynamics Academic (Pty) Ltd 40 Monte Carlo Crescent Kyalami Business Park Midrand 1685 Telephone: 062 217 0063 Bill To: UNI002 University of Cape Town Private Bag X3 Rondebosch 7701	Banking Details First National Bank Branch Code: 250655 Account: 62757260080		
Reg: 2018/231545/07 VAT: 4270282355	Ship To: Collection Quote Valid: 14 Days Delivery Period: 6-10 Weeks Payment Terms: Current	VAT: 4540125707 Ref:		
Item Code	Item Description	Quantity	Price (Ex)	Total (Ex)
511	Coupled Tanks	1.00	75 396.44	75 396.44
843	VoltagePAQ-X1 Amplifier	1.00	25 684.00	25 684.00
842	Q2- USB Dataacquisition Device	1.00	32 104.00	32 104.00
971	Quanser QUARC Essentials Software License	1.00	10 500.00	10 500.00
Notes: Prices are subject to change without notice due to ZAR/USD volatility Please note in some circumstances we have delayed shipping upto 12 weeks due to global component shortages which are out of our control.		Sub Total: R 143 684.44	VAT: R 21 552.67	Grand Total R 165 237.11

10.2 GitHub repository link

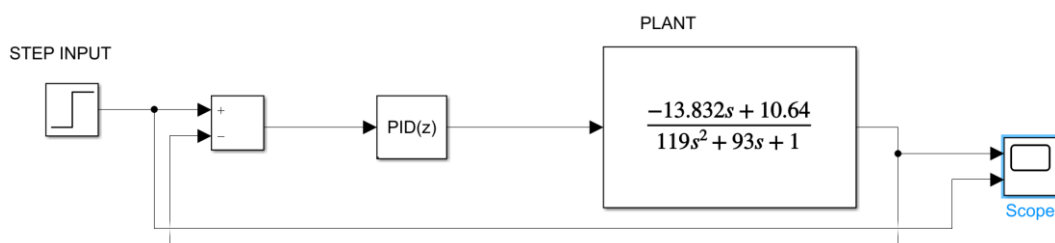
<https://github.com/rtnyakonda/EEE4022S>

10.3 Controller simulations in Simulink

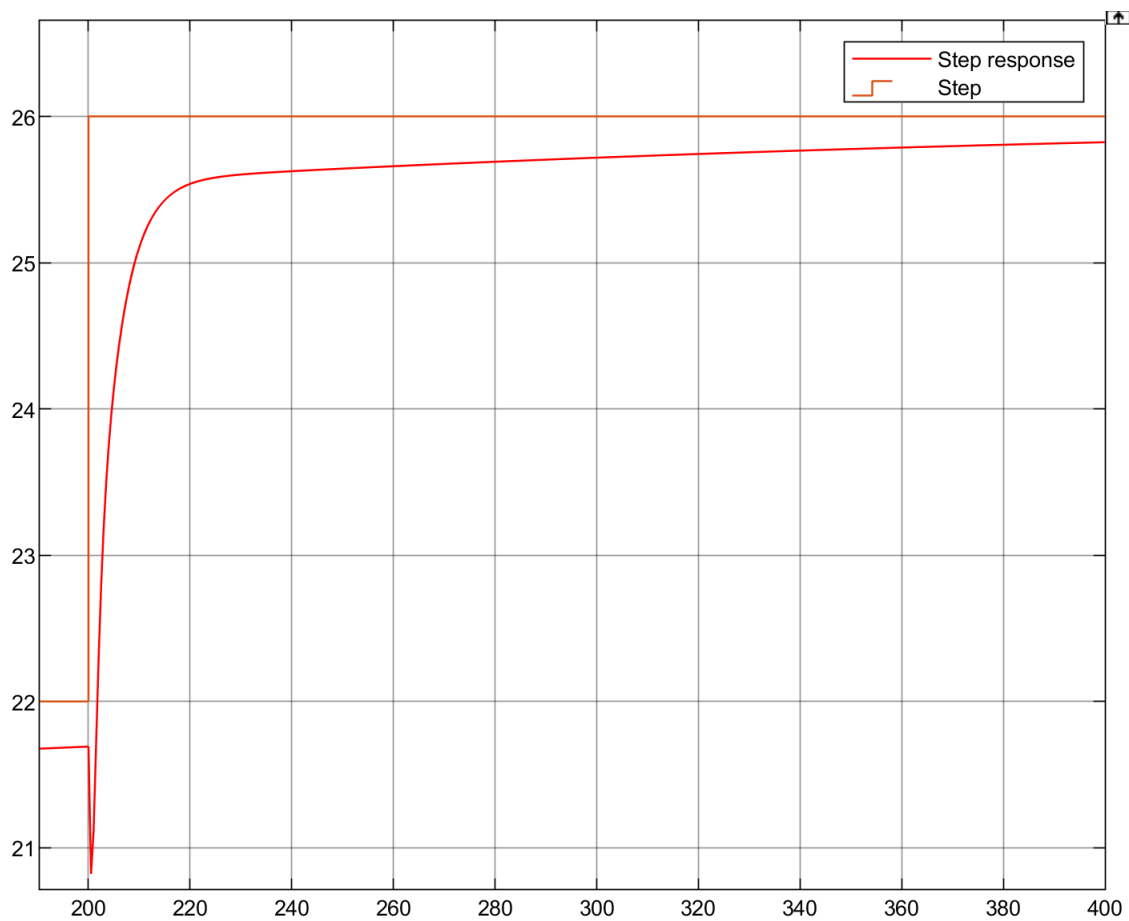


The PololuVL53L0X s function block was obtained from <https://github.com/PeterChmurciak/Simulink-Pololu-VL53L0X>

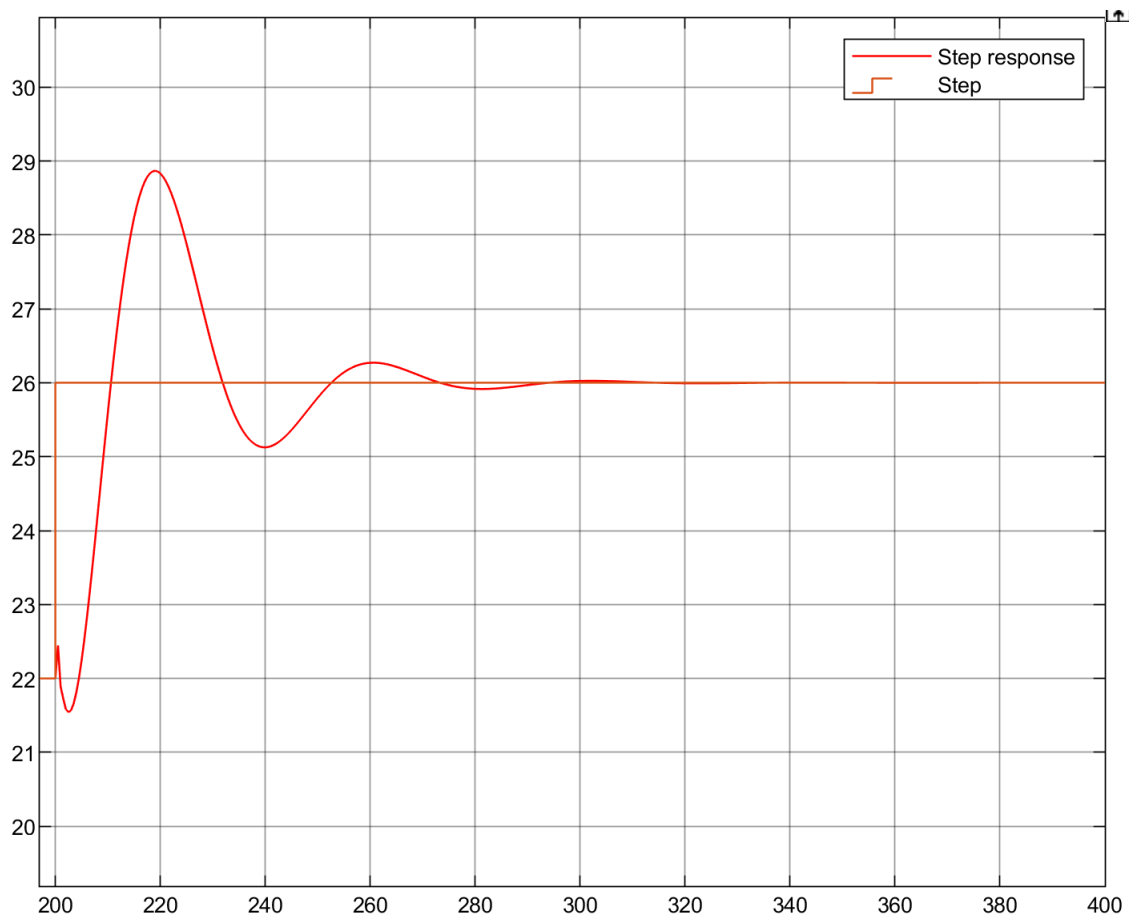
10.4 PID controller validation in software



The above setup was used to test the controllers on the $G_{12}(s)$ transfer function



The above step response was for controller simulation with $k_p=1.481$, $k_i = 0.007148$ and $k_d=2.108$



Above step response was made with $K_p = 0.9138$, $K_i = 0.1$, $K_d = -1.917$

11. EBE Faculty: Assessment of Ethics in Research Projects

Any person planning to undertake research in the Faculty of Engineering and the Built Environment at the University of Cape Town is required to complete this form before commencing research work such as collecting or analysing data. When completed it should be submitted to the supervisor (where applicable) and from there to the Head of Department. If any of the questions below have been answered YES, and the applicant is NOT a fourth year student, the Head should forward this form for approval by the Faculty EIR committee: submit to Ms Zulpha Geyer (Zulpha.Geyer@uct.ac.za; Chem Eng Building, Ph 021 650 4791). Students must include a copy of the completed form with the final year project when it is submitted for examination.

Name of Principal**Researcher/Student:** REGINALD TAMUKA NYAKONDA**Department:** ELECTRICAL ENGINEERING**If a Student:** YES **Degree:** BScEng Electrical Engineering**Supervisor:** Dr M.S Tsoeu**If a Research Contract indicate source of funding/sponsorship:****Research Project Title:** Design and control of a portable take-home laboratory rig for control systems teaching

Overview of ethics issues in your research project:

Question 1: Is there a possibility that your research could cause harm to a third party (i.e. a person not involved in your project)?	YES	NO
Question 2: Is your research making use of human subjects as sources of data? If your answer is YES, please complete Addendum 2.	YES	NO
Question 3: Does your research involve the participation of or provision of services to communities? If your answer is YES, please complete Addendum 3.	YES	NO
Question 4: If your research is sponsored, is there any potential for conflicts of interest? If your answer is YES, please complete Addendum 4.	YES	NO

If you have answered YES to any of the above questions, please append a copy of your research proposal, as well as any interview schedules or questionnaires (Addendum 1) and please complete further addenda as appropriate.

I hereby undertake to carry out my research in such a way that

- there is no apparent legal objection to the nature or the method of research; and
- the research will not compromise staff or students or the other responsibilities of the University;
- the stated objective will be achieved, and the findings will have a high degree of validity;
- limitations and alternative interpretations will be considered;
- the findings could be subject to peer review and publicly available; and
- I will comply with the conventions of copyright and avoid any practice that would constitute plagiarism.

Signed by:

	Full name and signature	Date
Principal Researcher/Student:	REGINALD TAMUKA NYAKONDA R.T.N	06 November 2021

This application is approved by:

Supervisor (if applicable):	Mohohlo Tsoeu	06 November 2021
HOD (or delegated nominee): Final authority for all assessments with NO to all questions and for all undergraduate research.	Janine Buxey	06 November 2021
Chair : Faculty EIR Committee For applicants other than undergraduate students who have answered YES to any of the above		

ADDENDUM 1:

Please append a copy of the research proposal here, as well as any interview schedules or questionnaires:

ADDENDUM 2: To be completed if you answered YES to Question 2:

It is assumed that you have read the UCT Code for Research involving Human Subjects (available at <http://web.uct.ac.za/depts/educate/download/uctcodeforresearchinvolvinghumansubjects.pdf>) in order to be able to answer the questions in this addendum.

2.1 Does the research discriminate against participation by individuals, or differentiate between participants, on the grounds of gender, race or ethnic group, age range, religion, income, handicap, illness or any similar classification?	YES	NO
2.2 Does the research require the participation of socially or physically vulnerable people (children, aged, disabled, etc) or legally restricted groups?	YES	NO
2.3 Will you not be able to secure the informed consent of all participants in the research? (In the case of children, will you not be able to obtain the consent of their guardians or parents?)	YES	NO
2.4 Will any confidential data be collected or will identifiable records of individuals be kept?	YES	NO
2.5 In reporting on this research is there any possibility that you will not be able to keep the identities of the individuals involved anonymous?	YES	NO
2.6 Are there any foreseeable risks of physical, psychological or social harm to participants that might occur in the course of the research?	YES	NO
2.7 Does the research include making payments or giving gifts to any participants?	YES	NO

If you have answered YES to any of these questions, please describe below how you plan to address these issues:

ADDENDUM 3: To be completed if you answered YES to Question 3:

3.1 Is the community expected to make decisions for, during or based on the research?	YES	NO
3.2 At the end of the research will any economic or social process be terminated or left unsupported, or equipment or facilities used in the research be recovered from the participants or community?	YES	NO
3.3 Will any service be provided at a level below the generally accepted standards?	YES	NO

If you have answered YES to any of these questions, please describe below how you plan to address these issues:

ADDENDUM 4: To be completed if you answered YES to Question 4

4.1 Is there any existing or potential conflict of interest between a research sponsor, academic supervisor, other researchers or participants?	YES	NO
4.2 Will information that reveals the identity of participants be supplied to a research sponsor, other than with the permission of the individuals?	YES	NO
4.3 Does the proposed research potentially conflict with the research of any other individual or group within the University?	YES	NO

If you have answered YES to any of these questions, please describe below how you plan to address these issues: